Quantum size effects in metal particles

W. P. Halperin

Department of Physics, Northwestern University, Evanston, Illinois 60201

The subject of small metallic particle properties is outlined with emphasis on quantum electronic effects. The theoretical background for interpretation of experiments is discussed beginning with the work of Kubo. More recent amendments to this have been included, taking into account the techniques of random matrix theory and effects of the spin-orbit interaction. A general review of experimental work is presented in order to permit a comprehensive evaluation of current understanding of the quantum size effect on the electronic spectrum. This survey includes magnetic susceptibility, nuclear magnetic resonance, electron spin resonance, heat capacity, optical, and infrared absorption measurements. These are discussed in many instances from the point of view of there being competing size effects arising from a reduced volume contrasted with those from the surface. A number of stimulating and provocative results have led to the development of new areas of research involving metallic clusters such as cluster beam techniques, far-infrared absorption by particle clusters, adsorbate NMR, and particle-matrix composites. Although there is little question that the experiments themselves indicate the existence of quantum effects, there are as yet, insufficient results to test the theoretical predictions for electron-level distribution functions based on fundamental symmetries of the electron Hamiltonian. A new suggestion for measurement of the electron-level correlation function is made using the magnetic field dependence of the NMR Knight shift. Particle preparation methods are also reviewed with commentary on the problems and advantages of these techniques for investigation of quantum electronic effects.

CONTENTS

I. INTRODUCTION

Small clusters of atoms of metallic elements have intriguing physical and electronic properties. Some of these characteristics have diverse technical applications, of key importance to our society. Others must be understood with quantum statistical theories whose development shares a common background with problems in nuclear physics. In this scientific arena, progress in fundamental and applied research has gone hand-in-hand. It is of central importance to recognize that our observations, and

Copyright ©1986 The American Physical Society

the properties with which we are concerned, usually entail measurement on a collection of a vast number of similar but not identical particles. From experiments determining the average behavior we might hope to deduce a correct description of a single particle. Unfortunately, only certain aspects of single-particle behavior can be determined. One of these is the average electronic level spacing. From the theoretical side it has been suggested that electronic properties of collections of small metal particles depend on fundamental symmetries of the electron Hamiltonian. This point of view is the basis for the discussion of Sec. II of this paper. Measurement of the temperature, or magnetic field dependence of the electronic susceptibility or specific heat can indicate what these symmetries are, giving another aspect of the single-particle properties. Experimental evidence in support of the statistical theory is reviewed in Secs. III and IV.

The central question is, "How does metallic behavior develop with increasing particle size starting with the atomic state?" Answers to this have been pursued from a wide range of experimental and theoretical directions, and indeed, such answers depend on which physical properties are under scrutiny. For instance, optical and magnetic measurements may indicate the existence of size effects, but of different origins. The optical experiments, see Sec. VI, are particularly sensitive to surface plasmon modes that depend on both small size and collective interaction between individual particles and with the matrix that supports them. Magnetic measurements presented in Secs. III and V have shown that the parity of electron number per particle is crucial. The purpose of this paper is to critically review the experimental work and its theoretical basis for electronic size effects in metal particles. Generally this means that they are smaller than several hundred angstroms in diameter and larger than 10 Å, corresponding to clusters of several hundred to many millions of atoms.

One might picture the process of forming a conducting solid from its constituent atoms in terms of band theory. Each atom on its own has a well-defined set of electronic states. An N-atom cluster of noninteracting atoms must have an N-fold degeneracy for each electronic energy level. The interatomic electron interactions of the cluster remove this degeneracy and the allowed energy states spread out into a band. In the bulk we are not at all concerned with the details of this process, rather it is the density of energy states which plays the crucial role. By contrast, the properties of the small particle, representing the nascent metallic condition, are determined by the statistics of the electron-level distribution in addition to the density of states. More precisely, the density of states is the inverse of the energy-level spacing averaged over this distrbution.

The most obvious experimental technique that might be applied in order to define the electronic spectrum involves direct electronic transitions from allowed states. Photoemission measurements (Colbert *et al.*, 1983; Mason, 1983) can give a sense of the evolution from atomic-to-bulk, for properties such as the work function, and how these are affected by the matrix or particle support. However, their limited energy resolution makes it impossible to directly determine the electronic level spectrum by observation of transitions from different discrete levels to the continuum. Alternatively, one might consider optical absorption measurements between levels. The appropriate range of frequencies falls in the far-infrared for reasonable particle sizes and has been studied theoretically by Gor'kov and Eliashberg (1965). Apparently this approach has insurmountable technical difficulties (Devaty and Sievers, 1980). This leaves the problem of exploring the electronic level spectrum to a class of measurements that are essentially thermodynamic, such as the magnetic susceptibility and the specific heat. Much of the theory and experimental effort in the last twenty years has been directed toward understanding this aspect of small metal particles.

On the theoretical side a considerable impetus in the field followed from the pioneering work of Kubo (1962) who recognized the inherent statistical nature of the problem. He pointed out that the detail of the level spectrum of an individual particle would be determined by its precise geometry. Other particles with similar size but different shape or surface conditions should have a different spectrum even though they have the same average level spacing. He then proposed that one should approach this problem, which had been originally enunciated by Fröhlich (1937) in terms of metal cubes, with the ansatz that there are random surface potentials that are reflected in a Poisson distribution of the energy levels. Later work by Gor'kov and Eliashberg (1965) showed that there was a connection between this problem and random matrix theory as had been developed for interpreting nuclear level spectra. They clarified that energy-level repulsion should be taken into account resulting in different energy-level distributions depending on the symmetry of the electron Hamiltonian. This was predicted to show up in the temperature dependence of the susceptibility and the specific heat for measurements on a collection of particles. Most experimental activity has been concentrated on demonstrating just the existence of these quantum size effects. In only a few cases has it been possible to deduce more information related to the level distribution functions themselves. Nonetheless, the process of developing and refining the experimental methods has led to the discovery and understanding of other phenomena including particle-matrix interactions and surface electronic effects. These may be of fundamental and technical importance in their own right and, to a limited extent, these are discussed in this review as well.

There are important applications of small metal particle technology to a number of areas; heterogeneous catalysis, surface enhanced Raman scattering, fields of research where surface and interface properties are important such as in heat exchangers and thermometers at ultralow temperatures, magnetic devices, and superconductivity, to name but a few. In many of these the essential properties are specifically a consequence of the small size and do not exist in the bulk material at all. Enhanced

catalytic activity is one example recently reviewed by Bond (1985). In other cases, such as is the situation with heat exchangers, the immediate concern is to obtain a large surface area that is clearly more efficiently achieved with smaller particles. On the other hand, it is essential to know that the metallic characteristics of the particle, important to the application, are not altered with decreasing size. Applications of platinum particles to very-low-temperature thermometry and heat exchange is a case in point. Here one requires that the nuclear-spin lattice relaxation time not be too long. Quantum effects may substantially increase the relaxation time with sufficiently small size at low temperatures compromising the efficacy of the increase in surface area. An understanding of the size effects is obviously important in this case too.

Even in the field of heterogeneous catalysis it is not easy to isolate effects which are strictly dependent on metal particle size since other factors such as the metal support interaction and preparation conditions are not easily controlled in an independent way. Nonetheless, it appears that there is compelling evidence for intrinsic size effects on a number of reactions and processes such as the activation energy for hydrogen desorption from platinum supported on silica gel. (See the review of this work by Bond, 1985.)

The electronic spectrum of the metal cluster has much in common with that of the highly excited vibrational states of polyatomic molecules (Buch, Gerber, and Ratner, 1982; Pechukas, 1983). In both cases a statistical description of the level spectrum is required. For the small-particle problem the theoretical techniques that have been applied rely on the random matrix methods developed for classifying excited nuclear states. In fact questions have been raised by Barojas *et al.* (1977) and Brody *et al.* (1981) as to the appropriateness of this approach. It is therefore particularly important in clarifying the right direction for these ideas to have clear-cut experimental results. This paper attempts to bring together a discussion of the existent measurements in order to have a better picture of compliance between experiment and theory.

The scope of the paper is to include a review of magnetic susceptibility, specific heat, electron spin resonance, nuclear magnetic resonance, optical, and far-infrared experiments on metal particles. Most of the work cannot be related to quantum size effects. Some of it is found to be affected by the metal surface. Other results are a consequence of collective interactions with the matrix or with other particles. Finally a number of key results indicate unambiguously that the metal particles have a discrete electronic level spectrum. From these, however, there is not yet sufficient evidence to give the statistical theory a rigorous test.

Since many different elements and a variety of techniques have been used in particle preparation these are summarized at the end. There are important size effects in metal particles on superconductivity for those elements which are superconducting in the bulk. These effects are only briefly referred to, insofar as they bear on the normal state electronic properties and the interpretation of such experiments. Size effects in ferro- or antiferromagnetic particles are not addressed at all. Although very interesting, this work was deemed to be outside of the scope of this paper.

Different aspects of the subject have been discussed in review format before. A rough guide to the literature should be helpful at this point. Those more comprehensive articles describing experimental work related to the quantum size effect include work by Marzke (1979), Baltes and Šimànek (1981), Perenboom, Wyder, and Meier (1981a), Morokhov, Petinov, Trusov, and Petrunin (1981), and Kubo, Kawabata, and Kobayashi (1984). Marzke includes, in an abbreviated format, a discussion of the Kubo theory and compares with the results of a number of magnetic and optical experiments. The article of Baltes and Šimànek is not restricted to just metal particles having a fairly extensive discussion of the theoretical basis for size effects on the vibrational specific heat, Bose-Einstein condensation, and optical properties, as well as a discussion of size effects in superconductors. These topics complement their treatment of the quantum size effect. Perenboom *et al.* (1981a) give a very complete account of this subject including a discussion of size effects in superconductors and particle preparation techniques. They present detailed derivations of the thermodynamic parameters with exact results for the equal-level spacing problem and limiting cases for a statistical distribution of levels. Morokhov *et al.* (1981) discuss the effects of small size on the physical structure of metal particles as well as electronic effects. Their review gives a more complete guide to the Soviet literature than was possible here. The more recent paper by Kubo *et al.* (1984), although quite brief, gives a useful, concise overview of the material.

Other authors have focused on certain aspects of size effects in metal particles. Brody *et al.* (1981) have reviewed random matrix physics largely in the context of problems in nuclear physics. In a section devoted to the quantum size effect they discuss critically some of the assumptions of the Kubo theory. A review of theoretical methods used to calculate properties of metal clusters, with emphasis on models that can describe adsorbate interactions, has been given by Messmer (1979,1981). These are based mostly on semiempirical methods. A related review has been written by Kunz (1980). Monot (1983) has presented a summary of microscopy and x-ray work on noble-metal clusters that indicates which are the preferred cluster structures, growth habits, and size effects on the melting tempertature and binding energies. A very pedagogical review of the quantum size effect on the magnetic susceptibility of small particles has been given by Buttet (1981), and a discussion of optical absorption in metal particles was presented recently by Kreibig and Genzel (1985).

The subject of metal and inorganic clusters has been the central theme of a series of three international conferences. Many interesting topics have been discussed there and are presented in the proceedings, but are not included in this review. In order to survey the variety of subfields

of cluster physics it may be helpful to search directly in the proceedings of these conferences. The first symposium was held in Lyon in 1976 for which the proceedings appeared in the colloque series of the Journal de Physique, vol. 38, C2 (1977). The second meeting was in Lausanne in 1980 and was published in Surface Science, vol. 106 (1981). The third conference was held in Berlin in 1984 and its proceedings have appeared in Surface Science, vol. 156 (1985).

II. DISCRETENESS OF THE ELECTRONIC LEVEL STRUCTURE

For practical purposes the conduction electron energy spectrum of a metal is usually considered to be a continuum. Indeed, this is always an appropriate point of view at high temperatures and for samples of macroscopic size. However, for small metal particles having a small number of conduction electrons, the discreteness of the spectrum has an important consequence at low temperatures. All of the thermodynamic properties, such as the specific heat and the magnetic susceptibility are significantly altered from their bulk values owing to the discrete character of the allowed energy states. This point was first discussed by Fröhlich (1937) but it was not until Kubo and his collaborators independently addressed this problem (Kubo, 1962; Kawabata and Kubo, 1966) that the subject developed widespread interest. The essential idea is that the spacing between adjacent conduction energy states increases inversely with the volume of the particle. Energy-level spacings of about 1 K can be found for particles of 100 Å in size. This can be seen from the following qualitative discussion. In a free-electron model the Fermi energy itself depends only on the density of electrons n,

$$E_F=\hbar^2\left[\frac{3\pi^2 n}{2m}\right]^{2/3} \tag{2.1}$$

and consequently is independent of the particle size. However, with smaller particle size there are fewer conduction electrons N and so the number of filled electronic states at $T=0$ is smaller as well. Since all states are filled up to E_F and E_F is fixed, then the energy spacing δ between the states increases with decreasing particle volume V according to

$$\delta\approx E_F/N\propto V^{-1} \tag{2.2}$$

and is given more precisely by $\delta=4E_F/3N$. The quantity δ is just the inverse of the average density of electronic states for a single spin at the Fermi energy. For approximately spherical particles with diameter d the level spacing varies as d^{-3}. These are restatements of the well-known fact that the density of electronic states is proportional to the volume.

Suppose that it were possible to make measurements on a single metal particle at a temperature T, sufficiently low that two conditions maintained: k_BT much less than δ and that the lifetime τ of the electronic states be much larger than $\hbar/\delta$. In this situation the Fermi energy would be found, most likely, in a gap between adjacent sharp energy levels, and the measurements should indicate that the particle has passed into a "nonmetallic" state. As an indication of the magnitude of this effect we find that for a free-electron metal such as silver with an electron density of $n=6\times10^{22}$ cm^{-3} the density of electronic states per spin is

$$D(E_F)=\delta^{-1}=\frac{Vmk_F}{2\hbar^2\pi^2}=\frac{Vm(3\pi^2 n)^{1/3}}{2\hbar^2\pi^2}\ , \tag{2.3}$$

$$\delta/k_B=\frac{1.45\times10^{-18}}{V}\ \text{K cm}^3\ . \tag{2.4}$$

In order to have a level spacing of $\delta/k_B=1$ K, such a particle would have to have a diameter of $d=140$ Å. This size depends on the metallic element considered but varies only within a range of about 50%. The level spacings presented in Fig. 1 are determined from the average density of states per spin band at the Fermi surface. These are found from heat capacity measurements, rather than using the free-electron formulations given above and consequently they include enhancement in the density of states at the Fermi surface from the electron-phonon interaction (Ashcroft and Mermin, 1976). There is not much difficulty in making particles of this and smaller sizes for most metals. Furthermore, refrigeration techniques to temperatures that satisfy the condition $k_BT\ll\delta$ are readily available. Since the experimental domain is reasonably accessible it is somewhat surprising at first sight that the observations of this phenomenon are not more clearly established. For example, it could be expected that the specific heat of a metal particle with a gap at the Fermi energy would be similar to that of the bulk metal at high temperatures ($k_BT\gg\delta$) showing a linear dependence upon temperature. However, at low temperatures ($k_BT\ll\delta$), this should switch to an exponential dependence,

$$C(T)=k_B\exp(-\delta/k_BT)\ ,\quad T\to0\ . \tag{2.5}$$

Similarily, dramatic alterations from the temperature-independent Pauli magnetic susceptibility of the bulk material might be anticipated for the small-size particle. Unfortunately it is not possible to perform thermodynamical experiments with just one particle. A sample suitable for experimentation normally includes a very large number of these. In this case, the temperature dependence of the specific heat and the magnetic susceptibility can be found by averaging the behavior of a single particle over the size and shape distributions for all the particles in the sample. In so doing, one finds that the exponential dependence on temperature, Eq. (2.5), is replaced with a simple integral power law. Which power is appropriate depends on the symmetry of the electron Hamiltonian. These results are based on a considerable literature which has developed for the description of the statistical properties of nucleon energy levels in nuclear physics. We will present derivations of the low-temperature limiting

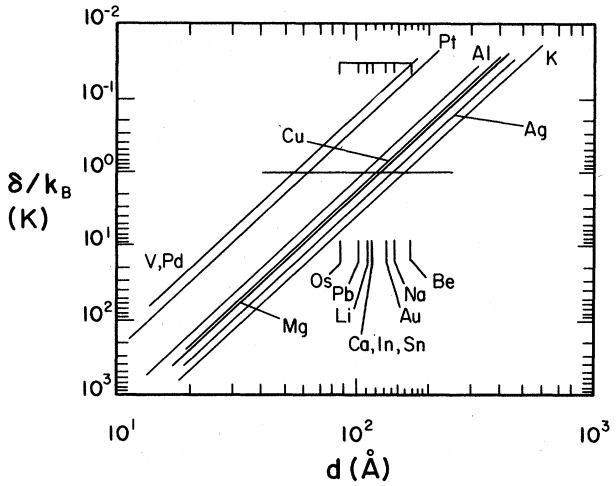

FIG. 1. Average electron-level spacing as a function of particle diameter for a selection of the metallic elements. The particle diameter d, calculated for an average level spacing of 1 K, is found from the measured heat capacity of the bulk metal according to the expression $d(\delta/k_BT=1\ \text{K})=55.8\ \text{Å}(v/\gamma)^{1/3}$ where the molar volume v is expressed in units of $\text{cm}^3\,\text{mole}^{-1}$ and the Sommerfeld constant γ is taken from the measured heat capacity and is in units of $\text{mJ}\,\text{mole}^{-1}\,\text{K}^{-2}$. For a number of elements only one size is shown by vertical marks and these correspond to a level spacing of 1 K. Other level spacings can be easily inferred from this using the indicated slope.

behavior for both the specific heat and the magnetic susceptibility showing that the predicted temperature dependence is markedly different from that of the bulk metal. Despite the simplicity of the concept and the very fundamental nature of the specific heat, no measurements of it have yet been performed that clearly show quantum size effects. However, there is strong evidence supporting some of the size-effect predictions for the electronic magnetic susceptibility despite the fact that we do not have a clear quantitative understanding for all of the experimental results. In this review a discussion of this theory will be presented and compared with available experimental results. Suggestions will be made for a number of directions in which new experiments might clarify ideas concerning the quantum size effect in metal particles.

A. Kubo theory

The theory of the electronic properties of metallic particles presented by Kubo and his colleagues (Kubo, 1962; Kawabata and Kubo, 1966; Kawabata, 1970) has recently been summarized and updated in a review (Kubo, Kawabata, and Kobayashi, 1984). The latter work incorporates important contributions concerning the statistical character of the energy-level distributions (Gor'kov and Eliashberg, 1965; Denton, Mühlschlegel, and Scalapino, 1973) that have evolved since Kubo's original work in 1962.

The simplest notion is to consider just one particle and try to develop a calculational scheme of the energy-level spectrum for its particular geometry (Buttet *et al.*, 1982; Delley *et al.*, 1983). We expect that at high temperatures there is really no distinguishable difference between our single small particle and that of the bulk material. At low temperatures there should be some simple limiting behavior. In between there will be a crossover regime that we need not discuss here in order to grasp the basic ideas. At low temperatures only the first few levels near the Fermi energy will be important. Consequently the low-temperature behavior for the single particle might be effectively modeled by an *equal level spacing* approximation: all levels are assumed to be equidistant. This model has a specific heat given by Eq. (2.5) and has only one adjustable parameter. Although this is appealing from the viewpoint of simplicity, nonetheless it is totally unrealistic as was first discussed by Kubo (1962). He introduced the notion that one must consider a large ensemble of particles for which the statistics of the distribution of level spacings plays a key role. His theory was based on these being randomly distributed following Poisson statistics. Subsequent to this landmark work important modifications of the ideas were introduced by others and will be discussed in a later section.

In a presentation of Kubo's theory there are two important aspects that require emphasis at the very beginning. First, the degenerate, size-restricted electron gas is treated in the context of Fermi liquid theory. This is in contrast to the approximate one-electron description, despite the fact that the latter leads to a conceptually facile account of electronic properties in terms of individual electronic states. In the Kubo theory the discrete energy levels are those of quasiparticle states. The use of a noninteracting quasiparticle model was justified by Kubo (1969) and he estimated that the effect of the quasiparticle interactions was negligible (Kubo, 1962). The lifetime broadening of the quasiparticle states in units of temperature is approximately 10 K at room temperature (300 K) and 0.5 K at liquid-nitrogen temperature (77 K), varying as T^2 . It is clear that the measurements of quantum size effects at liquid-helium temperature (4.2 K) will be unaffected by these interactions and that the energy levels can be considered to be quite sharply defined. Furthermore, it can be easily shown that the second condition for observation of quantum effects, $k_BT \ll \delta$, is more restrictive for all reasonable particle sizes.

Second, in the Kubo theory it is necessary to assume that each particle is electrically neutral (Kubo, 1962,1977). This point was discussed at some length by Kawabata (1977). Neutrality is determined by a comparison of the work function for a particle and thermal fluctuations. At sufficiently low temperatures the thermal energy k_BT can be expected to be much less than W, the work against the Coulomb interaction required to extract an electron from the particle. They have expressed this condition in the form

$$k_BT \ll W \approx e^2/d = 1.5\times 10^5 k_B/d\ \text{K Å}\,, \qquad (2.6)$$

where d is the diameter of the particle. This always holds for the quantum size effect regime. Even for particles of

10 Å, Eq. (2.6) is 2 orders of magnitude weaker than the stronger limit $k_B T \ll \delta$, that signals onset of quantum size effects.

However, the simple representation of W given by Eq. (2.6) has been called into question by recent experiments on electron tunneling from small metal particles (Cavicchi and Silsbee, 1984). These are consistent with there being a uniform distribution of absolute values of W from zero to e^2/d. This distribution might be attributed to varying amounts of electron transfer from the metal particle to an oxide support or to whatever matrix is used to hold the sample. This suggests that the canonical condition for electron neutrality may not be easily satisfied for an ensemble of particles unless care is taken that they are well segregated. In the limit where large tunneling rates are possible then the properties of the metal particle sample should be indistinguishable from that of the bulk. Even if thermal fluctuations do not drive electron tunneling the distribution of the work function indicates that there is an important static metal-support interaction. Consequently one should be wary of assuming that divalent metals such as Sn and Mg have strictly even integer numbers of electrons per particle.

Having made these two preliminary remarks let us return to the question of treating the energy-level spectrum of a single particle from a statistical point of view. By a single particle we mean a particle of almost spherical shape but having microscopic variations in the roughness at the surface. These surface conditions can be thought of as giving rise to a random potential that removes the large electronic orbital degeneracy that might otherwise be associated with such a highly symmetrical shape. This approach was first taken by Kubo (1962) where he assumed that the spacing between energy levels near the Fermi energy could be taken to be a random variable. He introduced the probability density for finding an energy state with a separation Δ from a given one with precisely n levels in between. This is given by the Poisson distribution

$$P_n(\Delta) = \frac{1}{n!\delta}(\Delta/\delta)^n \exp(-\Delta/\delta) \ . \tag{2.7}$$

The single important parameter that enters this theory is the average spacing of adjacent levels δ. The distribution of adjacent levels separated by energy Δ corresponds to $n=0$ in Eq. (2.7) and is an exponential function, becoming constant at small values of Δ. This is inappropriate for most circumstances since the probability of finding two levels in the same particle arbitrarily close together should be suppressed by level repulsion effects as is well known in nuclear physics problems. This application to the small-particle problem was pointed out by Gor'kov and Eliashberg (1965) and has been discussed by Kubo (1977). Taking this into account, the probability of finding adjacent energy levels with spacing Δ depends upon the transformation properties of the Hamiltonian. For example, in the case of weak spin-orbit interaction and small externally applied magnetic fields the electron Hamiltonian is invariant under space inversion and time reversal and it can be shown that the correct probability density decreases proportional to Δ for small Δ. A similar situation exists in nuclear physics where the highly excited states of the atomic nucleus may be thought of as being determined by random nucleon interactions having definite symmetry (Wigner, 1951,1955; Dyson, 1962; Porter, 1965; Mehta, 1967). This work was applied to the small-particle problem by Gor'kov and Eliashberg (1965) and developed further by Denton, Mühlschlegel, and Scalapino (1973) who found an approximate technique for determining the temperature and magnetic field dependence of the specific heat and magnetic susceptibility over the full range of temperature from the bulk metal limit $\delta \ll k_B T$ to the low-temperature limit, $\delta \gg k_B T$. Although the latter has been one of the most comprehensive theoretical accounts to date one important point was not fully recognized at that time. This was the effect of strong spin-orbit interaction on the quasiparticle states and on the predictions for the temperature dependence of the magnetic susceptibility. Theoretical treatments of this topic have since been presented by Shiba and Sone (Shiba, 1976; Sone, 1977) giving qualitative agreement with experiment. In the next section we will review the amendments to the Kubo theory principally as they were presented by Denton *et al.* and then in a subsequent section discuss how the effects of spin-orbit interaction can be taken into account.

B. The statistics of electron energy levels and thermodynamics

A real sample of small metal particles always has some distribution in size. Here we define size only in the context of the corresponding mean energy-level spacing near the Fermi energy, δ, the parameter with which the theory is most easily formulated. First we will discuss the properties of a monodispersion of particles having a unique value for δ, and then later we will average over the size distribution. For all particles falling in the range of sizes with average spacings δ to $\delta + d\delta$, the energy-level spectrum for the electrons is considered to depend on random surface potentials and fundamental symmetries of the electron Hamiltonian. Consequently the spectra in this subensemble of the particles are distributed according to a probability density. An illustration of this situation might be to consider all particles to be nearly spherical each with roughness on the atomic scale. The orbital degeneracy of a spherical particle increases as $N^{1/3}$ and can be removed by the hypothesized random surface conditions. Numerical analogs to this problem have been studied by Barojas *et al.* (1977), Tavel *et al.* (1979), and Ratcliff (1979). Selection of the appropriate probability density depends on the transformation properties of the Hamiltonian. This, in turn, depends on the relative strength of the spin-orbit interaction $\langle H_{so} \rangle$ or the external magnetic field $\mu_B H$ as compared with δ (μ_B is the Bohr magneton). We will classify the four possible combinations of weak and strong $\langle H_{so} \rangle$ and H by an index a

TABLE I. Assignment of the energy level distribution functions to different combinations of external conditions. These are specified by the magnitude of the applied field through its determination of the Zeeman energy ($\mu_B H$) and the spin-orbit interaction (H_{so}) as compared to the average electron level spacing δ.

a	Distribution	Magnetic field	Spin-orbit interaction
0	Poisson	large	small
1	orthogonal	small	small
		small	large (even particles)
2	unitary	large	large
4	symplectic	small	large (odd particles)

labeling the corresponding probability density P_N^a. Values of $a=0,1,2,4$ indicate Poisson, orthogonal, unitary, and symplectic distributions. These are summarized in Table I along with the conditions under which they apply. A complete description of the problem must specify the probability of finding an entire spectrum ($H=0$), which can be notated in order of increasing energy as

$$\ldots,-\Delta_2',-\Delta_1',\Delta_0,\Delta_1,\Delta_2,\ldots . \tag{2.8}$$

Here Δ_0 is the lowest occupied state at $T=0$. All of the filled levels at $T=0$ are primed. Such a specification is given by a distribution function for N levels,

$$P_N^a(\ldots,-\Delta_2',-\Delta_1',\Delta_0,\Delta_1,\Delta_2,\ldots) \tag{2.9}$$

suitably normalized and for which

$$\delta=\int P_N^a(\cdots\Delta_n\cdots)\,|\,\Delta_j-\Delta_{j-1}\,|\,d\Delta_n\ , \tag{2.10}$$

for all levels j near the Fermi energy. In practice we will only need to consider a small number of levels ($N\leq 3$) for which approximate distribution functions for all cases have been constructed (Denton, Mühlschlegel, and Scalapino, 1973). By integrating over Δ_0, distributions of level *spacings* relative to Δ_0 can be obtained. Next, if all spacings Δ_j are integrated over with the exception of $j=1$, then the resulting distribution is for the spacing of only the next highest level to that of Δ_0. If integration is performed over all the variables except Δ_1 and Δ_1', then the three-level problem can be described by the resulting distribution over two-level spacings. These functions are the only ones that are needed to solve the problem in the low-temperature limit $k_BT\ll\delta$ and so they are reproduced here in the approximate form given by Denton *et al.* (1973) appropriate for the cases $a=1$, 2, and 4,

$$p_2^a(\Delta)=\Omega_2^a\delta^{-1}(\Delta/\delta)^a\exp[-B^a(\Delta/\delta)^2]\ , \tag{2.11}$$

$$P_3^a(\Delta,\Delta')=\Omega_3^a\delta^{-(3a+2)}[\Delta\Delta'(\Delta+\Delta')]^a \times\exp[-a(\Delta^2+\Delta\Delta'+\Delta'^2)/3\delta]^2\ . \tag{2.12}$$

The normalization constants and parameters Ω_2^a, Ω_3^a, and B^a are listed in Table II. Exact results are given for Ω_2^a and Ω_3^1, whereas the other normalization constants have been calculated numerically (Tarczon, 1984).

The specific heat C and the magnetic susceptibility χ can be calculated from the partition function Z and the spectrum of energies E_j of allowed configurations such as displayed in Fig. 2.

$$Z=1+\sum_{j\neq 0}e^{-\beta E_j}\ , \tag{2.13}$$

$$C=k_B\beta^2\frac{\partial^2}{\partial\beta^2}\ln Z\ , \tag{2.14}$$

$$\chi=\beta^{-1}\frac{\partial^2}{\partial H^2}\ln Z\ ,\quad \text{where } \beta=(k_BT)^{-1}\ . \tag{2.15}$$

The averages of these thermodynamic quantities over the appropriate statistical distributions are

$$\langle C\rangle=k_B\beta^2\frac{\partial^2}{\partial\beta^2}\langle\ln Z\rangle\ . \tag{2.16}$$

$$\langle\chi\rangle=\beta^{-1}\frac{\partial^2}{\partial H^2}\langle\ln Z\rangle\ . \tag{2.17}$$

As a final step, the heat capacity and magnetic susceptibility are averaged over the experimentally determined size distribution to find the expected temperature and magnetic field dependences of the real sample, $\overline{\langle C\rangle}$ and $\overline{\langle\chi\rangle}$. Before we illustrate the method by calculating the

TABLE II. Parameters of the approximate distribution functions for two- and three-electron energy levels taken from Denton *et al.* (1973). The index a indicates orthogonal, unitary, or symplectic distributions and the subscript 2 or 3 identifies parameters of either the two- or three-level distributions.

a	Distribution	Ω_2^a	Ω_3^a	B^a
1	orthogonal	$\pi/2$	$(3\pi)^{-1/2}$	$\pi/4$
2	unitary	$32/\pi^2$	0.7017	$4/\pi$
4	symplectic	$(64/9\pi)^3$	2.190	$64/9\pi$

limiting low-temperature behavior of $\langle C \rangle$ and $\langle \chi \rangle$, it is worthwhile emphasizing the importance of the choice of distribution function.

There is an extensive discussion in the theoretical literature regarding the suitability of the functions P_N^a and the premises on which their choice is based. In the nuclear physics problem mentioned earlier there have been two hypotheses advanced regarding how random interactions should be treated. Following work by Wigner (1951,1955) an assumption was introduced of the statistical independence of the matrix elements of the random Hamiltonians. This allowed a convenient Gaussian formulation. The effect of Wigner's surmise is evident in the Gaussian factors in the approximate single-level spacing distributions given above, Eqs. (2.11) and (2.12) (Rosenzweig and Porter, 1960). According to Dyson (1962) the problem should be enunciated in terms of $N \times N$ unitary matrices where N is the number of levels. Then it is assumed that each possible unitary matrix is equally probable and the statistics are based on this ansatz. An extensive and clearly presented discussion is given by Perenboom, Wyder, and Meier (1981a). Recent work by Efetov with a supersymmetry method has led him to the conclusion that the Dyson hypothesis is, in fact, correct (Efetov, 1982a,1982b). Leading-order expansions for small Δ of some of the distribution functions are known exactly (Porter, 1965; Mehta, 1967) and so the error in the approximate forms given here, based on the Wigner surmise, can be evaluated and this is found to be unimportant (Denton, Mühlschlegel, and Scalapino, 1973).

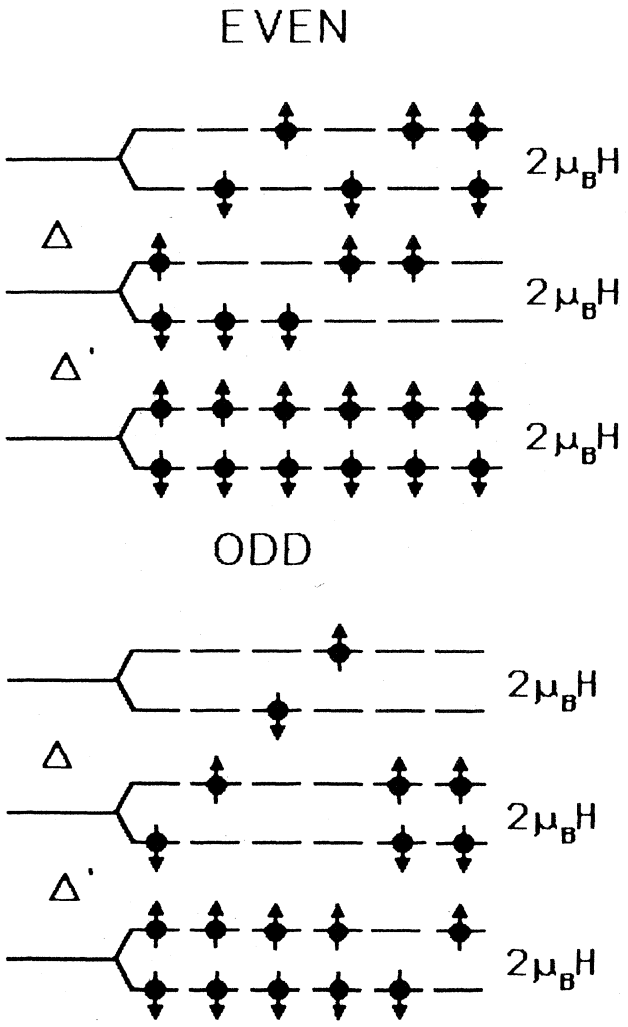

FIG. 2. Electron-level structure diagrams for the two cases of particles with an even number of electrons, and for particles with an odd number of electrons. Only the lowest-energy configurations are shown with the ground state at the left and progressively higher excited states to the right for each of the even and odd cases.

If the Hamiltonian is invariant under time inversion and is either invariant under space rotation or total angular momentum is an integral multiple of $\hbar$, then the *orthogonal* distribution is appropriate, $a=1$. This situation holds when both spin-orbit coupling and the external magnetic field are small compared to δ. $\langle H_{so} \rangle$ is small for light elements such as Li, Na, Mg, K, and Al. In this case spin is a good quantum number and the electronic spectrum consists of Zeeman doublets in a small applied magnetic field.

If the ensemble of random Hamiltonians is invariant only under time reversal and total angular momentum is half-integral, then the *symplectic* distribution applies, $a=4$. This holds for the case of strong spin-orbit interaction and weak applied magnetic fields. For this situation the electronic spectrum consists of a collection of Kramers doublets. Perenboom, Wyder, and Meier (1981a) point out that the case of strong spin-orbit coupling and weak magnetic fields should be discussed carefully on the basis of the parity of the number of electrons in the small particle. For a particle with an even number of electrons the total angular momentum is integral and the orthogonal distribution is correct; otherwise the symplectic distribution should be used as noted previously.

When there is a strong spin-orbit interaction, and time reversal invariance is destroyed by a large applied magnetic field then the *unitary* distribution is appropriate with $a=2$.

Lastly when the magnetic field is strong and the spin-orbit interaction is weak, different spin states are decoupled. Here it is argued that the correct distribution is close to being *Poisson* for which $a=0$ (Kubo, Kawabata, and Kobayashi, 1984). It should be noted that in earlier work (Gor'kov and Eliashberg, 1965; Denton, Mühlschlegel, and Scalapino, 1973; Efetov, 1982a,1982b) it was inferred that the *unitary* distribution would apply in this case.

For large magnetic fields the thermodynamical behavior of a single particle within the framework of the equal-level spacing approximation becomes a periodic function of the applied magnetic field (Denton, Mühlschlegel, and Scalapino, 1973); however, for a statistical distribution of level spacings, as one must have in a real sample, this effect is washed out and the magnetic

susceptibility is equal to its Pauli value.

1. Even and odd particles and the magnetic susceptibility

A very interesting aspect of the small metal particle problem was pointed out by Greenwood, Brout, and Krumhansl (1960) before the work of Kubo (1962). There is a fundamental difference between the partition functions for particles with a spectrum of doublets depending upon whether there are an even or odd number of electrons per particle. This leads to a difference in heat capacity and magnetic susceptibility associated with the parity of electron number. This is sketched in Fig. 2. For metals with one conduction electron per atom we should envisage that by chance, half of the particles have even numbers of electrons with the remainder having an odd number. For metallic elements with an even number of conduction electrons per atom such as Mg, Sn, Zn, Cd, Hg, or Pb we might expect that all particles have even electron number. However, as was suggested earlier, a metal-support interaction may permit partial electron transfer from a metal particle to the supporting matrix invalidating this hypothesis.

Even from a qualitative point of view one can see that there will be dramatic effects of electron number parity. Consider a particle with an even number of electrons in a small magnetic field H compared to δ ($\mu_B H \ll \delta$). For a spin-flip transition to take place, as may be necessary in the measurement of the magnetic susceptibility, an electron must be excited to the triplet state shown in Fig. 2. This requires energy $\Delta - 2\mu_B H$ which is of the order of δ. Consequently at low temperatures where $k_B T \ll \delta$ the magnetic susceptibility of an even particle must decrease exponentially in the temperature as does the specific heat, Eq. (2.5). By the same argument an odd particle would have an electron trapped in a state with twofold spin degeneracy ($H \approx 0$) and should respond as a free spin to the applied magnetic field. The susceptibility in this case can be expected to be Curie-type, $\chi = \mu_B^2 / k_B T$ where the g factor is taken to be 2.0 and the total angular momentum is $\frac{1}{2}$. These low-temperature results for the susceptibility and for the specific heat can be deduced from the grand canonical ensemble which was first applied to the small-particle problem by Fröhlich (1937). However, when allowance is made for a distribution in energy-level spacings these conclusions must be substantially modified as we will see in the next section. Finally, in the limit of large magnetic fields the spin-up and spin-down bands are decoupled and even-odd effects become washed out. A large spin-orbit interaction has a similar effect where spin-up and spin-down wave functions must be admixed to find eigenstates of the Hamiltonian. In either case of strong magnetic field or large spin-orbit coupling ($a = 0, 2$, or 4),

$$\chi_{\text{even}} = \chi_{\text{odd}} = \chi_{\text{Pauli}} , \quad H_{\text{so}} \text{ or } \mu_B H \gg \delta . \tag{2.18}$$

2. The partition function, specific heat, and magnetic susceptibility at low temperatures

One of the the most interesting aspects of the quantum size effect in small particles appears at low temperatures. In this regime the heat capacity and magnetic susceptibility have a temperature dependence deviating substantially from that of the bulk metal, the details of which directly reflect the statistical character of the electronic spectrum. It seems useful therefore to derive their dependences on temperature in this restrictive, but simple case, $k_B T \ll \delta$.

At low temperatures only electronic states adjacent to the ground state are important. It is sufficient to consider the three-level problem with two energy spacings Δ_1 and Δ_1', setting Δ_0 to be zero in the notation of Eq. (2.8), we can also drop the use of the subscript. For the level structure sketched in Fig. 2 it is straightforward to tabulate the energy of each possible electron configuration and to write out the complete partition functions, Z_{even} and Z_{odd} (note that only the least energetic configurations are shown explicitly in Fig. 2)

$$Z_{\text{even}} = 1 + 2(1 + \cosh 2\beta\mu_B H)(e^{-\beta\Delta} + e^{-\beta(\Delta+\Delta')} + e^{-\beta(2\Delta+\Delta')}) + e^{-2\beta\Delta} + e^{-2\beta(\Delta+\Delta')} , \tag{2.19}$$

$$Z_{\text{odd}} = 2(\cosh\beta\mu_B H)(1 + e^{-\beta\Delta} + e^{-\beta\Delta'} + 3e^{-\beta(\Delta+\Delta')}) + e^{-\beta(2\Delta+\Delta')} + e^{-\beta(\Delta+2\Delta')} + e^{-2\beta(\Delta+\Delta')}) + 2(\cosh 3\beta\mu_B H) e^{-\beta(\Delta+\Delta')} . \tag{2.20}$$

Following the prescription outlined earlier we should average $\ln Z$ in each of the two cases and then differentiate with respect to β and H. It is clear that in the low-temperature limit only the leading-order behavior of the distribution functions, Eqs. (2.11) and (2.12), needs to be considered. For the case of Z_{even} only the two-level (single-level-spacing) distributions are important. For Z_{odd}, however, the three-level functions, Eq. (2.12), must be used. Further simplification can be made in this limit:

$$Z_{\text{even}} \approx 1 + 2(1 + \cosh 2\beta\mu_B H)(e^{-\beta\Delta}) + e^{-2\beta\Delta} , \tag{2.21}$$

$$Z_{\text{odd}} \approx 2(\cosh\beta\mu_B H)(1 + e^{-\beta\Delta} + e^{-\beta\Delta'}) . \tag{2.22}$$

The electron configurations represented in Eqs. (2.21) and (2.22) are those displayed in Fig. 2. Carrying through the differentiation of $\ln Z$ for these approximate forms of the partition function gives, in zero magnetic field,

$$C_{\text{even}}^{a} / k_B = \int P^{a}(\Delta) 4\beta^2 \Delta^2 \frac{(e^{-\beta\Delta} + e^{-2\beta\Delta} + e^{-3\beta\Delta}) d\Delta}{(1 + 4e^{-\beta\Delta} + e^{-2\beta\Delta})^2} , \tag{2.23}$$

$$C^a_{\rm odd}/k_B = \int P^a(\Delta,\Delta')\beta^2 \frac{[\Delta^2 e^{-\beta\Delta}+\Delta'^2 e^{-\beta\Delta'}+(\Delta-\Delta')^2 e^{-\beta(\Delta+\Delta')}]d\Delta\, d\Delta'}{(1+e^{-\beta\Delta}+e^{-\beta\Delta'})^2}\ , \tag{2.24}$$

$$\chi^a_{\rm even}=8\mu_B^2\beta\int P^a(\Delta)(e^{-\beta\Delta})(1+4e^{-\beta\Delta}+e^{-2\beta\Delta})^{-1}d\Delta\ , \tag{2.25}$$

$$\chi^a_{\rm odd}=\beta\mu_B^2\ ,\ \text{independent of the distribution } a\ . \tag{2.26}$$

Using the distribution functions given in Eqs. (2.11) and (2.12) and numerically integrating the above expressions gives the results tabulated by Denton *et al.* (Denton, Mühlschlegel, and Scalapino, 1973):

$$\begin{aligned} &C^0_{\rm even}/k_B=5.02(k_BT/\delta)\ , \\ &C^0_{\rm odd}/k_B=3.29(k_BT/\delta)\ , \qquad \text{Poisson} \\ &C^1_{\rm even}/k_B=30.2(k_BT/\delta)^2\ , \\ &C^1_{\rm odd}/k_B=17.8(k_BT/\delta)^2\ , \qquad \text{orthogonal} \\ &C^4_{\rm even}/k_B=3.18\times10^4(k_BT/\delta)^5\ , \\ &C^4_{\rm odd}/k_B=1.64\times10^4(k_BT/\delta)^5\ ; \qquad \text{symplectic} \end{aligned} \tag{2.27}$$

$$\begin{aligned} &\chi^0_{\rm even}=3.04\mu_B^2/\delta\ ,\ \text{Poisson} \\ &\chi^1_{\rm even}=7.63\mu_B^2k_BT/\delta^2\ ,\ \text{orthogonal} \\ &\chi^4_{\rm even}=2.02\times10^3\mu_B^2\delta^{-1}(k_BT/\delta)^4,\ \text{symplectic} \\ &\chi_{\rm odd}=\mu_B^2/k_BT\ ,\ \text{all distributions}\ . \end{aligned} \tag{2.28}$$

The indices $a=0$, 1, 2, and 4 correspond to the Poisson, orthogonal, unitary, and symplectic distributions. According to Perenboom *et al.* (1981a) even electron particles are described by the orthogonal ensemble. These results can be compared with those of the bulk, that is to say the high-tempertature limit,

$$\begin{aligned} &C/k_B=\frac{2\pi^2}{3}(k_BT/\delta)-\tfrac{1}{2}\ , \\ &\chi_{\rm Pauli}=2\mu_B^2/\delta\ . \end{aligned} \tag{2.29}$$

The correction term $-k_B/2$ to the heat bulk capacity is of order N^{-1} where N is the number of electrons in the particle and can be usually neglected (Denton *et al.*, 1973). The Pauli susceptibility is expressed in terms of the single spin band density of states δ. However, it is known that the electron-phonon enhancement to the density of states which increases the heat capacity and is included in the plot of δ given in Fig. 1, does not contribute to the Pauli susceptibility. Consequently, one should not use the results from this figure and Eq. (2.29) to determine the susceptibility of the bulk metal.

Since the results given above are only valid for $H\approx0$ we do not show the case of the unitary ensemble, $a=2$, which is applicable to the small-particle problem for large magnetic fields and large spin-orbit interaction. The Poisson distribution, $a=0$, is also expected to be inappropriate (with the exception noted by Kubo, Kawabata, and Kobayashi, 1984 for $H\neq0$) but is shown for illustrative purposes. Consequently we expect that for small magnetic fields the experimental results for the light elements should be described by the orthogonal ensemble, $a=1$. As the spin-orbit interaction becomes more important, such as for the heavier metals, the symplectic ensemble should be used for the odd particles. We shall see shortly that a correct calculation of the magnetic susceptibility in the event of large spin-orbit interaction requires that admixing of the spin-up and spin-down wave functions be taken into account as well as the use of the symplectic or orthogonal distribution of energy levels. Consequently the calculation of Denton *et al.* (1973) is incomplete and the prediction that $\chi_{\rm even}$ goes to zero at low temperatures proportional to $(k_BT/\delta)^4$ or (k_BT/δ) is incorrect. In fact with increasing $H_{\rm so}$ it is found from the theory, presented later, that the magnetic susceptibility at zero temperature tends to the Pauli value. Lastly, in an actual sample we will have a superposition of results from both even and odd particles. This means that the even- and odd-particle results need to be averaged together in some proportion in order to compare with experiment. If it were possible to have particles with precisely an even number of electrons per particle as one might naively expect for an element with even valence then direct comparison between experiment and theory could be made with $C_{\rm even}$ and $\chi_{\rm even}$ using Eqs. (2.27) and (2.28). This may be inappropriate in view of the implications of the tunneling measurements of Cavicchi and Silsbee (1984). On the other hand, Knight shift experiments seem to be sensitive only to even-numbered particles, as will be explained in Sec. III, thus giving a direct means for measuring $\chi_{\rm even}$.

There are no experiments on the heat capacity at this time that show clear evidence of the quantum size effect (QSE). However, direct and indirect measurements of the magnetic susceptibility for a number of elements confirm that a power-law temperature dependence is followed at low temperatures for small particles. These experimental results will be reviewed in detail in Sec. III.

3. The specific heat and susceptibility at all temperatures

In Figs. 3(a) and 3(b), and 4 the calculations of Denton *et al.* (Denton, Mühlschlegel, and Scalapino, 1973) are displayed for the specific heat and susceptibility at low magnetic fields over a wide range of temperature. These results are obtained from an iterative interpolation scheme between, on the one hand, the equal-level spacing approximation which holds at high temperatures, and on the other hand, the low-temperature limit that has just been discussed. From their work it appears that the low-temperature limit applies for $\beta\delta\gtrsim10$. One limitation of this work is that spin-orbit coupling has not been taken into account in an explicit way. The first evidence that

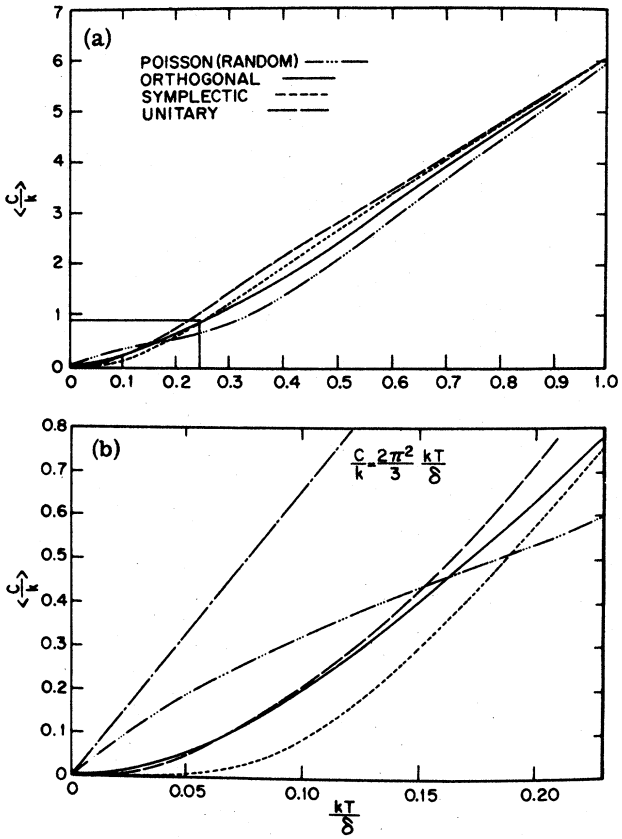

FIG. 3. The small-particle electronic heat capacity as a function of temperature, taken from Denton, Mühlschlegel, and Scalapino (1973): (a) An average of the even and odd particle calculations; (b) the linear heat capacity for the continuum case, shown for comparison (dashed-dotted line). Note the displacement of the high-temperature asymptote by $-k_B/2$ consistent with Eq. (2.29).

this needed to be included followed from experiments performed by Yee and Knight (1975) on copper particles. The interpretation of NMR measurements of the Knight shift indicated that the magnetic susceptibility of even particles does not go to zero as might be expected from the symplectic or orthogonal ensemble predictions given in Eq. (2.28). The extension of the theory to account for spin-orbit effects has been presented by Shiba (1976) and Sone (1977) and will be summarized in a later section.

4. The magnetic susceptibility in a large magnetic field

For the equal-level spacing hypothesis there is a very simple picture for the evolution of the electronic spectrum with increasing magnetic field. Referring to the diagram shown in Fig. 2 and setting $\Delta=\Delta'$, one can easily see that there appears a coincidence of levels as the magnetic field is increased to the point that $\mu_B H=\delta/2$. Then the lowest level is a singlet and all the others are doubly degenerate. This is in contrast to the zero-field case where all the levels are doubly degenerate. This fact means that an odd particle is effectively converted into an even particle in zero field and vice versa at just this value of the magnetic field. Increasing the field again until $\mu_B H=\delta$ leads to another coincidence. Here all levels become doubly degenerate except the lowest two, which are singlets. At this point even and odd particles are reconverted to their original parity. The level structure is now identical to that in zero field, with the exception of the lowest two levels which can be ignored. We expect therefore that the partition function will be perfectly periodic as a function of the field strength. This situation has been studied in detail by Denton, Mühlschlegel, and Scalapino (1973) and is probably only of academic interest given that the aforementioned periodicities depend critically on the unrealistic assumption of equal-level spacing. If one considers a statistical distribution of levels it is possible to show analytically that the field dependence is given in terms of the two-level correlation functions, $R^a(\Delta_1,\Delta_2)$. This has been investigated by Gor'kov and Eliashberg (1965) for the even-particle case and more generally for both cases by Denton, Mühlschlegel, and Scalapino (1973). The two-level correlation function is the probability density for finding two electronic levels in their respective intervals $\Delta_1,\Delta_1+d\Delta_1$ and $\Delta_2,\Delta_2+d\Delta_2$, irrespective of the number of levels in between. This function can depend only on the level separation $\Delta_1-\Delta_2$ and has been calculated by Dyson (1962). Efetov (1982b) has also calculated these simple expressions for $R^a(x)$, $x=\pi(\Delta_1-\Delta_2)/\delta$, for the three interesting statistical distributions ($a=1,2,4$):

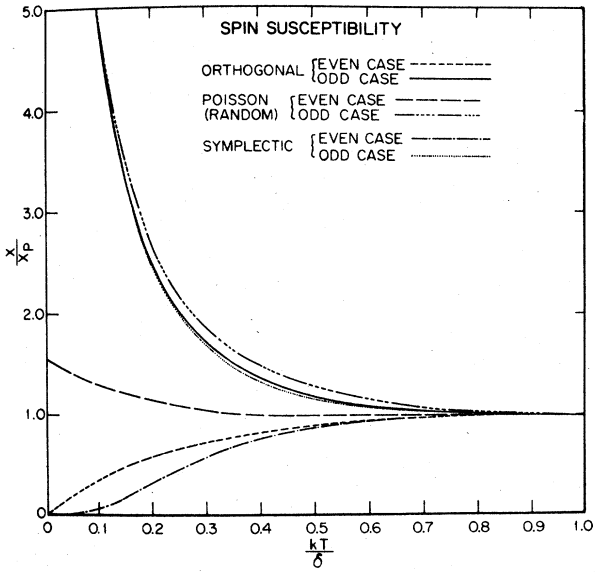

FIG. 4. The small-particle magnetic susceptibility calculated by Denton, Mühlschlegel, and Scalapino (1973). The calculated spin susceptibilities are normalized to the Pauli value taken here to be $\chi_P=2\mu_B^2/\delta$.

$$R^1(x)=1-\frac{\sin^2 x}{x^2}-\frac{d}{dx}\left[\frac{\sin x}{x}\right]\int_1^\infty \frac{\sin xt}{t}dt\ , \tag{2.30}$$

$$R^2(x)=1-\frac{\sin^2 x}{x^2}\ , \tag{2.31}$$

$$R^4(x)=1-\frac{\sin^2 x}{x^2}+\frac{d}{dx}\left[\frac{\sin x}{x}\right]\int_0^1 \frac{\sin xt}{t}dt$$

$$=R^1(x)+\frac{\pi}{2}\frac{d}{dx}\left[\frac{\sin x}{x}\right]\ . \tag{2.32}$$

These functions are graphed in Fig. 5 showing oscillatory behavior for the unitary and symplectic ensemble distributions where level repulsion effects are strongest. The two-level correlation functions are also essential in describing physical phenomena that require a calculation of the transition probability between levels; for example, optical absorption in the infrared or the nuclear spin-lattice relaxation time. In the limit of small x the correlation function $R^a(x)$ approaches the near-neighbor level distribution $P^a(x)$.

Returning to the calculation of the magnetic susceptibility Denton, Mühlschlegel, and Scalapino (1973) find in the low-temperature limit, $k_BT \ll \delta$,

$$\chi_{\rm odd}=\frac{\mu_B^2}{k_BT}\,\mathrm{sech}^2(\beta\mu_BH)\ , \tag{2.33}$$

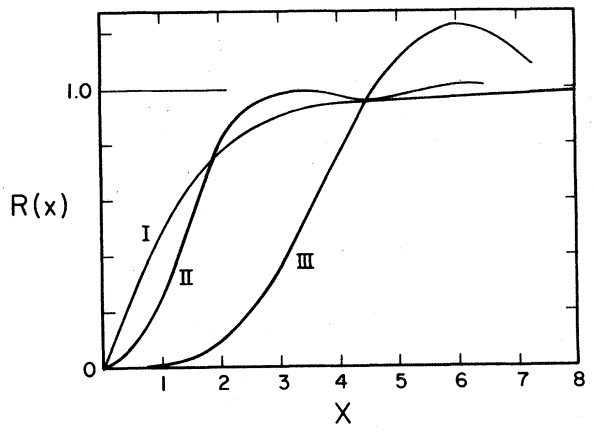

FIG. 5. The two-level correlation function for different statistical ensembles. The correlation functions for orthogonal, unitary, and symplectic ensembles are shown in this figure by the symbols I, II, and III, respectively. The two-level correlation $R(x)$ gives the probability of finding two levels with a spacing $\Delta_1-\Delta_2$ where $x=\pi(\Delta_1-\Delta_2)/\delta$. The expected field dependence of the even-particle susceptibility normalized to the Pauli susceptibility, $\chi_P=2\mu_B^2/\delta$, is equal to the two-level correlation function $R^a(x)$ in the limit $T\to 0$. This function is calculated from the expressions reported by Dyson (1962) and Efetov (1982b) as a function of the parameter $x=2\mu\pi_BH/\delta$.

$$\chi^a_{\rm even}=2(\mu_B)^2/\delta\{R^a(x_0)$$
$$+\pi^2/6[d^2R^a(x)/dx^2]_{x=x_0}(\beta\delta)^{-2}$$
$$+\cdots\}\ , \tag{2.34}$$

where $x_0=2\pi\mu_BH/\delta$ and $\beta^{-1}=k_BT$. The form of Eq. (2.34) is consistent with Eq. (2.18) in the limit of large magnetic fields. The remarkable thing is that the field dependence of the even-particle susceptibility at $T=0$ is a *direct* measure of the two-level correlation function. Other measurements of the level-structure distributions such as optical absorption in the infrared and nuclear spin-lattice relaxation compare experiment with an integral, or average, of the correlation functions and are thereby decidedly less sensitive, particularly so when an average over particle sizes, and hence δ, is taken. Despite this fact there has been no effort to explore the small-particle spectral character through the field dependence of the even-particle susceptibility as might be done, for instance, using the NMR Knight shift technique.

5. The effect of the spin-orbit interaction

The presence of a gap in a continuous electron spectrum, or a sequence of electronic levels mutually isolated, have much in common. The transition to superconductivity is an example of the former from which a considerable amount can be learned and carried over to the problem of discrete levels in a small particle. In particular the electronic susceptibility is expected to reduce to zero for the s-wave pairing theory (usual BCS theory) except when there is a large spin-orbit interaction. The early theoretical work in this area (Anderson, 1959; Ferrell, 1959; Abrikosov and Gor'kov, 1960; Appel, 1965) was found to be in excellent agreement with interpretation of NMR Knight shift measurements on superconductors (Wright, 1967; Hines and Knight, 1971). The Knight shift is usually proportional to the electronic susceptibility. It was this experience that led Yee and Knight (1975) to suggest that the spin-orbit interaction might also be the reason why the Knight shift did not reduce to zero in the limit of low temperatures for their samples of small Cu particles.

Where there are both a large spin-orbit interaction and the presence of crystal lattice imperfections, such as at a particle surface, then a mixture of the spin-up and spin-down electron states must be taken to find the correct eigenstates of the Hamiltonian. Although it was found for a pure singlet state that the electronic susceptibility went smoothly to zero as temperature is reduced, now, with some admixture of spin-up and spin-down states in the ground-state wave function, this will no longer be the case: $\chi_{\rm even}$ will be nonzero at $T=0$. By the same token the Curie law for $\chi_{\rm odd}$ will be reduced in strength. This effect can be calculated in perturbation theory in a weak applied magnetic field where the unperturbed states are a set of Kramers doublets that are eigenstates of the spin-orbit Hamiltonian (Shiba, 1976; Sone, 1977; Buttet, 1981). Both Shiba and Sone have used the equal-level spacing

approximation. In Buttet's (1981) more pedagogical presentation these results are reviewed and in addition he indicates how averages over the appropriate distribution functions might be taken in an approximate way. This is in general a very difficult problem since the spin-orbit matrix elements depend on the level spectrum and should be averaged over self-consistently as well.

In the following we will assume that only a few levels close to the Fermi energy are important as suggested in Fig. 2. These correspond to eigenstates of the Hamiltonian:

$$H = H_0 + H_{so} , \tag{2.35}$$

which we write in the form of Kramers doublets $\{\phi_{n\uparrow}, \phi_{n\downarrow}\}_n$. The symbols $\uparrow$ and $\downarrow$ are to suggest predominantly spin-up and predominantly spin-down, respectively. The $\phi_{n\uparrow}$ and $\phi_{n\downarrow}$ are degenerate and are chosen for each n to diagonalize the z-component spin operator. These properties are

$$\phi_{n\uparrow} = u_n |+\rangle + v_n |-\rangle , \quad \phi_{n\downarrow} = -v_n^* |+\rangle + u_n^* |-\rangle ,$$
$$H\phi_{n\uparrow} = \Delta_n \phi_{n\uparrow} , \quad H\phi_{n\downarrow} = \Delta_n \phi_{n\downarrow} , \tag{2.36}$$
$$R\phi_{n\uparrow} = \phi n_{\downarrow} ,$$

where R is the time-reveral operator and $|+\rangle$, $|-\rangle$ are eigenstates of σ_z. The matrix elements of the Pauli spin operator σ_z are

$$\langle n\uparrow | \sigma_z | n\uparrow \rangle = u_n^2 - v_n^2 , \quad \langle n\downarrow | \sigma_z | n\downarrow \rangle = -(u_n^2 - v_n^2) ,$$
$$\langle n\uparrow | \sigma_z | m\uparrow \rangle \neq 0 , \quad \langle n\uparrow | \sigma_z | n\downarrow \rangle = 0 , \tag{2.37}$$
$$\langle n\downarrow | \sigma_z | m\downarrow \rangle \neq 0 .$$

Now introduce the Zeeman Hamiltonian as a perturbation,

$$H_z = \sigma_z \mu_B H .$$

H is the external field directed along the z axis and the g factor is taken to be 2.0. Indicating the perturbed energies as $\underline{\Delta}$ one finds in second order,

$$\underline{\Delta}_{m\uparrow} = \Delta_m + \mu_B H (u_m^2 - v_m^2) - (\mu_B H)^2 \sum_{n \neq m} \frac{|\langle n\uparrow | \sigma_z | m\uparrow \rangle|^2 + |\langle n\downarrow | \sigma_z | m\uparrow \rangle|^2}{\Delta_n - \Delta_m} ,$$
$$\underline{\Delta}_{m\downarrow} = \Delta_m - \mu_B H (u_m^2 - v_m^2) - (\mu_B H)^2 \sum_{n \neq m} \frac{|\langle n\uparrow | \sigma_z | m\downarrow \rangle|^2 + |\langle n\downarrow | \sigma_z | m\downarrow \rangle|^2}{\Delta_n - \Delta_m} . \tag{2.38}$$

The second-order terms are similar to what one expects for Van Vleck paramagnetism. The partition function can be written in terms of these perturbed energies for the even and odd cases consistent with the low-temperature truncation used in Eqs. (2.21) and (2.22) from which both heat capacity and susceptibility may be calculated. However this can be viewed in a slightly simpler way. Sone has shown (Sone, 1977) that the second-order terms in Eq. (2.38) produce an approximate uniform shift in energy of each state m near the Fermi energy, by an amount

$$\mu_B^2 H^2 [1 - \overline{(u_m^2 - v_m^2)^2}] \delta^{-1} ,$$

giving a contribution to χ_{even} of

$$2\mu_B^2 [1 - \overline{(u_m^2 - v_m^2)^2}] \delta^{-1} .$$

The overbar indicates an average over states near the Fermi energy. From Eq. (2.38) it can be seen that the effect of the first-order terms is just to renormalize the effective magnetic moment by an amount $(u_m^2 - v_m^2)$, which can also be represented by its average and expressed in terms of a phenomenological parameter ρ,

$$\overline{(u_m^2 - v_m^2)} \approx \overline{(u_m^2 - v_m^2)} = (1 - \rho) . \tag{2.39}$$

The physical interpretation of ρ is that it is a measure of the average strength of the spin-orbit interaction since the relative amount of spin-up compared to spin-down in each of the states ϕ_n is given by the expectation value of σ_z,

$$\langle n\uparrow | \sigma_z | n\uparrow \rangle = u_n^2 - v_n^2 \approx 1 - \rho ,$$
$$\langle n\downarrow | \sigma_z | n\downarrow \rangle = -(u_n^2 - v_n^2) \approx -1 + \rho . \tag{2.40}$$

Then for the simple model sketched in Fig. 2 the susceptibility of a single even-electron particle becomes

$$\chi_{even} = 8\mu_B^2 \beta (1-\rho)^2 e^{-\beta\Delta} / (1 + e^{-2\beta\Delta} + 4e^{-\beta\Delta}) + 2\mu_B^2 (2\rho - \rho^2) \delta^{-1} . \tag{2.41}$$

The above was deduced with the assumption that the magnetic field would be small but no constraint on the magnitude of the spin-orbit interaction was imposed. Averaging over the orthogonal and symplectic level distributions gives, in the low-temperature limit,

$$\chi^1_{even} = 7.63\mu_B^2 \delta^{-1} (k_B T/\delta)(1-\rho)^2 + 2\mu_B^2 (2\rho - \rho^2)\delta^{-1} , \quad \text{orthogonal} , \ T \to 0 ,$$
$$\chi^4_{even} = 2.02 \times 10^3 \mu_B^2 \delta^{-1} (k_B T/\delta)^4 (1-\rho)^2 + 2\mu_B^2 (2\rho - \rho^2)\delta^{-1} , \quad \text{symplectic} , \ T \to 0 . \tag{2.42}$$

It will be noticed here that the first term in each case is the familiar form of the susceptibility obtained earlier, Eq. (2.28), without the spin-orbit interaction, only now with the magnetic moment reduced by a factor of $1-\rho$.

From the definition of ρ it is qualitatively evident that in the absence of H_{so} it will be zero and that for very large spin-orbit interaction ρ will be equal to 1. Consequently the first-order perturbation term vanishes for large spin-orbit coupling independent of the temperature. This leaves the temperature-independent second term which is just χ_{Pauli} for $\rho=1$. In this case the quantum size effect in the magnetic susceptibility for even particles is washed out. At intermediate values of ρ we find that χ_{even} is nonzero at $T=0$ in contrast with the results derived by Denton *et al.* (Denton, Mühschlegel, and Scalapino, 1973).

Although the results for both orthogonal and symplectic distributions are given for the susceptibility of particles with even numbers of electrons in Eq. (2.42), nonetheless, it is expected that only the orthogonal distribution is appropriate for the even case. This situation was discussed earlier in Sec. II.B.

Now we turn to the calculation of χ_{odd} following a similar procedure as above. In the low-temperature limit we find that the diagonal matrix elements in Eq. (2.38) reduce the effective magnetic moment weakening the Curie constant obtained previously in Eq. (2.28). In addition a constant susceptibility must be added coming from the off-diagonal contributions. This takes the form

$$\chi_{\text{odd}}=\mu_B^2(1-\rho)^2/k_BT+2\mu_B^2(2\rho-\rho^2)\delta^{-1}\ ,\quad T\to 0\ , \tag{2.43}$$

and can be compared with the earlier results without the spin-orbit interaction of Eq. (2.28). Again, in the limit of very strong spin-orbit interaction $\rho=1$, and we find that the susceptibility is independent of even or odd considerations and is equal to χ_{Pauli}.

In the equal-level spacing approximation the susceptibility differs from that of Eq. (2.42) in that the first term would have an exponential dependence on temperature, proportional to $\exp(-\delta/k_BT)$. Such approximate calculations were reported by Sone (1977) and Shiba (1976) and the results of Sone are shown in Fig. 6. The heat capacity has not been explicitly discussed in the literature for the case in which spin-orbit effects are included. Nonetheless, it is quite clear from Eq. (2.33) that in zero magnetic field in the low-temperature limit there should be no difference from that given previously in Eq. (2.27) where H_{so} was taken to be negligible.

It remains to discuss briefly what might be the relation between the phenomenological parameter ρ and the spin-orbit interaction. Apart from the general comments that were made earlier that strong spin-orbit interaction implies that $\rho=1$ and that in the other extreme it is zero, it is possible to deduce approximate expressions relating ρ to average matrix elements,

$$\overline{|\langle H_{so}\rangle|^2}\ .$$

Following Sone (1977) a perturbation expansion for weak spin-orbit coupling can be made. Let $A_{n\uparrow}$ and $A_{n\downarrow}$ represent the unperturbed eigenstates of H_0, Eq. (2.35). We have in first order

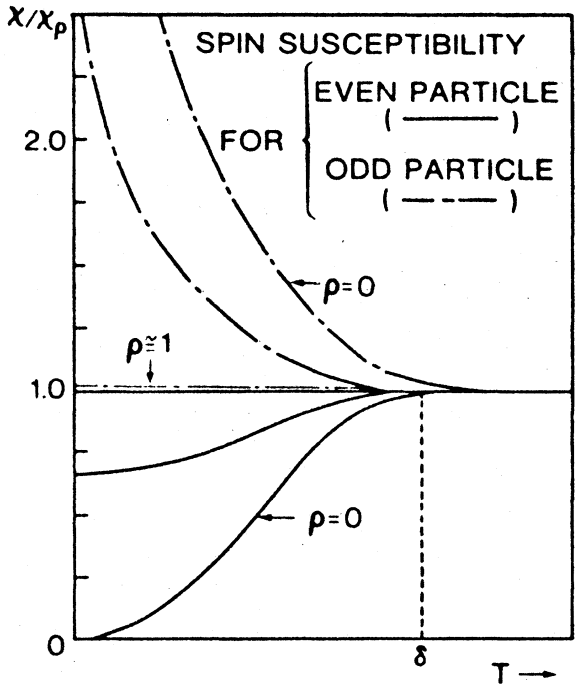

FIG. 6. The spin susceptibility, including the effect of spin-orbit interaction, is shown as a function of the temperature as calculated by Sone (1977) in an equal-level spacing approximation. Allowing for a statistical distribution in the energy levels would replace the exponential low-temperature behavior for even particles with a power law as described by Eq. (2.42). It is thought that this power law should be linear in the temperature. Various values of Sone's spin-orbit coupling parameter ρ are used as defined in the text. The temperature at which $\delta/k_BT=1$ is indicated.

$$\phi_{n\uparrow}=A_{n\uparrow}+\sum_{m\neq n}\frac{\langle A_{m\uparrow}|H_{so}|A_{n\uparrow}\rangle A_{m\uparrow}}{\Delta_n-\Delta_m}+\frac{\langle A_{m\downarrow}|H_{so}|A_{n\uparrow}\rangle A_{m\downarrow}}{\Delta_n-\Delta_m}$$

with a similar expression for $\phi_{n\downarrow}$. The perturbed states ϕ_n are the same as those introduced before, Eq. (2.36), except that they are not normalized in the perturbation expansion here. In order to find an expression for ρ we need to evaluate the matrix elements of σ_z for these perturbed states [see Eq. (2.37)], keeping in mind that $\sigma_z A_{n\uparrow}=A_{n\uparrow}$, $\sigma_z A_{n\downarrow}=-A_{n\downarrow}$,

$$\langle\phi_{n\uparrow}|\sigma_z|\phi_{n\uparrow}\rangle=1+\sum_{m\neq n}\frac{|\langle A_{m\uparrow}|H_{so}|A_{n\uparrow}\rangle|^2}{(\Delta_n-\Delta_m)^2}-\frac{|\langle A_{m\downarrow}|H_{so}|A_{n\uparrow}\rangle|^2}{(\Delta_n-\Delta_m)^2}$$

and

$$\langle\phi_{n\uparrow}|\phi_{n\uparrow}\rangle=1+\sum_{m\neq n}\frac{|\langle A_{m\uparrow}|H_{\rm so}|A_{n\uparrow}\rangle|^2}{(\Delta_n-\Delta_m)^2}+\frac{|\langle A_{m\downarrow}|H_{\rm so}|A_{n\uparrow}\rangle|^2}{(\Delta_n-\Delta_m)^2}$$

Hence we get for the expectation of σ_z,

$$\frac{\langle\phi_{n\uparrow}|\sigma_z|\phi_{n\uparrow}\rangle}{\langle\phi_{n\uparrow}|\phi_{n\uparrow}\rangle}\approx 1-2\sum_{m\neq n}\frac{|\langle A_{m\downarrow}|H_{\rm so}|A_{n\uparrow}\rangle|^2}{(\Delta_n-\Delta_m)^2}$$

$$=u_n^2-v_n^2 .$$

And similarily,

$$\frac{\langle\phi_{n\downarrow}|\sigma_z|\phi_{n\downarrow}\rangle}{\langle\phi_{d\uparrow}|\phi_{n\downarrow}\rangle}\approx -1+2\sum_{m\neq n}\frac{|\langle A_{m\uparrow}|H_{\rm so}|A_{n\downarrow}\rangle|^2}{(\Delta_n-\Delta_m)^2}$$

$$=-(u_n^2-v_n^2) .$$

Averaging this over the states near the Fermi energy in the equal-level spacing approximation and comparing with Eq. (2.39) gives

$$\rho=2\sum_{m\neq n}\frac{\overline{|\langle A_{M\downarrow}|H_{\rm so}|A_{n\uparrow}\rangle|^2}}{(\Delta_n-\Delta_m)^2}\approx\frac{2\pi^2}{3\delta^2}\overline{|\langle H_{\rm so}\rangle|^2} . \tag{2.44}$$

A number of theoretical efforts have been directed at the problem of determining the importance of the spin-orbit interaction for small-size particles. Kawabata (1970) has calculated the effect of discreteness of the electronic spectrum on electron spin resonance (ESR). He has defined an electron relaxation time τ_s in terms of the average matrix elements above,

$$\frac{1}{\tau_s}=\frac{2\pi}{\hbar\delta}\overline{|\langle H_{\rm so}\rangle|^2} , \tag{2.45}$$

such that the Elliott relation (Elliott, 1954; Dyson, 1955) is satisfied,

$$\frac{1}{\tau_s}=\frac{1}{\tau_r}(\Delta g_\infty)^2 , \tag{2.46}$$

and where the particle size is sufficiently small that the perturbation expansion in $H_{\rm so}$ is valid. In a small particle the "resistivity" relaxation time τ_r is given by d/v_F, in terms of the particle diameter and the Fermi velocity, and Δg_∞ is the bulk ESR g shift. Combining Eqs. (2.44), (2.45), and (2.46) we have

$$2\rho\approx h v_F(\Delta g_\infty)^2/(3\delta d) \quad \text{for small } d . \tag{2.47}$$

This expression is similar to that for a spin-orbit parameter defined by Abrikosov and Gor'kov (1960) or Shiba (1976). That given in Eq. (2.47), however, is not a definition but only the limiting case for small spin-orbit coupling, $\langle H_{\rm so}\rangle \ll \delta$. In particular, Sone's parameter varies between the limits of zero and one, while the others vary between zero and infinity. For small values they are essentially the same except for numerical factors of order one. A comparison of these different parameters is presented later in Sec. III, Eq. (3.16).

In bulk metals the g shift is large for materials that have significant spin-orbit interaction and is generally used as a measure for the importance of spin-orbit effects (Elliott, 1954). The g shift in small particles can be expected to differ from this owing to quantum effects (Kawabata, 1970; Buttet, Car, and Myles, 1982), a topic that is discussed further in Sec. III.C. Estimates from Kawabata's semiclassical theory (1970) for the magnitude of the average matrix elements are in excellent agreement with orthogonalized-plane-wave (OPW) calculations of Buttet, Car, and Myles (1982) for a cube of sodium. This comparison is shown in Fig. 7, from which it is clear that the average matrix element of $H_{\rm so}$ decreases with increasing particle diameter as d^{-2}. Since δ varies as d^{-3} we can see from Eqs. (2.42) and (2.44) that the size dependence of the residual even-particle susceptibility is given as follows:

$$\chi_{\rm even}/\chi_{\rm Pauli}=2\rho-\rho^2$$

$$\approx 4\pi^2\frac{\overline{|\langle H_{\rm so}\rangle|^2}}{3\delta^2}\propto d^2 \tag{2.48}$$

for $T\to 0$ and small d. The restriction on particle size in Eqs. (2.47) and (2.48) comes from the requirement that the perturbation expansion in $H_{\rm so}$ remains valid. NMR Knight shift measurements can be interpreted directly in terms of the susceptibility ratio given above. Consequently, this is a prediction which can be tested by experiment and will be discussed in Sec. III.B. An estimate of the g

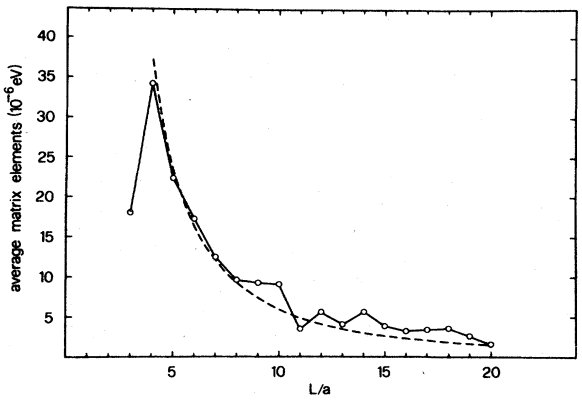

FIG. 7. Average spin-orbit matrix elements $H_{\rm so}^2$ calculated with an orthogonalized standing-wave technique (OSW) for a cube of sodium by Buttet, Car, and Myles (1982) compared with the calculation of Kawabata (1970), shown as a dashed line. In both cases it appears that the matrix elements, averaged over states near the Fermi energy, increase with decreasing particle size as the inverse square of the particle dimension L. This is expressed in units of the lattice constant a, for sodium.

shift, Δg_∞, from the low-temperature residual Knight shift measurements can be made using Eqs. (2.47) and (2.48) and this can be compared with ESR data. From the above we find that this can be expressed as

$$\Delta g_\infty \approx \frac{6\delta d}{h v_F}\{1-[1-\chi_{\text{even}}(0)/\chi_{\text{Pauli}}]^{1/2}\} . \quad (2.49)$$

6. The effect of a particle-size distribution

Until this point we have assumed that each particle in our sample of particles has an identical average level spacing δ. Small variations in the shape or surface roughness from particle to particle can be expected to give rise to a different electronic level spectrum for each case. In a realistic sample the large variation in the geometry of particles must also include a distribution in the average level spacing. In the literature this is qualitatively referred to as *the size distribution* and in principle can be directly related to a measured physical size distribution with the caveat that the shapes remain approximately the same from one particle to another. One can see from Eqs. (2.23)—(2.28) that the heat capacity and susceptibility at low temperatures can be expressed as a series expansion in $k_B T$ for which the coefficients are functions of δ. Although only the lowest-order terms are given explicitly in Eqs. (2.27) and (2.28), it is nonetheless clear that the effect of a distribution in δ can be found by averaging each term over the appropriate measured size distribution. Let us further assume that the particles are of the same approximately *spherical* shape for which $\delta \propto d^{-3}$. Then for the orthogonal and symplectic statistical ensembles of energy-level spacings, the lowest-order temperature dependence for both the heat capacity and the susceptibility will be proportional to $\overline{d^6}$ and $\overline{d^{15}}$, respectively. The overbars refer to the size distribution average. Although the algebraic form of the dependence on temperature will not be affected by the size distribution, the fact that such high moments must be computed from size measurements indicates that a meaningful quantitative comparison of theory and experiment will be difficult to achieve, particularly for the symplectic case.

In most experiments the quantum effects are sought through the direct measurement of the thermodynamic parameters for which the above discussion holds. These measurements are intensive functions of the number of particles. However, this is not the case for the NMR Knight shift method. Here one relies on an indirect probe, that of the nuclei for which the signal intensity is proportional to the number of atoms and not the number of particles. This approach will tend to weight even more highly the larger size particles which will dominate the NMR spectrum reducing the apparent quantum size effects on the absorption frequency. Consequently, one should be cautious of using the peak in the particle-size distribution as an indication of the temperature at which one can expect onset of quantum effects.

To address this question quantitatively we extend the above assumptions concerning the geometry of a typical small-particle sample to include the postulate that the particle-size distribution is log-normal (Granqvist and Buhrman, 1976a),

$$\frac{dn}{N} = \frac{1}{\sqrt{2\pi}\ln\sigma}\exp\left[-\frac{\ln^2(d/d_0)}{2\ln^2\sigma}\right] d\ln(d/d_0) , \quad (2.50)$$

where dn/N is the fraction of particles in the interval $\ln(d/d_0)$, $\ln(d/d_0)+d\ln(d/d_0)$; d_0 is the peak diameter of the distribution; and σ is a parameter that determines the width of the distribution. For measured particle samples it has been found that it may be difficult to produce a narrower distribution than $\sigma=1.3$ and that $\sigma=1.5$ is more typical of inert gas evaporation methods. The moments of the distribution are simple Gaussian integrals,

$$\overline{d^m}/(d_0)^m = \sigma^{(m^2/2)\ln\sigma} . \quad (2.51)$$

The heat capacity and susceptibility have the same leading-order dependence on δ at low temperatures as was noted previously. For the various statistical ensembles this means the leading-order temperature coefficients are proportional to the mth moment of the size distribution for which particular cases are listed in Table III. The last two columns give the average particle diameters to which an experiment is sensitive, expressed as a ratio to the peak diameter in the size distribution. For reasonable size distributions this can be as much as 3.5 times the peak diameter in the size distribution. It is this average diameter that should be used to estimate the temperature range for onset of quantum effects in the Kubo theory using Eq. (2.4). Table III should serve only as a rough guide where a more reliable determination of the average particle sizes and the leading-order coefficients of the low-temperature expansion of the thermodynamic functions can be obtained directly from measured particle-size distributions.

III. MEASUREMENTS OF THE ELECTRONIC SUSCEPTIBILITY

The electronic magnetic susceptibility is an experimental parameter which can be expected to show dramatic effects from discreteness of the electronic level spectrum. The low-temperature susceptibility for even particles reduces with decreasing temperature by an amount of the order of the Pauli susceptibility. The odd-particle susceptibility, on the other hand, diverges according to a Curie law. Assuming that the number of even- and the number of odd-electron-numbered particles in a sample are about the same, then the total measured susceptibility will be dominated by the odd-particle effects, if they are indeed present. If the number of conduction electrons per atom is strictly even, then the magnetic susceptibility will exhibit only even effects. Ideally such is the case for a number of elements with even valence Mg, Be, Pt, Hg, Pb, to name a few, provided there is no electron transfer from the particle to its host matrix. It might then seem that the most obvious experiment to try would be to perform direct magnetization measurements on a series of small-particle samples of different sizes as a function of tem-

TABLE III. High-order moments of a log-normal particle size distribution are important in determining the low-temperature leading-order behavior of the magnetic susceptibility and heat capacity. If the peak size in the distribution is d_0 then the coefficients of the first-order terms in a low-temperature expansion of the thermodynamic functions, given in Eqs. (2.28) and (2.29), can be expressed in terms of a value of the average level spacing δ evaluated for a particle size that is substantially larger than d_0 by a factor given in the last two columns of the table. This depends on the width parameter σ of the size distribution. For example, for a reasonable width parameter $\sigma=1.5$ one finds that the thermodynamic measurements will be sensitive to an average particle size that can be 3.5 times larger than the peak size in the distribution.

m	Distribution	$\overline{d^m}/d_0^m$		$(\overline{d^m}/d_0^m)^{1/m}$	
		$\sigma=1.3$	$\sigma=1.5$	$\sigma=1.3$	$\sigma=1.5$
3	Poisson	1.36	2.09	1.11	1.28
6	orthogonal	3.44	1.93	1.23	1.64
15	symplectic	2.31×10^3	1.10×10^8	1.67	3.43

perature in order to identify the dominant odd-particle effect Eqs. (2.28) or (2.43). However, this is not so straightforward. If 50% of the particles are odd, we see that there will be only $\frac{1}{2}\mu_B$ per particle and the expected signal will therefore be quite small. Combining Eqs. (2.4) and (2.28), this is of the order $\tilde{\chi}\approx 6\times10^{-6} f\delta/k_BT$ for a volume filling factor of metal, f, and $\tilde{\chi}=\chi/V$. For supported metal particles ($f\approx10^{-2}$) this requires the measurement of susceptibilities with a resolution of $\lesssim10^{-8}$ emu/cm^3. A number of techniques are generally available with this level of sensitivity. The problem however, is to reduce the unwanted background signals from the matrix or particle support, and from the particle surface, to below this value. Methods that measure the total magnetization of the sample will be referred to here as direct magnetization techniques: Faraday balance, SQUID magnetometer, etc. In applying these direct methods to search for small-particle effects a number of interesting surface phenomena have been reported. Unfortunately, there is not much compelling evidence in favor of the quantum size effect from direct static magnetization measurements. One exception is the recent Faraday balance measurements of Kimura, Bandow, and Sako (1985) on 20-Å Mg particles showing the even-particle effect. These direct methods and the corresponding results will be discussed in the next section. Resonant methods employing either electron spin resonance or interpretation of nuclear magnetic resonance spectra will be reviewed subsequently. We note parenthetically at this point that, in contrast to the majority of the magnetization measurements, the resonance data clearly indicate the existence of quantum size effects.

A. Direct magnetization measurements

1. Interpretative phenomenology

Recall that the dominant temperature-dependent behavior expected from the quantum size effect regime for odd-electron particles is approximately that of a Curie law plus a temperature-independent Pauli susceptibility. We should keep in mind that typical small-particle samples have the fraction of surface atoms compared to the total number of atoms approaching unity. Consequently surface effects can become rather important. At the surface of a metal both the physical and electronic structure may be significantly altered from that of the bulk metal. There may also be chemical effects associated with oxides, adsorbed gases, or impurities. In addition the metal particle susceptibility may be masked by that of the support matrix, particularly if the metal concentration relative to the matrix is small. Most of the reported work takes advantage of the measurement of control samples or other subtraction methods to allow removal of the matrix susceptibility and interpretation of the results in terms of the metal particle sample itself. Nonetheless considerable care must be exercised in order to unravel contributions to the susceptibility from different sources. As a reasonably general phenomenological model that can account for local moments (impurities, surface states) and odd-electron quantum effects, we write the susceptibility from either the surface or from the interior of the metal particle in the form

$$\tilde{\chi}=\tilde{\chi}_b(T)+(\mu_0\mu_B)^2 n/3k_B(T-\theta)\ . \tag{3.1}$$

This describes the usual volume susceptibility, an intensive unitless quantity (emu/cm^3) as distinct from the total susceptibility previously used in Eqs. (2.28) and (2.29) having the units of volume and for which the tilde is omitted, $\tilde{\chi}=\chi/V$. A background contribution, $\tilde{\chi}_b(T)$, can be assumed for the simplest case to be temperature independent, measured without ambiguity at high temperature, $\tilde{\chi}_b(\infty)$. A local moment term is included having a Curie-Weiss temperature dependence with a magnetic moment expressed as μ_0 Bohr magnetons, and a Curie-Weiss temperature θ. The density of moments is n. To distinguish between contributions in the form of Eq. (3.1) from either the surface or from the particle interior, we will use the subscripts s and v, respectively.

Although Eq. (3.1) is not a specific prediction of the odd-electron particle quantum size effect it can serve as a

rough guide for interpretation of experiment. The odd-particle susceptibility corresponds to a local moment having behavior given by the second term with $\theta=0$. For measurements in very large magnetic fields at low temperatures saturation in the magnetization per unit volume should be observable for these local moments,

$$M=n\mu_0\mu_B\tanh(\mu_0\mu_B H/k_B T) \tag{3.2}$$

for which the leading-order behavior is the Curie law, Eq. (3.1), modified to include the effects of interaction between the moments in the form of the Curie-Weiss law. Standard treatments of this subject can be found in introductory solid state physics texts (Ashcroft and Mermin, 1976; Kittel, 1976). For a free-electronic spin, $\mu_0^2=3$, such as one might expect for an odd-electron particle at low temperatures, saturation is observable in a field of 50 kOe at a temperature of $T\approx 6$ K where the argument of the tanh function in Eq. (3.2) is equal to 1. Measurements as a function of magnetic field are necessary in order to infer the magnitude of μ_0. Otherwise the measurements in low field represented by the Curie-Weiss form have the ambiguity that only the product $\mu_0^2 n$ can be determined, complicating the interpretation of the measured susceptibility. A convenient normalized form for the susceptibility with contributions from both surface and bulk can be expressed as

$$\frac{\tilde{\chi}}{\tilde{\chi}_{bv}(\infty)}=\left[\frac{\tilde{\chi}_{bs}(\infty)}{\tilde{\chi}_{bv}(\infty)}+\frac{T_s}{T-\theta_s}\right]f_s + \left[1+\frac{T_v}{T-\theta_v}\right](1-f_s)\,, \tag{3.3}$$

where

$$T_s=\frac{(\mu_{0s}\mu_B)^2}{3k_B\tilde{\chi}_{bv}(\infty)}n_s\,,\quad T_v=\frac{(\mu_{0v}\mu_B)^2}{3k_B\tilde{\chi}_{bv}(\infty)}n_v\,, \tag{3.4}$$

and the fraction of atoms at the surface is f_s. The assumption that there is only the superposition of a Curie-Weiss temperature dependence and a temperature-independent part in each term in Eq. (3.3) is overly simplistic, but can represent most experimental observations in small particles other than the even-electron quantum effect. The bulk metal can be expected to have a temperature-independent Langevin diamagnetic susceptibility (frequently referred to as the Larmor or orbital susceptibility, $\tilde{\chi}_{\rm dia}$); a temperature-independent paramagnetic susceptibility the Van Vleck contribution, $\tilde{\chi}_{VV}$; and the itinerant electron susceptibility, $\tilde{\chi}_{\rm Pauli}$. The latter is essentially temperature independent except for certain transition metals, notably Pt and Pd, for which the temperature variations are less than 30% for $0\le T\le 300$ K. Writing the metal particle susceptibility as in Eq. (3.3), we are expressing all of these terms by $\tilde{\chi}_{bv}(\infty)$. Further details, including some discussion of individual metallic elements, are given by Kittel (1976) and Ashcroft and Mermin (1976).

In order to identify different contributions to the magnetic susceptibility, it is imperative to separate surface and volume effects. In Eq. (3.3), the surface contribution (i.e., the first term) depends on particle size through the factor $f_s\propto d^{-1}$. In the second term, the factor $(1-f_s)$ depends only weakly on size for larger particles, $d\gtrsim 50$ Å; however, T_v can vary as d^{-3} owing to odd particle quantum effects discussed in Sec. II. The case of quantum effects can be summarized as

$$\mu_{0v}=3^{1/2}(1-\rho),\quad \theta_v=0\,,$$
$$n_v=\text{odd-electron particle density}\,. \tag{3.5}$$

Using Eq. (2.4) for silver, assuming in this case 50% of the particles are odd, gives $n_v=f(\delta/k_B)3.7\times 10^{17}\ \text{K}^{-1}\text{cm}^{-3}$ which varies as d^{-3}. For a clear identification of the quantum size effects in an odd valence element, it is necessary to show that there is a Curie law contribution to the low-temperature susceptibility and that the Curie constant, which is proportional to n_v, varies as d^{-3}. As mentioned before, this has not been satisfactorily demonstrated so far for any particle sample investigated by direct magnetic susceptibility techniques. If there are impurities with local moments uniformly distributed throughout the sample then no size dependence of χ should be observed. A Curie or Curie-Weiss law temperature dependence may have a number of explanations. Measurements of the particle-size dependence of the susceptibility can help to indicate the nature of the observed local moments. An inverse dependence of the Curie constant on d suggests a surface effect. Size-independent results suggest a bulk impurity problem. If the Curie constant has a dependence d^{-3}, then this is consistent with a quantum effect.

For even-electron-number particles one expects that on reducing the temperature the magnetic susceptibility will remain constant until $k_B T\ll\delta$. Substantial reduction of the magnetic susceptibility should be observed as the temperature is reduced further as indicated in Figs. 4 and 6. This effect is not represented by Eqs. (3.1) and (3.3), however, when it is observed it should be relatively unambiguous and not easily confused with local moment and impurity contributions as is the case with the odd-electron susceptibility.

Before discussing the individual experiments, it is worthwhile commenting on the significance of $\theta_v=0$ for the quantum size effect, Eq. (3.5). At sufficiently low temperatures the coupling between odd particles can produce magnetic ordering. This point has been discussed in the context of a Hubbard model by Kawabata (1977) while presenting calculations of the effects of electron tunneling between particles on nuclear spin-lattice relaxation. He estimates that the coupling should be antiferromagnetic with a possible magnetic transition at $T_c\approx 0.2$ K for $d=100$ Å.

2. Measurements of the susceptibility

The investigations of metallic powders by direct magnetization measurements are discussed in this section in

the following order: Cu, In, Pt, Pd, V, Os, Be, and Mg. This arrangement is chronological in terms of the first reported studies of each element.

One of the earliest low-temperature susceptibility measurements was performed by Kobayashi, Takahashi, and Sasaki (1972). Two samples of small Cu particles were prepared with mean size 40 and 90 Å by inert gas evaporation methods. Cu NMR and SQUID susceptibility measurements were performed both indicating existence of a strong Curie or Curie-Weiss temperature dependence. The size of the Curie constant was estimated to be of order $10\mu_B$ per particle. They interpreted these results as being most likely an effect of Cu oxide.

A technique for embedding small indium particles in a paraffin support was developed by Meier and Wyder (1973). They evaporated In into a flowing He stream that was passed through molten paraffin producing approximately 50-Å-diam spherical particles. Initial measurements using a vibrating magnetometer in the range 1.5—4.2 K with applied fields up to 50 kOe showed the presence of a large diamagnetic susceptibility plus an easily saturable paramagnetic contribution. The saturation fields were inconsistent with Eq. (3.2), leading them to suggest that orbital quantum magnetic effects (size effects on $\tilde{\chi}_{\rm dia}$) might account for the results. Further theoretical interpretation of this result was made by van Gelder (1974). Subsequently, Perenboom *et al.* (1981b) improved on these techniques. They studied many samples with a wide range of mean sizes, and most importantly, investigated blank paraffin samples. As a consequence of the work, both diamagnetic and paramagnetic susceptibilities ($\approx 10^3\mu_B$ per particle in the latter case) could be associated with just the paraffin matrix which they speculated might include some molecular oxygen. No evidence for quantum effects were claimed.

Marzke, Glaunsinger, and Bayard (1976) fabricated quite uniform platinum particles of mean size 22 Å using chemical reduction of H_2PtCl_6 followed by embedding in a gelatin matrix. Measurements from 1.5 to 200 K were performed in fields of 2—13 kOe using a Faraday balance. A Curie law behavior was observed consistent with Eq. (3.1) with about $2\mu_B$ per particle. These measurements were initially interpreted in terms of the quantum size effect. However, later work by Marzke and Glaunsinger (1984) and Marzke *et al.* (1983) expanded on this effort by varying the particle size and preparation conditions. Some of this data is shown in Fig. 8. They found that the Curie constant was proportional to d^{-1} strongly suggesting that the observed behavior, proportional to f_s, could be identified with a surface effect. In both investigations it was found that the high-temperature susceptibility $\tilde{\chi}_{bs}(\infty)/\tilde{\chi}_{bv}(\infty)$ was less than 1, a point that might be clarified by an investigation of the size dependence of the high-temperature susceptibility. In their later work Marzke and co-workers (Marzke *et al.*, 1983; Marzke and Glaunsinger, 1984) found a definite antiferromagnetic tendency with a Curie-Weiss temperature $\theta_s = -5$ K. Furthermore, the Curie constants appeared to be much larger than previously reported (Marzke *et al.*, 1976) and, of order 7—50 μ_B per particle.

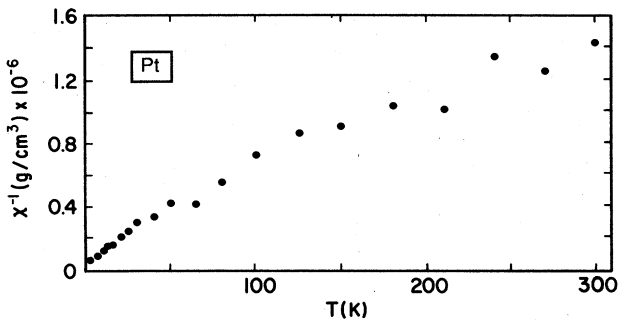

FIG. 8. The inverse susceptibility of a Pt particle sample of average diameter 22 Å is shown as a function of the temperature reported by Marzke and Glaunsinger (1984). Note that deviations from a Curie-Weiss law are apparent; that a negative intercept at $\chi^{-1}=0$ suggests antiferromagnetic coupling; and that the high-temperature susceptibility is less than that of the bulk which is about 0.9 on the vertical axis.

Yu and Halperin (1981b) and Yu (1980) have measured the susceptibility of Pt powder with nominally 33 Å diameter made by H_2 reduction of H_2PtCl_6 impregnated into a silica support. Measurements with a SQUID ac susceptometer were performed from 20 mK to 0.6 K in a steady field of 1 Oe. Different sizes were not investigated and so it is not possible to determine whether this work reflects a surface or volume effect. Nonetheless, clear evidence for a Curie-Weiss law was obtained with approximately $1\mu_B$ per particle and a Curie temperature $\theta = -0.07$ K. Below this temperature, distinct saturation of the susceptibility deviating from the Curie-Weiss law was observed. Without a determination of the size dependence of the Curie constant, however, it is not possible to relate this work to the quantum size effect.

A number of magnetic measurements have been reported on transition-metal-supported heterogeneous catalysts. In general, these samples suffer from the point of view that background susceptibility measurements for the matrix are not easy to perform and that the concentration of metal particles is very dilute. For instance, Bylina, Evidokimov, and Kobozev (1962) used Faraday balance techniques to measure the magnetization of several Pt catalysts over a range of temperature from 80 to 300 K. It was recognized that the existence of iron, particularly in the support material (SiO_2) could seriously affect this sort of measurement. It was claimed that this effect could be identified in blank experiments in high fields and subtracted from the measurement. They found the qualitative result that, the smaller the particle size, the larger the susceptibility. Critical comments relevant to this class of materials and preparation techniques are presented by Ladas, Dalla Betta, and Boudart (1978) whose work with Pd catalysts will be discussed next.

A unique differential susceptibility technique has been employed by Ladas, Dalla Betta, and Boudart (1978), applicable to the measurement of the susceptibility of particles of Pd. They used SiO_2-supported Pd catalysts sam-

ples made by standard techniques including hydrogen reduction of $PdCl_2$ or $Pd(NH_3)_4Cl_2$ following impregnation. Special care was exercised to clean the support using HCl. Magnetic measurements were performed with a Faraday balance on particles in the range 20—100 Å. Ladas *et al.* have made use of the fact that Pd particles in an environment of H_2 at moderate pressure absorb hydrogen resulting in a filling of the hole in the metallic d band. This almost completely eliminates the Pauli spin susceptibility which is principally of d character. Subtraction of two measurements before and after exposure to hydrogen allows a direct measure of the d-electron susceptibility. Moreover, when the hydrogen is pumped out of the experimental region, it is claimed that the hydrogen in the interior of the metal can be readily removed while that on the surface remains relatively strongly bound. This means that with a second subtraction experiment, it is possible to measure the d-electron susceptibility of the surface Pd atoms. Indeed, their measurements as a function of dispersion (f_s = dispersion) indicate a good linear dependence of the susceptibility on dispersion, consistent with what would be expected for the first term in Eq. (3.3). Extrapolation to zero dispersion gives, as expected, the accepted value χ_{Pauli} for Pd and this was found to have the correct temperature dependence between 150 and 298 K. The extrapolation to a dispersion of 1 gives the surface susceptibility. This has a negligible dependence on temperature and is substantially reduced ($\approx 27\%$) compared to that of the bulk, $\tilde{\chi}_{bs}(\infty)/\tilde{\chi}_{bv}(\infty) < 1$. This demonstration of the hydride-subtraction technique appears quite successful. It might be possible to extend this method to lower temperatures to measure the temperature dependence of the bulk and surface susceptibilities of Pd particles in a regime where quantum effects may play an important role. Another observation made by Ladas *et al.* (1978) is that the presence of Pd can catalytically convert Fe that is natively present in the SiO_2 support, into metallic form. This can explain the qualitative observation that the total sample susceptibility prior to subtraction increases with decreasing Pd particle size, whereas the electronic susceptibility of the palladium actually decreases with decreasing size. In this regard, one might note a similar observation for Pt particles made by Bylina *et al.* (1962).

Magnetic measurements of vanadium small particles produced by inert gas evaporation methods have been reported by Akoh and Tasaki (1977). Their particles cover the size range from 90 to 300 Å and the magnetic susceptibility detection was performed with a Faraday balance in the temperature range from 4.4 to 300 K. No diamagnetic signals were found that might have been associated with superconductivity ($T_c \approx 5.3$ K). However, a strong paramagnetic susceptibility was observed consistent with Eq. (3.1). In this case, $\tilde{\chi}_b(\infty)$ corresponded to that of bulk vanadium for most particle sizes. For the smallest size, $d = 90$ Å, there appeared to be a reduced susceptibility consistent with $\tilde{\chi}_{bs}(\infty)/\chi_{bv}(\infty) < 1$. This can be seen in their data reproduced in Fig. 9. The particle size dependence d^{-1} of the susceptibility indicated clearly that the observed Curie law behavior was a surface effect, amounting to $115—370\mu_B$ per particle depending on their size. The Curie constant T_s in Eq. (3.3), was found to be a well-defined characteristic for all samples provided the fraction of surface atoms f_s was interpreted to include two atomic layers. Then the magnetic moment per surface atom of vanadium was found to be $\mu_{0s} = 1.2$. In addition it was found that the surface paramagnetism was of antiferromagnetic character having $\theta_s = -2$ K for the case of $d = 100$ Å. Substantial deviations from the Curie-Weiss law were observed below 10 K, in a manner remarkably similar to that observed for Pt particles of smaller size by Yu and Halperin (1981b). Akoh and Tasaki (1977) suggested that the observed surface paramagnetism of vanadium was unrelated to the presence of vanadium oxide since exposure of their samples to air and heat treatment did not significantly change the results.

The work of Akoh and Tasaki was followed by simila. experiments on vanadium particles performed by Morozov (1980) who was motivated to investigate further the possibile mechanism for the observed surface paramagnetism. He prepared a variety of sample sizes: 170, 280,

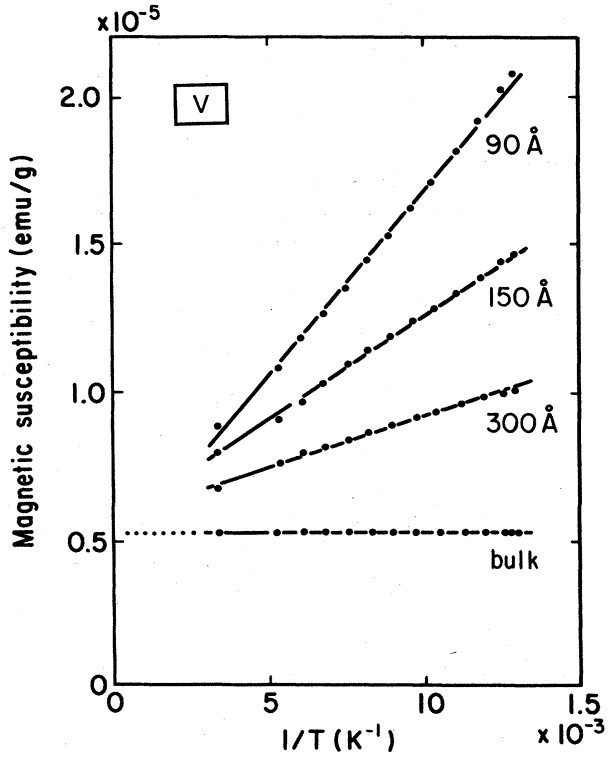

FIG. 9. The magnetic susceptibility of vanadium particles measured using Faraday balance techniques by Akoh and Tasaki (1977). The Curie constants given by the slopes of the lines shown in this figure were found to be proportional to the inverse of the particle diameter. This suggests that the magnetic effects are associated with the particle surface. Other work on vanadium suggests that the results in this figure may not be intrinsic to the vanadium surface (Morozov, 1980; Ohnishi *et al.*, 1985) but may be accounted for in terms of nonstoichiometric oxides (Morozov, 1980).

410, 600, 990, and 1250 Å, by inert gas evaporation followed by embedding in paraffin. Similar paramagnetic behavior to that discussed above was found using a SQUID magnetometer. However, these results were attributed to the formation of nonstoichiometric vanadium oxides on the particle surface. Identification of the nature of the oxide formation was possible through analysis of x-ray experiments. In light of this work the interpretation of the surface paramagnetism of vanadium as an intrinsic effect needs to be viewed with some caution. This point is strengthened by a recent full-potential linearized augmented plane wave (FLAPW) calcuation of the local spin density for the V(100) surface where no enhancement in the surface magnetism was found (Ohnishi, Fu, and Freeman, 1985).

There has been a recent report (Benfield, Edwards, and Stacy, 1982) of observation of paramagnetism in a precisely defined ten-atom cluster of osmium. This was interpreted by the authors as evidence of the quantum size effect. The technique of forming metal cluster molecules for such investigations is appealing in that monodispersed size distributions can be obtained. The molecule $H_2Os_{10}C(CO)_{24}$, which has an even number of osmium electrons, was studied by Faraday balance methods from 4.2 to 300 K. Since three- and six-atom Os clusters were found to be diamagnetic with no temperature dependence, it was concluded that the observed paramagnetic effects were intrinsic to the ten-atom cluster and not associated with impurities. They found a Curie law with a Curie constant of $0.6\mu_B$ per cluster. Without being able to vary the cluster size over a significant range, it will be difficult to interpret these results in terms of a specific model. One puzzling inconsistency with the proposed theory for the quantum size effect, is that a large Curie paramagnetism is observed for an ostensibly even electron system.

Recent experiments on Mg and Be particles by Kimura, Bandow, and Sako (1985) have shown the first clear indication of quantum effects in static magnetization measurements. Particles were made by inert gas evaporation methods followed by matrix isolation in hexane or in tetrahydrofuran. Faraday balance magnetic measurements were performed on a 20-Å sample of Mg particles and a 30-Å sample of Be particles from 2.1 to 150 K in a magnetic field of 10 kOe. ESR experiments were also conducted over a comparable temperature range at 9.1 and 35 GHz.

The susceptibility of the Be particles indicated a slight increase with decreasing temperature that could not be explained in any clear-cut way. On the other hand, the susceptibility of the Mg sample ($\delta/k_B \approx 250$ K) reproduced in Fig. 10 showed a dramatic decrease of order of magnitude χ_{Pauli} as the temperature was reduced below 30 K. This decrease was superimposed on a modest increase as had been observed for the case of the Be particle sample. The increasing susceptibility with decreasing temperature was tentatively assigned to surface impurities consistent with the observation of a narrow line (1 Oe) contribution to the ESR spectrum that increased in intensity with decreasing temperature. Noting that the alkali earths are of

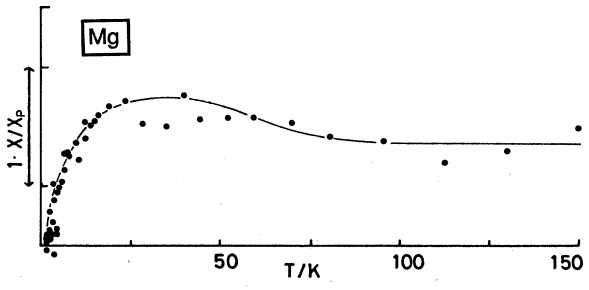

FIG. 10. Magnetic susceptibility of Mg particles in a hexane matrix performed by Faraday balance methods by Kimura, Bandow, and Sako (1985). The sample size was 20 Å with an estimated average level spacing of $\delta/k_B \approx 250$ K. The slight increase in magnetic susceptibility with decreasing temperature may be associated with extrinsic or impurity effects, while the dramatic decrease in susceptibility near 25 K is consistent with expectation of quantum size effects for even-number electron particles.

even valence the observed net decrease in susceptibility is consistent with the expected behavior predicted by Greenwood *et al.* (1960) and Kubo (1962). Experiments with different particle size samples are necessary to confirm this interpretation as was noted in Sec. III.A.1.

In many cases careful measurements as a function of particle size have been crucial in making compelling identification of the origin of the magnetic susceptibility. When this has been done the measured temperature-dependent part of the susceptibility was attributed to surface paramagnetism. In addition, it was found in a number of experiments (Pt,V) that the magnetic coupling was antiferromagnetic in nature. It is also interesting that there is an apparently consistent result for a number of transition metals (Pt,Pd,V) that the temperature-independent part of the surface susceptibility, $\tilde{\chi}_{bs}(\infty)$, may be reduced below that of the bulk metal.

B. NMR measurements: the Knight shift and line shapes

Even before Kubo's landmark work (Kubo, 1962), it had been suggested that very interesting and unusual magnetic effects might be observed for metals of very small size. Greenwood, Brout, and Krumhansl (1960) showed that the conduction electronic properties of metal particles would have even and odd anomalies. They were the first to point out that the Knight shift measurement might distinguish separately the behavior of even- and odd-electron-numbered particles. They remarked that the magnetic susceptibility would go to zero for the even particles, as has been discussed in Sec. II, and that this would be indicated by a reduction of the NMR Knight shift from its bulk metallic value at high temperatures, to zero at low temperatures, $T \ll \delta/k_B$. At the same time, another resonance should separate from the high-

temperature spectrum moving away from the bulk metallic NMR frequency in the opposite direction from that above, and that this one should have a strongly temperature-dependent frequency shift associated with the Curie law susceptibility of the odd particles, Eq. (2.28). It is along these general lines that a large number of experiments have been analyzed in the last twenty years. One important addendum to these ideas is that the inevitable particle-size distribution will produce a wide range of odd-particle NMR frequency shifts, since for this case the susceptibility varies as d^{-3}. By contrast all even particles have the same limiting low-temperature susceptibility. From this argument it follows that half of the NMR line will have moved toward the zero Knight shift frequency at low temperatures, while the other half will become so broad as to be essentially unobservable. Thus the NMR Knight shift technique gives the possibility of selective measurement of the magnetic susceptibility of the even-electron-numbered particles. According to the quantum size effect theory, this should be linear in the temperature having a residual nonzero value at zero temperature in the case of strong spin-orbit coupling. Otherwise the Knight shift, and the even-electron susceptibility, should be simply proportional to the temperature, where in both cases we only consider the region $k_B T \ll \delta$. A second comment of technical significance is that the Knight shifted NMR resonance determination of the electronic susceptibility is independent of background contamination in the sample, from the surface, or the support matrix. It will be recalled from the last section that direct measurements of the magnetic susceptibility have had interpretational difficulties owing to these effects.

From the theoretical side, it is well understood how the NMR frequency is affected by the Pauli electronic susceptibility (Bennett, Watson, and Carter, 1970; Clogston, Jaccarino, and Yafet, 1964). The contributions to the shift $\Delta\nu$ in the NMR frequency ν are defined (Slichter, 1978) relative to a suitable reference compound with NMR frequency $\nu_{\rm dia}$

$$\nu=\nu_{\rm dia}+\Delta\nu\ , \tag{3.6}$$

giving a Knight shift

$$K=\Delta\nu/\nu_{\rm dia}=K_s+K_d+K_{\rm VV}\ . \tag{3.7}$$

Each term can be expressed in terms of the product of a hyperfine coupling constant a and a corresponding electronic susceptibility $\tilde{\chi}$

$$\begin{aligned} K_s&=a_s\tilde{\chi}^{\,s}_{\rm Pauli}\ ,\\ K_d&=a_d\tilde{\chi}^{\,d}_{\rm Pauli}\ ,\\ K_{\rm VV}&=a_{\rm VV}\tilde{\chi}_{\rm VV}\ . \end{aligned} \tag{3.8}$$

These are the contributions from the Fermi contact interaction a_s, core polarization a_d, and the nuclear spin-electron orbital interaction $a_{\rm VV}$. For the nontransition metals the first term is dominant and to an excellent approximation $K\approx K_s$. However, for Pt and some other transition metals this is not the case. Here, the core-polarization term is the most important amounting to $K_d\approx -4\%$, dependent on temperature, about four times larger than K_s and with opposite sign. We will be concerned with measurements of the Knight shift for the metals Li, Cu, Al, and Sn, for which the approximation

$$K\approx K_s \tag{3.9}$$

is probably satisfactory. A discussion of the hyperfine coupling constants is beyond the scope of this article, but is extensively reviewed in the literature (Bennett *et al.*, 1970; Carter *et al.*, 1977). Nonetheless, it is interesting to observe that the Fermi contact interaction contribution to the Knight shift has the form (Slichter, 1978),

$$K_s=(8\pi/3)\langle\,|\,\phi_k(0)\,|^2\rangle_F\tilde{\chi}^{\,s}_{\rm Pauli}\ , \tag{3.10}$$

where the average is over all electronic states k with energy close to the Fermi energy. For very small size particles, one can imagine that the hyperfine coupling may be different from that of the bulk since there will be contributions from surface states to the average $\langle\ \rangle_F$. Such effects have been observed by Yu and co-workers (Yu *et al.*, 1980; Yu and Halperin, 1981a,1981b) in platinum particles. When the particles are not too small ($d>30$ Å) it was found that a separation of the size effects on $\langle\ \rangle_F$ and $\tilde{\chi}_{\rm Pauli}$ in Eq. (3.10) was possible. In this case oscillatory variations in $\langle\ \rangle_F$ contribute mainly to an inhomogenous Knight shift distribution leading to NMR line broadening. The center of mass of the line is controlled by $\tilde{\chi}^{\,s}_{\rm Pauli}$.

According to the above discussion, we expect that a small metal particle will have a temperature-dependent NMR spectrum attributable to quantum effects on the electronic susceptibility. Let us presume, for the time being, that the applied magnetic field H is quite small, $\mu_B H\ll\delta$. Then Eqs. (2.28), (2.42), and (2.43) together with Eqs. (3.6)—(3.9) indicate that on decreasing the temperature, the NMR line should begin to broaden where $\delta\approx k_B T$. With further decrease in temperature half of the line intensity will shift toward the zero Knight shift position (in the direction of lower frequency or, for a fixed frequency, to higher field), while the other half will spread out on the low-field side of the bulk metal resonance line. If the metallic element has an even number of electrons per atom in each particle, then the low-field tail will be missing and the full intensity of the line should move up-field toward zero Knight shift. If the metal is free-electron-like with a weak spin-orbit coupling, then the resonance frequency at low temperature should be at the zero Knight shifted position.

At high temperatures, it might be anticipated that the NMR linewidth is just what one would expect for bulk material. There are two reasons why this might not be the case. They both have to do with the effect of the particle surface. The surface of a metal represents an interruption in the translationally periodic potential felt by the conduction electrons. It is well known that if such a disturbing potential is spatially abrupt compared to π/k_F (of the order of a lattice constant) then the conduction elec-

tron wave functions respond in an arrangement that has a damped oscillatory probability density where k_F is the Fermi wave vector. These Friedel or Ruderman-Kittel oscillations have been extensively studied for the problem of dilute impurities in metals. Both the electronic spin density and the electronic charge density can be expected to oscillate in response to the presence of the metal particle surface. The spin density is proportional to the local Knight shift which must therefore be oscillatory as well. This will produce a distribution of Knight shifts throughout the particle, but with the largest variations concentrated near the surface, decreasing with increasing distance from the surface according to the inverse second power and having period π/k_F (Adawi, 1966; Yu and Halperin, 1981b). This means that the NMR linewidth of a small metal particle can be larger than that of the bulk even at high temperatures. The first work demonstrating this surface effect was performed by Charles and Harrison (1963) using Pb particles and more recently has been studied extensively for Pt particles by the Northwestern University group (Yu, 1980; Yu *et al.*, 1980; Yu and Halperin, 1981a,1981b). In a similar way the electron charge density oscillations produce an oscillatory electric field gradient near the particle surface. For nuclei with spin $I > \frac{1}{2}$, the nuclear level spectrum splits into a $2I+1$ multiplet for which the splittings depend on the nuclear quadupole moment and the strength of the electric field gradients. Since the latter has a wide range of values for atomic sites near the surface, line broadening will result. In both cases, we can understand that the surface of the metal particle gives rise to inhomogeneous NMR line broadening, which should scale as the surface-to-volume ratio d^{-1}, but which will be temperature independent. In any case, these oscillatory distributions of effective local fields should not appreciably shift the average resonance frequency despite their effect on the linewidth. We will assume that the frequency of the peak in the NMR spectrum gives the average even-particle Knight shift that may be taken to be proportional to the electronic susceptibility, χ_{even}. This approximation may only be suitable for larger particles where relatively few atoms are at the surface itself. (If $d \geq 50$ Å, we might expect that the fraction of surface atoms f_s is less than $\approx 20\%$.)

A substantial amount of work has been done on superconducting small particles. Here there are two effects that come into play. If the size of the particle is small compared to the superconducting coherence length then the superconducting properties are markedly changed (Buhrman and Halperin, 1973). The second effect appears if the size of the particle is made still smaller. Then one can have $\bar{\delta} = \delta/k_B T_c \gtrsim 1$. This gives an interplay between "zero-dimensional" superconductivity and discreteness of the electronic level structure that will be briefly discussed here.

For bulk superconducting metals, the Knight shift decreases as a function of temperature owing to the formation of the superconducting energy gap in the quasiparticle spectrum and a concomitant reduction in the Pauli susceptibility. For the light elements such as Al, it has been found that the Knight shift tends to zero as the temperature decreases (Hammond and Kelly, 1967). In the heavier metals where spin-orbit coupling is important there is a residual Knight shift at low temperatures (Androes and Knight, 1961; Wright, 1967; Hines and Knight, 1971) consistent with theoretical expectation (Ferrell, 1959; Anderson, 1959). This situation is not unlike that which has been already discussed here in the context of small, even-electron particle effects on the electronic susceptibility, Eq. (2.48). Since the superconducting energy gap is only weakly dependent on particle size, one might suppose that the effects of superconductivity and discreteness of the level structure could be easily distinguished from each other in a superconducting small particle sample by examining the size dependence of the reduction in the Knight shift. Unfortunately, it is not so straightforward. The small-size superconductor or "zero-dimensional" superconductor experiences large temporal fluctuations of the order parameter which are strongly affected by size, particularly in the vicinity of T_c. If the particle size is very small and consequently the average level spacing is of order or larger than the superconducting condensation energy, $\delta/k_B T_c \geq 1$, then the behavior of the Knight shift at temperatures well below T_c is similar to that of a normal metal particle (Shiba, 1976; Sone, 1983), which is predominantly determined by the quantum effects of discreteness of the electronic levels. Otherwise, at temperatures of the order of T_c, the size dependence of the Knight shift is more complicated. In the following sections, we will discuss experimental results, grouped with nonsuperconducting metals appearing first: Li, Cu, Pt, Al, Sn, and Pb.

1. Normal metals

a. Lithium

Samples of LiF when irradiated with neutrons at liquid-nitrogen temperature develop precipitates of lithium metal. It is believed that there are principally two kinds of metallic clusters that result from this treatment: large particles of size ≈ 100 Å and small platelets about 20 Å. Charvolin *et al.* (1966) and Taupin (1967) have reported NMR measurements that show evidence for three ^{7}Li lines. One broad resonance is associated with the Li of the LiF matrix. The other two are narrow and considered to be that of metallic lithium. Of these, one is at the expected Knight shifted position for bulk Li and corresponds to the large particles in the irradiated sample. The other appears at the zero Knight shift position and this was interpreted as a manifestation of the quantum size effect in small Li "platelets" with even electron number. These first experimental results have stimulated extensive NMR work with other metal particle samples; however, they remain as the only Li particle NMR measurements reported to date. There is sufficiently poor sample characterization in this early work that it is impossible to quantitatively evaluate the measurements in

terms of the quantum size effect. Moreover, the observation of a zero Knight shift, independent of the temperature up to 368 K, appears qualitatively at odds with the estimated particle size distribution and the simple theory. From Fig. 1, we find that an 18-Å Li particle would have $\delta/k_B \approx 250$ K seemingly inconsistent with $\delta/k_B \gg 368$ K as would be necessary to interpret the experimental results in terms of Eqs. (2.28) and (3.6)—(3.10). At this juncture it may be worthwhile to point out that ESR measurements on lithium metal particles (Borel and Millet, 1977) have also been interpreted as showing evidence of the quantum size effect. Anomalies in the electron spin resonance intensity have been observed for 32-Å particles at a temperature of about 20 K, a temperature at which one might more reasonably expect quantum effects to show up.

b. Copper

Copper is the normal metal that has been most widely studied using the Knight shift technique. Hines (1971) first reported results on copper particles of size 110 and 150 Å obtained at temperatures from 0.5 to 77 K. These samples were made by vacuum evaporation techniques using a SiO matrix. The substantial quadrupolar moment of ^{63}Cu ($I=\frac{3}{2}$) was interpreted as giving rise to broadening of the NMR line leaving only the central $\frac{1}{2} \rightarrow -\frac{1}{2}$ transition. Hines was mainly interested in the linewidth. He first subtracted an amount from the measured linewidth that he attributed to a nonuniform conduction electron spin density as was indicated by Charles and Harrison (1963), as well as a contribution from the bulk metal, leaving an excess temperature-dependent linewidth. This was attributed to a Knight shift distribution arising from the quantum size effect. A temperature-dependent linewidth is suggestive of effects of odd particles on the NMR line. However, without observations of either the frequency shift of even particles or there being more systematic studies of the size dependence one cannot rule out other explanations such as that of surface paramagnetic impurities.

A series of experiments from a Tokyo group have made very extensive contributions to the understanding of small particle NMR. This work includes ^{63}Cu, ^{27}Al, ^{119}Sn, and ^{65}Cu, of which we will review the copper measurements first (Kobayashi, Takahashi, and Sasaki, 1971,1972; Kobayashi, 1974; and Kobayashi, 1977). In the early work (Kobayashi *et al.*, 1971) 60-Å particles were made by inert gas evaporation and insulated from one another through oxidation. Later (Kobayashi *et al.*, 1972) samples of 40 and 90 Å were made by similar methods and all of these measurements were consistent with the earlier work of Hines (1971). In addition, spin-lattice relaxation time (T_1) measurements were made. An increase in the linewidth was observed with decreasing temperature from 63 to 0.5 K and with decreasing particle size. A very extensive broadening on the low-field side of the resonance was found to be consistent with that expected from a line shape attributed to both even- and odd-electron number quantum effects. Two features that were not understood in the data from these samples were the rather large paramagnetic susceptibility (see our earlier discussion of this in Sec. III.A) and the short values of T_1 compared to those of the bulk. It was suggested that both of these features might be related to significant surface oxidation of the copper particles. In this first series of experiments (Hines, 1971; Kobayashi *et al.*, 1971,1972; Kobayashi, 1974) no shift of the even-particle resonance line toward the zero Knight shift frequency was found. However, it was recognized (Kobayashi *et al.*, 1972) that the large spin-orbit interaction in copper would tend to quench the quantum size effect in the Knight shift. [Later these ideas were quantified through the theoretical work of Shiba (1976) and Sone (1977).] It was also pointed out that the large quadrupole moment of copper couples to the surface electric field gradients and makes interpretation of both line shape and relaxation nontrivial.

Of all the normal metal particle Knight shift measurements yet reported, the experiment of Yee and Knight (1975) was the first work that can be convincingly understood in terms of the quantum size effect. A set of four samples of copper particles were vacuum evaporated and isolated in a SiO matrix. Two other samples were prepared by chemical methods involving impregnation of an alumina support with copper fluoride solution followed by hydrogen gas reduction at elevated temperatures. In a final step, these samples were encapsulated in paraffin to prevent oxidation. The particle sizes ranged from having peak values of 25—450 Å, were characterized by either electron microscopy or x-ray measurements, and were investigated by continuous wave NMR from 0.4 to 77 K. The NMR signal at 0.4 K and 8.8 kOe from the 100-Å sample is reproduced in Fig. 11, showing a considerably broadened NMR line centered at a frequency between that of the bulk metal and the reference position of a nonmetallic salt (the zero Knight shift position). There is also evidence in this figure of a low-field tail that is attributed to the odd-electron particles. Both the wide resonance line and the low-field tail are consistent with the previous measurements discussed above. The new results are the observation of a reduced Knight shift that was associated with even-numbered particles. This is clearest for the smallest sizes which have relatively well-defined, narrow size distributions. The temperature dependence of the Knight shifts for the four smallest particle samples is displayed in Fig. 12, appearing almost linear in the temperature except for the lowest temperature datum of the 40-Å size sample (solid dots). This result for the temperature dependence is exactly what is expected theoretically for the orthogonal distribution, appropriate to even-electron-numbered particles. Extrapolation of the Knight shifts to zero temperature clearly indicates that there is a residual Knight shift in each particle size sample where the residual shift is larger for larger sizes. Yee and Knight have analyzed their results in terms of the theory of Abrikosov and Gor'kov (1960) which was developed to account for residual Knight shifts of superconducting ele-

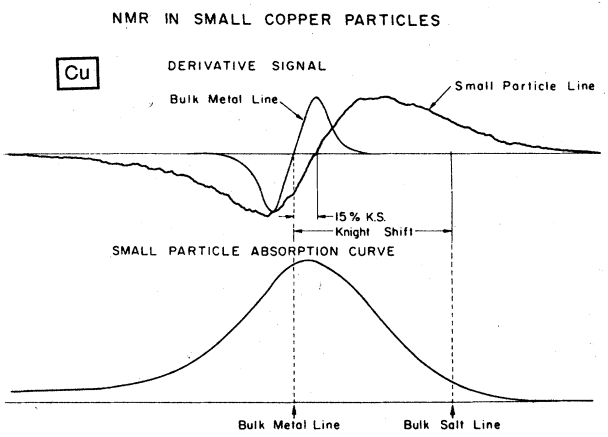

FIG. 11. The Knight shift of a copper particle sample of average diameter 100 Å can be deduced from the NMR derivative spectrum taken by Yee and Knight (1975) at a temperature of 0.4 K and magnetic field, 8.8 kOe. For this sample the residual Knight shift was determined to be 15% smaller than in the bulk metal and the line was found to be substantially broader as was characteristic of all the small particle specimens.

ments that have significant spin-orbit interaction. This adaption of the Abrikosov-Gor'kov treatment to the quantum size effect gives qualitatively the correct behavior for the Knight shift. However, the small-particle Knight shift problem in the presence of spin-orbit interaction was specifically addressed in the later theoretical work of Shiba (1976) or equivalently that of Sone (1977), outlined earlier in this paper. The measured residual Knight shifts are presented in Table IV. With these, we have determined Sone's spin-orbit coupling strength parameter ρ defined by Eq. (2.39), and the bulk g shift Δg_∞, using Eqs. (2.42) and (2.49). The accepted value for the bulk g shift of copper is $\Delta g_\infty = 0.031$ (Schultz, Shanabarger, and Platzman, 1967), which is of the same order of magnitude as that indicated in Table IV. The fact that the NMR measurements give values for the g shift that increase with smaller particle sizes indicates that the residual Knight shift apparently does not strictly scale as d^2 as might have been expected from the theory, Eq. (2.48). There are a number of possible reasons for this apart from inadequacy of the theory. First, the particle sizes themselves are only imprecisely known. Surface oxidation may reduce the metallic particle size from that estimated from electron microscopy. Second, NMR measurements give a resonance whose intensity is proportional to the number of nuclei in the small-particle sample. In such experiments, the large particles have a disproportionately large contribution to the signal. This means that the measured residual Knight shift is characteristic of particles larger than those at the peak of the size distribution and the shift is therefore overestimated. A more careful approach would be to numerically fit the NMR line using the measured size distribution to find the size dependence of the residual shift as was discussed earlier (Sec. II.B.6). Third, it is possible that the approximation in Eq. (3.9) is not valid. That is to say, that the Knight shift is not proportional to the Pauli susceptibility. If the Van Vleck contribution to the Knight shift were important, or if spin-orbit coupling to the crystal field were significant (Appel, 1965), then the residual Pauli susceptibility would be overestimated by our interpretation of the Knight shift experiments. An excellent discussion of these possibilities has been given by Wright (1967) as applied to the problem of residual Knight shifts in superconductors. The latter two arguments would tend to reduce the g shifts calculated from NMR measurements for the smallest samples, bringing theory and experiment into better agreement. With these uncertainties kept in mind, the agreement of the Yee and Knight data with the predictions of the quantum size effect, including spin-orbit coupling, is quite satisfactory.

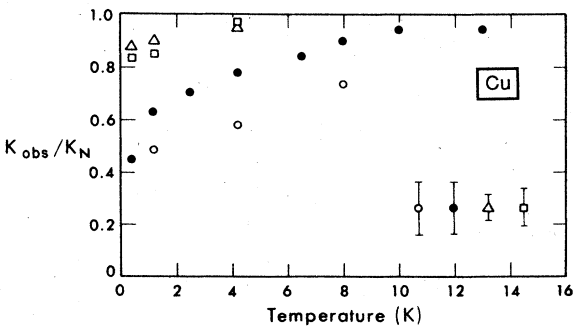

FIG. 12. The Knight shifts of copper particles observed as function of temperature by Yee and Knight (1975) for four samples with different particle sizes. The data correspond to average sizes of 25 Å (○); 40 Å (●); 100 Å (△); and 110 Å (□). Normalization of the measured shifts was made with respect to the Knight shift for the bulk metal. The reduction of the Knight shift with decreasing temperature is characteristic of the expected quantum size effects on the electronic susceptibility probed by the Knight shift.

Similar results to those obtained by Yee and Knight (1975) were obtained by Kobayashi (1977). He used continuous-wave ^{65}Cu NMR to investigate samples prepared by vacuum evaporation in a matrix of SiO, with four sizes in the range 15—110 Å. Measurements down to 0.66 K were reported. In addition, spin-lattice relaxation time measurements were obtained that showed significant enhancement over that of bulk copper. From this work, it was suggested that only the $\frac{1}{2} \rightarrow -\frac{1}{2}$ transition was observed in the smallest particles, broadened by the second-order quadrupolar interaction. In principle, this could have been identified by measurements as a function of magnetic field since the broadening in this case should decrease with increasing magnetic field according to H^{-1}. Nonetheless, it is probable that the NMR intensity measurements in this and previous work on copper are affected by the quadrupolar interaction to some extent and cannot be quantitatively interpreted. Furthermore, the quadrupolar line broadening makes it difficult to uniformly irradiate the resonance line in a pulsed NMR experiment and consequently spin-lattice relaxation times are not

TABLE IV. Extrapolated residual Knight shifts for copper particles from the measurements of Yee and Knight (1975). The particle size d, residual Knight shift expressed as χ/χ_P, and calculated average level spacing δ/k_B are listed. Values of Sone's (1977) spin-orbit parameter ρ are calculated and the results of the measurements are cast in the form of the expected g shift for copper using Eq. (2.49). The reasonable, although qualitative, agreement of these results with the known value for copper, $\Delta g_\infty = 0.031$, is a measure of the success of the theory invoking the spin-orbit interaction to account for the residual Knight shift in small copper particles at low temperatures. The fact that there are variations in the entries in the last column indicates that the size dependence of the residual Knight shift may not be accurately predicted by the theory. This disparity is shown graphically in Fig. 19.

d (Å)	χ/χ_P	δ/k_B (K)	ρ	$\Delta g(\infty)$
25	0.42	119	0.24	0.075
40	0.60	29	0.37	0.058
100	0.85	1.9	0.61	0.030
110	0.81	1.4	0.56	0.026

easily interpreted either (Kobayashi, 1977). A delicate but important point is the following. With quadrupolar broadening the observed resonance may be only that of the $\frac{1}{2} \rightarrow -\frac{1}{2}$ transition for which there is an average shift of the resonance line from the quadrupolar interaction in second-order perturbation theory. This could compromise the interpretation of the residual Knight shifts in copper. For this reason, higher magnetic field experiments than those presently reported would be preferred especially for small particle sizes where the number of surface atoms is appreciable, and hence, where the effect of the quadrupolar interaction is more significant.

c. Platinum

There have been reports of NMR work for Pt small particles, another nonsuperconducting material (Yu, Gibson, Hunt, and Halperin, 1980). No quantum size effects were observed. This is somewhat unfortunate from the following point of view. In choosing a suitable metallic element for the NMR investigation of the quantum size effect, one would like to find a material that is not superconducting and which does not have a quadrupole moment. The latter can lead to confusion in the interpretation of line shapes and possibly frequency shifts as noted above for the case of copper. This means that one should choose a nucleus with spin $I=\frac{1}{2}$. Measurements have been reported on both lead and tin that satisfy the spin-$\frac{1}{2}$ criterion, however, they are superconducting metals. This leaves only a few possibilities such as ^{195}Pt, ^{103}Rh, ^{89}Y, ^{183}W, and ^{109}Ag, of which only ^{195}Pt has a reasonably sensitive NMR signal. In the Northwestern University experiments on platinum particles, no frequency shifts were observed to an accuracy of 1% of the bulk Knight shift for particles as small as 33 Å and at temperatures down to 1.7 K (Yu, 1980; Yu and Halperin, 1981a,1981b). This can be accounted for by the significant spin-orbit interaction in Pt, which can be expected to quench the quantum size effect on the Pauli susceptibility. A rough estimate from Shiba's theory (1976) using an estimated g shift of 0.1 from Clogston, Jaccarino, and Yafet (1964) gives a residual Knight shift for 33-Å particles that is reduced by less than 1% from the bulk Knight shift. This is consistent with experiment. It is interesting to note that for comparable size particles of silver, the estimated residual Knight shift would be almost zero and might be the most suitable metal with which to perform these experiments except for a sensitivity problem compounded by a large Korringa constant.

Despite the limited information that is available concerning the quantum size phenomenon from Pt particles, there has been considerable interest in the study of this metal. Small particles of platinum of the order of 20 Å in size, supported in a porous SiO_2 or Al_2O_3 matrix, are one of the most important heterogeneous catalysts in use today. The application of NMR to explore their electronic structure with, and without, adsorbates is an obvious, if not easy, approach that has proven to be both interesting and fruitful. A brief review will be presented here of work on small-particle Pt NMR of three groups where each has investigated effects attributed to the particle surface. These are: the Northwestern group whose data has been referred to above (Yu, 1980; Yu, Gibson, Hunt, and Halperin, 1980; Yu and Halperin, 1981a,1981b); the University of Illinois—Exxon group (Slichter, 1981a,1981b; Stokes, Rhodes, Wang, Slichter, and Sinfelt, 1981,1982; Rhodes, Wang, Makowka, Rudaz, Stokes, Slichter, and Sinfelt, 1982; Rhodes, Wang, Stokes, Slichter, and Sinfelt, 1982), and finally the Lausanne group (van der Klink, Buttet, and Graetzel, 1984).

The Northwestern group has prepared small particles by standard techniques for chemical impregnation of a SiO_2 support with hexachloroplatinic acid solution followed by hydrogen gas reduction at elevated temperatures following the procedure of Uchijima *et al.* (1977). In a final step, the matrix was dissolved with NaOH and the particles that were recovered were washed repeatedly in water and collected after sedimentation. Several samples, 33 and 50 Å, were made in this way, the larger of which was heat treated in a series of steps to promote particle

growth giving a largest size of 200 Å. The sizes were determined from electron microscopy and total surface area measurements performed with nitrogen gas physisorption (BET method) and hydrogen gas chemisorption techniques. In each sample, a significant, but temperature-independent, NMR line broadening was observed in the range 77—1.7 K. This was identified as being inhomogeneous and was proportional to the externally applied field. However, no frequency shifts were observed and the temperature dependence of the spin-lattice relaxation time was accurately that of the bulk metal, $T_1T=29$ msec K. ^{195}Pt NMR is particularly favorable for investigating frequency shifts since the bulk metal Knight shift is very large at low temperatures -3.4%, and the dipolar linewidth is considerably narrowed through indirect exchange coupling to the conduction electrons. The linewidth data are shown in Fig. 13 and they scale as d^{-1}, clearly indicating a surface effect similar to that reported for Pb filaments by Charles and Harrison (1963). In the Pt experiment, the total surface area is measured directly and consequently, the detailed nature of the size distribution is unimportant for this interpretation. Spin echo experiments were performed from which it was found that the dominant contribution to the echo envelope could be attributed to nuclear spin diffusion in an inhomogeneous local field. Their analysis of these experiments gave a determination of the local magnetic field gradient averaged over the particles. Finally, a simple model calculation was performed without adjustable parameters treating the Pt s electrons as free and the d electrons as being highly localized. From this model, the spatial distribution of the electron spin density was found, Fig. 14, and the NMR line shapes and average magnetic field gradients were calculated and these were in excellent agreement with the experimental results, Figs. 13 and 14. Similar results for the electron density near the surface of a spherical particle have been calculated from self-consistent local-density functional theory (Ekardt, 1984). Although it was not reported at the time the Northwestern group performed ^{195}Pt NMR susceptibility measurements, calibrating these by comparison with a standard Pt sample of $\approx$5-μm-diam particles. It was found that the observed small-particle NMR signal intensity corresponded to that expected from the weight of each sample to an accuracy of 20%.

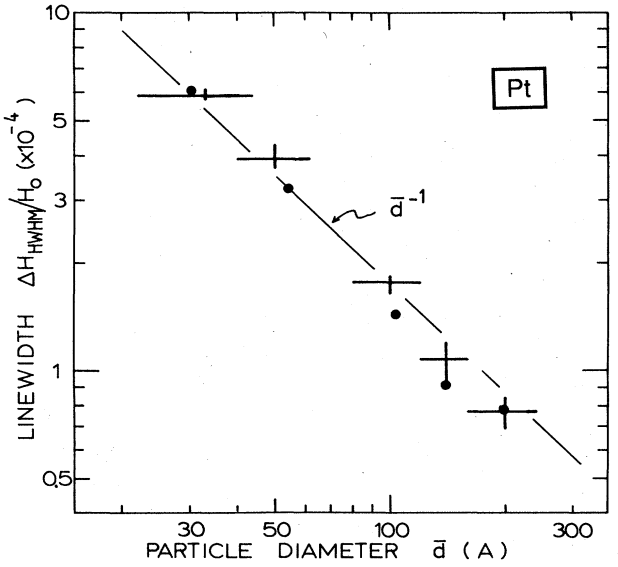

FIG. 13. The dependence of the NMR absorption linewidth as a function of particle diameter for platinum particles measured by Yu, Gibson, Hunt, and Halperin (1980). The inverse dependence on particle size suggests a surface effect. This is compared with the results of their simple two-band model calculation (●). The solid line shows a slope of -1 for comparison with the data.

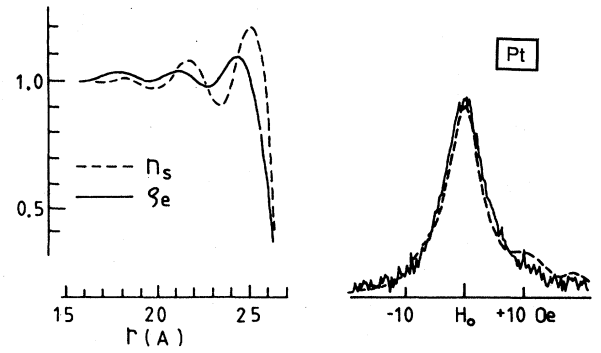

FIG. 14. The charge (ρ_e) and spin density (n_s) at the platinum metal particle surface calculated by Yu, Gibson, Hunt, and Halperin (1980) for a 54-Å size particle. These were used to generate an NMR line shown at the right as a dashed curve and compared to the experimentally determined spectrum for particles of average size 50 Å obtained at 4.2 K and 10 kOe. The agreement between these results confirms that the enhanced NMR linewidth can be accounted for by surface spin-density oscillations.

The University of Illinois—Exxon group have studied Al_2O_3-supported Pt particles with sizes in the range 9 to over 100 Å. Larger sizes were produced by heat treatment on the support. These were systematically characterized by hydrogen gas chemisorption and, for the smallest sizes, electron microscopy. One of the principal differences of this work and that discussed previously is the emphasis on very small particles. For this purpose the use of supported samples is essential in order to maintain isolation between them. The low filling factor then requires extensive signal averaging. Their results for the 39-Å sample are reproduced in Fig. 15. The principal features of the line-shape data for all samples are represented in this graph. A large prominent contribution to the resonance is evident at the bulk Knight shift position (-3.4%), however the NMR line is asymmetrically distributed up to a positive shift of 1%. The analysis consistently shows that this positive shift feature is the resonance of surface Pt atoms since the intensity of this peak for all samples scales accurately with the measured

dispersion (ratio of the number of Pt atoms available for surface chemisorption to the total number of Pt atoms). Surface treatment experiments led to the identification of this shift as being attributable to the surface compound $Pt(OH)_6$. The fact that this feature in the spectrum corresponds to surface Pt was later conclusively demonstrated by Makowka, Slichter, and Sinfelt (1982) using elegant double resonance NMR techniques. The surface resonance was missed by the Northwestern University group in their experiments possibly because their particle sizes were substantially larger than those used by the University of Illinois—Exxon group. A surface-atom Pt NMR peak has also been observed recently by the Lausanne group. Returning to the bulk Pt peak in the University of Illinois—Exxon work, one finds that its breadth for the largest particle samples (dispersion 4% and 11%) is approximately the same as that determined by the Northwestern University group. However, a dramatic increase in the linewidth of their bulk peak was found for dispersions just a bit larger, 15% and higher (Fig. 6 of Rhodes, Wang, Stokes, Slichter, and Sinfelt, 1982). This behavior leads to "slow-beat" echo envelopes and the conclusion that in these samples, with dispersion 15% and greater ($d \leq 39$ Å), the platinum particles have an electronic structure distinct from that of the bulk metal. It is noteworthy that the samples with 4% and 11% dispersion appear to come from a different batch than the others. Such an abrupt change with particle size was not observed by the Northwestern group, whose results are displayed in Fig. 13. They did find, however, that sample treatment was very important. This was evident in the observation that heating at elevated temperatures, $T > 400\,^{\circ}C$, in the presence of hydrogen produces dramatic broadening of the small-particle NMR line (Yu, 1980; Yu and Halperin, 1981a), a process that can be reversed by calcination (heat treatment in air). This phenomenon may be relevant to the results of the experiments of the University of Illinois—Exxon group.

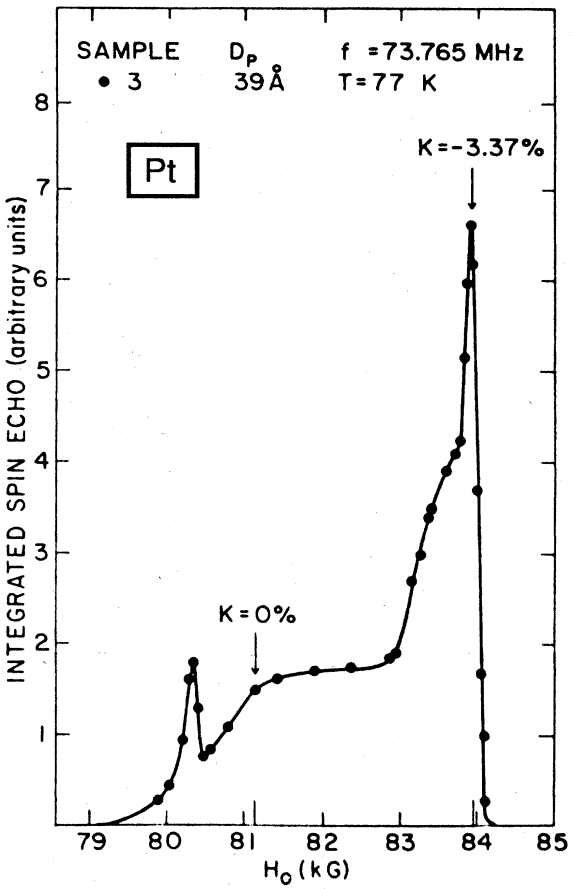

FIG. 15. The NMR line shape of a 39-Å sample of platinum particles vs applied field H_0 as reported by Slichter (1981b). Both the zero Knight shift and bulk metal Knight shift positions are indicated. Note the contributions to the spectrum at positive values of the Knight shift which were associated with a surface platinum oxide. In the work of Yu *et al.* (1980) only the prominent feature at the bulk Knight shift position was observed.

The samples of the Lausanne group were prepared by chemical reduction of H_2PtCl_8 producing 20-Å particles that were then distributed on a SiO_2 support. In this work, the existence of the surface resonance found by the University of Illinois—Exxon group, was confirmed and examined closely under clean surface conditions. By controlling the surface condition, they were able to show that the clean surface Pt atoms resonate at a frequency very close to the zero Knight shift position and that their spin-lattice relaxation measurements indicated that these atoms were in a metallic environment. This work is in excellent agreement with the theoretical calculation of Weinert and Freeman (1983) for which the (001) surface Knight shift was determined to be very small, only −0.6%.

2. Superconductors

a. Introduction and theoretical background

Small metal particles of superconducting elements that have been most intensively investigated by NMR are ^{127}Al, ^{119}Sn, and ^{207}Pb. The original motivation for studying small superconducting particles was to compare Knight shift measurements with the BCS theory for the reduction of the Pauli susceptibility below the transition temperature. A consequence of the theory is that this suppression should be complete at $T=0$. However, the superconducting condensate has a Kramer's degeneracy under time reversal. In the presence of spin-orbit coupling the ground state does not have well-defined spin character and it is possible to have a nonzero polarization at $T=0$ (Ferrell, 1959; Anderson, 1959; Appel, 1965). The use of extremely small particles to investigate this problem was required in any case to avoid distortion of the magnetic field from the Meissner effect. For a light element such as Al, in which there is negligible spin-orbit

interaction, the measurements (Hammond and Kelly, 1967) indicated that there is no residual Knight shift consistent with the theory. For the heavier metals a residual electronic susceptibility at low temperatures was first inferred from observation of a nonzero Knight shift in Hg particles (Reif, 1957). An investigation was then launched by Knight's group at the University of California, Berkeley in order to explore these spin-orbit effects, principally for Sn and Pb and some of their alloys (Androes and Knight, 1961; Wright, 1967; Hines and Knight, 1971). The picture that has emerged from this work is described very well by the spin-reverse scattering theory for spin-orbit coupling in impure superconductors by Abrikosov and Gor'kov (1960). Their principal prediction, relevant to the Knight shift measurements, was that the Pauli susceptibility would be nonzero at $T=0$ and would depend on the particle size

$$\chi(0)/\chi_{\text{Pauli}}=1-\rho_0^{-1}[\pi/2-(\rho_0^2-1)^{-1/2}\cosh^{-1}\rho_0] , \quad \rho_0>1 , \tag{3.11}$$

$$\chi(0)/\chi_{\text{Pauli}}=1-\rho_0^{-1}[\pi/2-(1-\rho_0^2)^{-1/2}\cos^{-1}\rho_0] , \quad \rho_0<1 , \tag{3.12}$$

Here ρ_0 is a spin-orbit coupling parameter and the spin-flip scattering length l_s is assumed to be of the same order as the superconducting coherence length. These are given by

$$\rho_0=2\hbar/(3\tau_s\Delta_{\text{BCS}})=2\hbar v_F(\Delta g_\infty)^2/(3d\Delta_{\text{BCS}}) . \tag{3.13}$$

The spin-flip scattering time

$$\tau_s=l_s/v_F=(\Delta g_\infty)^{-2}\tau_r=(\Delta g_\infty)^{-2}d/v_F$$

was introduced earlier, Eq. (2.46) (Appel, 1965), and the BCS energy gap function is written as Δ_{BCS}. It is interesting to note the similarity between Eqs. (2.47) and (3.13). In the limit of small spin-orbit coupling one finds by expanding Eq. (3.12)

$$\chi(0)/\chi_{\text{Pauli}}\approx\pi\frac{\rho_0}{4}=\frac{hv_F(\Delta g_\infty^2)}{12d\Delta_{\text{BCS}}} , \quad \rho_0\ll 1 . \tag{3.14}$$

With this result, it is clear that the residual susceptibility increases with decreasing particle size as d^{-1} for the superconducting case. For contrast with the quantum size effect one may substitute the average level spacing δ instead of the BCS energy gap in Eq. (3.14). Since δ varies as d^{-3} the expected behavior of the residual susceptibility is therefore proportional to d^2 as was shown earlier in Eqs. (2.47) and (2.48). On decreasing the superconducting particle size one expects to find two regimes, first one where the residual Knight shift increases, $\Delta_{\text{BCS}}\gg\delta$, and then one at much smaller particle sizes, where the residual Knight shift decreases, $\Delta_{\text{BCS}}\ll\delta$, owing to discreteness in the electronic level spectrum. A summary of a number of experiments that indicates this twofold behavior for Sn particles is given by Fukagawa, Kobayashi, and Sasaki (1982) and is shown in Fig. 16. The size that appears to separate these two regions is approximately 150 Å. The

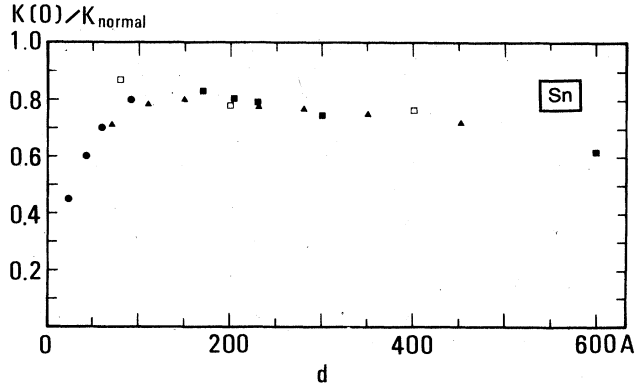

FIG. 16. The residual Knight shift of tin small particles extrapolated to $T=0$ as a function of particle size reported by Fukagawa, Kobayashi, and Sasaki (1982). This work is collected from four sources: (▲) Fukagawa, Kobayashi, and Sasaki (1982); (□) Kobayashi, Takahashi, and Sasaki (1974); (■) Wright (1967); and (●) Nomura, Kobayashi, and Sasaki (1977). The results are normalized to the bulk Knight shifts measured in the normal state. The quantum size effect is evident in the decrease at small diameters.

closed-form expression of Eq. (3.13) for the spin-orbit parameter is only an approximation since Δ_{BCS} is not a correct representation of the amplitude of the superconducting order parameter for a zero-dimensional particle (Sone, 1983).

For the superconducting particle a new parameter needs to be introduced to account for quantum size effects as suggested by the above relative comparison of Δ_{BCS} and δ. This can be represented by

$$\bar{\delta}\equiv\delta/k_BT_c=1.76\delta/\Delta_{\text{BCS}} . \tag{3.15}$$

There have been a number of theoretical papers describing the thermodynamic character of such small superconducting particles with $\bar{\delta}$ as an important scaling parameter. Some of the first work was that of Schmidt (1966) who correctly calculated the temperature dependence of the diamagnetic susceptibility near T_c in both the critical and mean field regions. The importance of the "zero-dimensional" limit was emphasized by Hurault, Maki, and Béal-Monod (1971) where temporal fluctuations of the order parameter are very important and the critical region very large. Mühlschlegel, Scalapino, and Denton (1972) considered the effects of discreteness in the level spectrum on small superconducting particles. They calculated the diamagnetic susceptibility and the spin susceptibility as well as the specific heat. The order parameter fluctuation effects on the spin-lattice relaxation were discussed by Šimánek, Imbro, and MacLaughlin (1973) and reviewed by MacLaughlin (1976). This theory was then extended by Sone (1976) to account for pair breaking and the effects of the Zeeman energy coming from magnetic field dependence of impurity vertex corrections. Sone calculated the spin-lattice relaxation comparing with experi-

ments of Takahashi, Kobayashi, and Sasaki (1975). His results for the spin susceptibility were compared with the Knight shift measurements of Ido and Hoshino (1975). This work was not limited to a temperature interval near T_c as had been the case for previous calculations, however the discreteness in the level spectrum was not taken into account. Shiba (1976) has calculated the spin susceptibility including both level discreteness in the equal-level spacing approximation and the effect of spin-orbit interactions. This paper deals with both normal and superconducting particles, recovering the Abrikosov and Gor'kov (1960) results, Eq. (3.11) and (3.12), for the limit of the continuous spectrum, $\delta \to 0$. The comparison with the Knight shift measurements for Sn (Kobayashi *et al.*, 1972) and Cu (Yee and Knight, 1975) was reasonably good. More recently, Sone (1983) has extended his previous theory to include effects of the spin-orbit interaction and has found that this gives quite good agreement for the spin-lattice relaxation and Knight shifts of Sn particles (Fukagawa, Kobayashi, and Sasaki, 1982) where, as might be inferred from Fig. 16 and comments made earlier, this comparison is restricted to larger particle sizes $d \geq 150$ Å. A review of magnetic resonance in superconductors including effects of thermodynamic fluctuations on the order parameter has been written by MacLaughlin (1976).

The discussion of Knight shift measurements in very small particles is organized by element in the order Al, Sn, and Pb. Extensive work on spin-lattice relaxation has also been performed, as might be gathered from the brief summary of some of the theoretical activity given above. This is presented later in Sec. V.

b. Aluminum

Three groups have made Knight shift measurements on small Al particles: the Nagoya—Osaka University group (Fujita, Ohshima, Wada, and Sakakibara, 1970); the University of Tokyo group (Kobayashi, Takahashi, and Sasaki, 1970,1971,1974; Kobayashi, 1974; Kobayashi, Nomura, and Sasaki, 1978; Nomura, Kobayashi, and Sasaki, 1980); and the Hokkaido University group (Ido and Hoshino, 1975; Ido, 1976). During the last fifteen years there has been development of both measurement technique and interpretative approach. On the other hand, the preparation technique of choice has mainly been that of inert gas evaporation. The results of some of the most recent experiments are displayed in Figs. 17 and 18. All work consistently shows that the Knight shift is suppressed to zero as the temperature approaches zero. Aluminum has a nuclear spin $I = \frac{5}{2}$, 100% natural abundancy, a relatively large quadrupole moment, $Q = 0.15$ b, and it is superconducting at 1.2 K in the bulk.

In the early work of Fujita *et al.* (1970) on particles of 70, 90, and 110 Å, no frequency shift was observed; however substantial decrease in the intensity of the observed signal below 10 K was attributed to inhibition of the spin-lattice relaxation mechanism owing to discreteness of

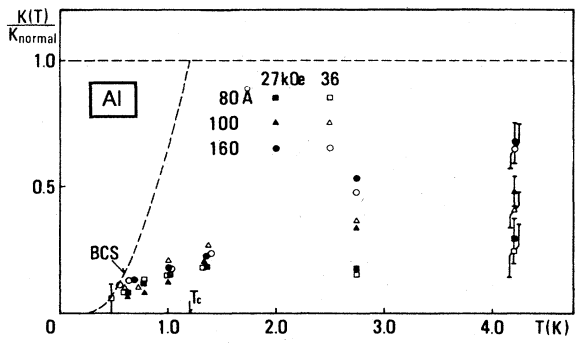

FIG. 17. The temperature dependence of the Knight shifts of Al small particles measured by Nomura, Kobayashi, and Sasaki (1980). The results are normalized to the bulk Knight shifts measured in the normal state, K_{norm}. The authors believe that the particle sizes are smaller than those indicated in their figure, reproduced here. For the largest size, spin-lattice relaxation measurements indicated that superconductivity was quenched by the application of a 36-kOe field. In this case one supposes that the reduced Knight shift is purely a quantum size effect.

the electron level spectrum. Direct measurement of T_1 by other groups (for example, Nomura, Kobayashi, and Sasaki, 1980) confirm that this interpretation, although qualitative, is basically correct.

Prior to 1978, almost all work has been with relatively modest magnetic fields, less than or of the order of 10 kOe. This will be discussed first. The University of Tokyo group has reported a wide range of experiments with different particle sizes from 45 to 350 Å. In this low-field range the results are internally consistent and furthermore, agree reasonably well with work of the Hokkaido University group summarized by Ido (1976). Typically the resonance exhibits a low-field tail producing an asymmetric line shape for particles with diameter less than 100 Å at low temperature, similar to that found for copper (Kobayashi, 1974; Kobayashi, Takahashi, and Sasaki, 1974). This effect was attributed to the odd-electron particles. Broadening was observed that was presumed to be caused by the interaction of the aluminum quadrupole moment and electric field gradients associated with the particle surface. Some of the broadening in the smallest sizes, $d < 100$ Å, may have been from NMR of the aluminum oxide on the particle surface (Ido, 1976) and this may also have been a factor that has not been satisfactorily considered in the other earlier measurements. The question of how thick the oxide is and, hence, how big the metallic particles really are, is not easy to answer. Ido (1976) used x-ray characterization in order to avoid problems of overestimating particle size. Nomura *et al.* (1980) have judged that half of their particle volume determined by electron microscopy was really oxide. This was estimated on the basis of their measurements of the slope of the Knight shift variation with temperature, as shown in Fig. 17. We will return to discuss this criterion

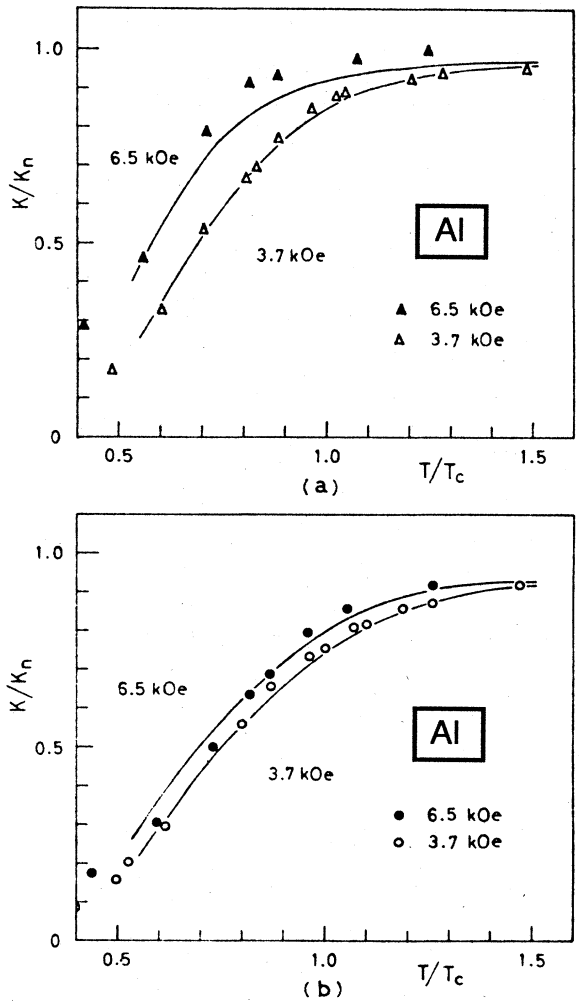

FIG. 18. The temperature dependence of the Knight shifts of Al small particles in several magnetic fields as reported by Ido (1976). Sample (a) corresponds to an average diameter of 170 Å. Sample (b) corresponds to an average diameter of 130 Å. The solid lines are fits to the theory of Sone (1976) which does not take discrete level effects into account. The good agreement suggests that for these particle sizes superconducting order parameter fluctuation effects, calculated by Sone, are dominant. Quantum size effects are not evident.

later on.

In Fig. 18 we show the comparison that has been made between the Sone (1976) theory and the experimental Knight shifts reported by Ido (1976). This is particularly striking when one recalls that this theory is for a "zero-dimensional" superconductor with a *continuous* spectrum. The effects of discreteness of the levels are not apparent above $T=0.5$ K and for particles larger than ≈ 100 Å. The calculated results with various values of δ are shown, from which interpolation was carried out to fit the experimental results. It was concluded that the fit values for $\bar{\delta}$ were a factor of 2 smaller than those estimated from the peak in the measured size distribution. This disagreement should not be considered unreasonable in the absence of a detailed fit of the NMR line shapes taking directly into account the measured size distribution. Some deviations of the experimental results (Ido, 1976) from the theory were noted at low temperatures for the smallest sample, $d=80$ Å and $T \lesssim 0.6$ K, and this was attributed to the effects of a noncontinuous electronic spectrum which had not been included in the theory.

The problem of sorting out the quantum size effects from those expected for the zero-dimensional superconductor is not straightforward, at least in the case of Al. To try to unfold this, a new approach was taken by the University of Tokyo group (Kobayashi, Nomura, and Sasaki, 1978; Nomura, Kobayashi, and Sasaki, 1980). Large magnetic fields up to 36 kOe were used. Spin-lattice relaxation data indicated that these fields were sufficient to suppress superconductivity, at least for the largest particle size $d=160$ Å. They argued that this implies that the observed depression of the Knight shift under these conditions could be attributed to the quantum size effect, and not to superconductivity. The data are shown in Fig. 17. It is apparent here that the Knight shifts are much closer to zero than that reported earlier by the same group, or by Ido (1976), for similar sizes. One can compare Figs. 17 and 18. This aspect of their data was addressed by Nomura *et al.* They suggested that the actual sizes of their particles were almost certainly less than that indicated from electron microscopy, attributable to some amount of surface oxidation. For this reason, the average sizes were estimated to be reduced by about 30% below those indicated in the figure. This would tend to produce a larger decrease of the Knight shift at any given temperature. Another complication revealed by the high-field NMR experiments was the observation of very broad resonance lines, 200 Oe, presumably because of the higher sensitivity at larger fields. This is to be compared with the linewidth of 10 Oe reported before for low-field resonance (Kobayashi *et al.*, 1974; Ido, 1976). This effect was interpreted by Nomura *et al.* (1980) as evidence of significant quadrupolar broadening which would lead to distortion of the low-field line shape for two reasons. This would tend to weight inordinately the upper side of the particle-size distribution for which such broadening would be less pronounced. In addition, second-order quadrupolar effects are known to be suppressed with increasing field and these were estimated to be large enough to compromise the earlier low-field data.

Before discounting the earlier work of the Tokyo University group which seems consistent with that of Ido (1976) and the Sone theory (1976), it is worthwhile comparing the data of Nomura *et al.* (1980) with the quantum size effect predictions. The ratio of the even-particle and Pauli susceptibilities in Eqs. (2.28) and (2.29) is just the relative Knight shift plotted in Fig. 17. For the orthogonal distribution, we expect a linear temperature dependence of the Knight shift at low temperatures, $K(T)/K(\infty)=3.8k_BT/\delta$, similar to that observed. From Fig. 16, one can estimate δ/k_B to be 58, 30, and 21 K for the three sizes given nominally as 80, 100, and 160 Å. This is to be compared with the calculation of the average

level spacing given by these authors, or taken from Fig. 1, of $\delta/k_B = 2.5$, 1.3, and 0.32 K. A factor of 3—4 reduction of particle diameter by oxidation would need to be invoked to account for this discrepancy which is substantially more than was suggested. Consequently it is not yet clear how this problem can be resolved.

A final important point should be brought forward at this time. All of the theoretical work concurs in that the suppression of the Pauli susceptibility of even particles by the quantum size effect is believed to be a low-field phenomenon. This is shown in Fig. 5. The residual susceptibility at $T=0$ normalized to the Pauli susceptibility in a magnetic field of 36 kOe is expected to be 0.94 for an Al particle of 100 Å. Even for a 50-Å Al particle, one might expect a substantially nonzero residual susceptibility of $\chi_{\text{even}}(0)/\chi_{\text{Pauli}} = 0.22$ in this magnetic field. It may be, therefore, that there are inherent difficulties in using large magnetic fields to suppress the effect of superconducting fluctuations on the Knight shift in order to separate the effects of superconductivity from the quantum size effect, since large magnetic fields suppress both. There have been no experiments reported to date that systematically study the field dependence of the even-odd electron number anomalies so one should bear in mind that the above comments are largely theoretically motivated.

c. Tin

Metallic tin has been prepared in the form of very small particles for the purpose of studying the Knight shift in the superconducting state. The University of California, Berkeley group (Androes and Knight, 1961; Wright, 1967; Hines and Knight, 1971) were mostly interested in clarifying the relation between BCS theory and the measured Knight shifts for which significantly nonzero values were found in the limit $T \to 0$. They were able to show convincingly that the spin-reverse scattering theory, Eqs. (3.11) and (3.12) (Abrikosov and Gor'kov, 1960) gave an adequate description of their experimental results for particles with sizes in the range of 150—850 Å. A second group, at the University of Tokyo (Kobayashi, Takahasi, and Sasaki, 1974; Normura, Kobayashi, and Sasaki, 1977; Fukagawa, Kobayashi, and Sasaki, 1982) extended measurements to particle sizes as small as 22 Å where the effects of discreteness of the electron-level spectrum were very clearly in evidence. Most of the samples have been made by a method of evaporation of Sn in vacuum so as to make a discontinuous film of isolated islands of metal. This was covered with an evaporated, insulating layer of SiO, and the process repeated in alternation, building up a sufficient amount of sample for observation of the NMR signal. Work with inert gas evaporated particles (Kobayashi, Takahashi, and Sasaki, 1974) has not been so successful for the smallest sizes. A comparison of the two methods is reviewed by Fukagawa *et al.* (1982). Wright (1967) also reported work with a sample of tin particles made by chemical impregnation of alumina with a solution of a tin salt followed by hydrogen reduction. The sample that was made this way produced results consistent with those from particles prepared by the vacuum evaporation method. Tin has an advantage from the point of view of interpretation of NMR signals in that it is free of quadrupolar effects. Each of the two principal isotopes, ^{117}Sn and ^{119}Sn has $I = \frac{1}{2}$, and their natural abundance is 7.6% and 8.6%, respectively. The bulk isotropic Knight shift of Sn is 0.72%. The anisotropic shift is only 0.027% and the superconducting transition temperature in the bulk is 3.72 K.

A summary of all of the residual ($T=0$) Knight shift data for tin is given in Fig. 16, taken from Fukagawa *et al.* (1982). In contrast to the results for Al, one sees in this figure that the Knight shift at $T=0$ is nonzero for all particle sizes. Only in the limit of $d \to 0$ does it appear that the residual Knight shift might be completely suppressed. The effect of the spin-orbit interaction on electron spin-flip scattering from the particle surface is to mix spin-up and spin-down states more effectively for small particles. In the superconducting state, this gives rise to a residual susceptibility of the conduction electrons that tends toward the Pauli value in the limit of small size. Following our earlier discussion associated with Eq. (3.14) when a gap Δ opens up at the Fermi energy the expected low-temperature Knight shift is proportional to $(\Delta d)^{-1}$. When superconductivity is a dominant effect, $\Delta_{\text{BCS}} \gg \delta$, then one substitutes $\Delta = \Delta_{\text{BCS}}$ and the low-temperature Knight shift increases with decreasing particle size. When electronic level discreteness is more important, $\delta \gg \Delta_{\text{BCS}}$, we should use $\Delta = \delta \propto d^{-3}$ and we find that the Knight shift decreases with decreasing particle size. If tin particles are sufficiently small, $d < 150$ Å, the residual susceptibility reduces with decreasing size qualitatively consistent with the theory of the quantum size effect (Shiba, 1976; Sone, 1977). The otherwise difficult problem of separating the effects of superconductivity from those of the quantum size effect is accomplished here by the different role played by the spin-orbit interaction in the two cases.

Wright (1967) analyzed his measurements on thin platelets of tin using the Abrikosov and Gor'kov (1960) theory, Eqs. (3.11) and (3.12), appropriate for that regime where superconducting effects are dominant. This can be expressed in terms of a g shift $\Delta g_\infty = 0.35$. Similarly, Nomura, Kobayashi, and Sasaki (1977) compared their results with the theory of Shiba (1976) estimating a value of $\Delta g_\infty = 0.25$ for the same range of particles. Sone's theory (1983) also appears to account for this data rather well (Fukagawa, Kobayashi, and Sasaki, 1982) with a g shift of $\Delta g_\infty = 0.31$. For the smallest particle data, $d \leq 150$ Å, discreteness of the electron-level spectrum can be clearly observed. Analysis of the results of Nomura, Kobayashi, and Sasaki (1977), with Eqs. (2.42) and (2.43), gives a somewhat smaller value of $\Delta g_\infty \approx 0.1$. We note further that the residual Knight shift does not closely follow the expected dependence on particle diameter in either size

range. This is shown in Fig. 19 by the lighter solid curve. If there were a contribution to the tin Knight shift other than that from the Pauli susceptibility (Wright, 1967) of approximately 20%, then there would be better agreement with the predicted size dependence for both large and smaller particles. Although this cannot be independently determined from the data, it seems that there is, in any event, qualitative agreement with existing theory over the entire range of particle sizes. More importantly, there is an unambiguous demonstration of the quantum size effect on the Pauli susceptibility for the smallest particles indicated by the data of Nomura *et al.* (1977). Two further comments regarding these data are appropriate, however. First, the measurements of Fukagawa *et al.* (1982) extend up to 30 kOe. In their largest applied field, $2\mu_B H/\delta \approx 2$ for a particle size of 110 Å. Although there are no explicit theoretical predictions for the susceptibility as a function of the field in the presence of strong spin-orbit interaction, one might, nonetheless, have expected from Fig. 5 an increase in the even-particle susceptibility with application of such large magnetic fields. However, only a modest increase in the residual Knight shift, if any, was observed for this size of particle. Second, it is interesting to recall that Sn has an even valence, and consequently, that all particles might be expected to exhibit only even-electron-number quantum effects under the ideal circumstances of negligible chemical interaction with the matrix. For small tin particles, $d < 150$ Å, Nomura, Kobayashi, and Sasaki (1977) found that the Knight shift was linear in the temperature. In the quantum size effect regime this is the result expected for an even valence element where total angular momentum is an integer. The observation of symmetric ^{119}Sn NMR lines (Fukagawa, Kobayashi, and Sasaki, 1982) also indicates that there are not very many odd-electron particles.

d. Lead

Charles and Harrison (1963) studied two sample sizes of lead particles, or filaments, prepared by impregnation of porous Vycor glass with molten metal under pressure. No frequency shifts were observed although information concerning the temperature range of the experiment was not provided. Observation of significant inhomogeneous line broadening was interpreted in terms of spin density oscillations associated with the particle surface. A similar interpretation was invoked for Pt particles (Yu *et al.*, 1980; Yu and Halperin, 1981a,1981b) and has been discussed earlier. Line broadening in tin particles (Wright, 1967) and in other lead particle work (Hines and Knight, 1971) was thought to have the same origin. In the latter case, frequency shifts in the superconducting state were observed for particles of 340 and 550 Å. The effect of the spin-orbit interaction in lead was evidently stronger than for comparable size particles of tin. No quantum size effects have been observed in any of the lead samples.

e. Summary of notation used to describe spin-orbit effects

In the above discussion the ESR g shift Δg_∞ is used as a spin-orbit coupling parameter. The observation of ESR has not been reported in either bulk tin or bulk lead and consequently comparison with actual measurements of the g shift cannot be made. Other parameters proportional to $(\Delta g_\infty)^2$ have been used to describe spin-orbit effects in metallic particles. These are listed below:

$$\rho = \frac{\pi \hbar v_f (\Delta g_\infty)^2}{3\delta d} \quad \text{(Sone, 1977)}$$

$$\rho_0 = \frac{3\hbar v_f f^{-1}}{4\delta d} \quad \text{(Yee and Knight, 1975), } \alpha f^{-1} = (\Delta g_\infty)^2 \text{ and } \alpha \text{ is a number of order unity}$$

$$\lambda = \frac{\hbar v_f (\Delta g_\infty)^2}{k_B T_c^{2/3} d(\delta/k_B)^{1/3}} \quad \text{(Sone, 1983), } T_c \text{ is the transition temperature for superconductivity}$$

$$\eta = \frac{\hbar v_f (\Delta g_\infty)^2}{\delta d} = \frac{\hbar v_f (\Delta g_\infty)^2)}{\Delta_{\rm BCS} d} \quad \text{(Fukagawa } et\ al.\text{, 1982)}$$

$$\rho = \frac{\pi \hbar v_f f_{\rm so}}{\delta d} \quad \text{(Shiba, 1976), } f_{\rm so} = (\Delta g_\infty)^2$$

$$\rho_0 = \frac{2\hbar v_f f^{-1}}{3\Delta_{\rm BCS} d} \quad \text{(Wright, 1967; Hines and Knight, 1971), } \alpha f^{-1} = (\Delta g_\infty)^2 \text{ as above, with } \alpha = 1$$

(3.16)

3. Summary of Knight shift experiments and the quantum size effect

The clearest indication of the quantum size effect comes from the work with copper particles of Yee and Knight (1975) as well as that of Kobayashi (1977), and the work with tin particles of Nomura, Kobayashi, and Sasaki (1977). In both the cases of copper and tin, significant spin-orbit interaction partially quenches the even-odd electron number anomalies. In both cases the Knight

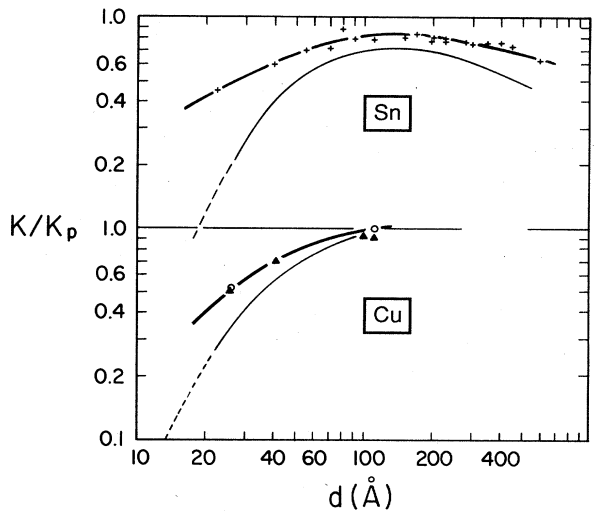

FIG. 19. Summary of residual Knight shift measurements K extrapolated to $T=0$ for copper and tin metal particles. These are materials for which spin-orbit coupling is important. Forcing agreement with quantum size theory, which predicts a d^{-2} dependence for small sizes, can only be made by subtracting a constant contribution K_0 (0.2 for Cu and 0.35 for Sn) from the measured Knight shifts. $(K-K_0)/(K_p-K_0)$ is plotted as a light solid curve, where K_p is the bulk metal shift. The dashed lines show the d^{-2} dependence. (○) Kobayashi (1977); (△) Yee and Knight (1975); (+) Fukagawa *et al.* (1982), Nomura *et al.* (1977), Kobayashi *et al.* (1974), and Wright (1967). The heavy solid lines represent the data as guides to the eye.

shift is a linear function of temperature as predicted by the quantum size effect theory with an orthogonal distribution of electron levels. For aluminum, where the spin-orbit interaction is negligible, the effects of superconductivity cannot be easily separated from those of the quantum size effect. At high fields, where superconductivity is suppressed, it is not obvious how to interpret the data quantitatively (Nomura, Kobayashi, and Sasaki, 1980). In the case of Cu, there is some possible difficulty in the interpretation of spectra owing to the quadrupolar interaction. For tin, there are no quadrupolar effects, however, there is a disadvantage that this metal is a superconductor for which the corresponding changes in the Knight shift must be understood independently and subtracted out.

C. ESR measurements: resonance intensity, *g* shift, and linewidth

1. Introduction and theoretical background

The measurements of the ESR of small metal particles fall in four categories: the resonance position, or g shift; the ESR linewidth; the saturability of the resonance or longitudinal relaxation time T_1; and the integrated intensity of the line. All of these factors may be expected to be altered in particles where the discreteness of the electron-level spectrum becomes apparent at low temperatures or where the average level spacing is large compared to the magnetic field. In this section we continue the discussion of the electronic susceptibility of small particles that is made evident, in the case of an ESR experiment, through the integrated intensity of the resonance line. First it is appropriate to describe the scope of ESR measurements and their interpretation, before specializing to the comparision of the electronic susceptibilities that have been extracted from them. The treatment of measurements of g shifts and linewidths is an integral part of the discussion of the resonance intensity. Consequently all of these quantities will be discussed in parallel. Relaxation times, on the other hand, will be presented later in Sec. V.

In some respects the ESR measurement may be thought of as the most direct and unambiguous approach to determining the electronic susceptibility of small particles and therefore particularly suitable for investigating the quantum size effect. For instance it is relatively straightforward to distinguish between atomic and conduction electronic signals. In most cases the atomic ESR is split by the hyperfine interaction giving a characteristic signal for the nucleus of the element under scrutiny. It is also quite convenient that the conduction electron g shift is different for different materials, at least in the bulk. This can be of considerable importance in helping to identify the origins of various signals. In principle, one can expect to monitor the evolution of the ESR signal from the atomic state to the bulk metal during particle growth and thereby have considerable confidence that the results for the intermediate, small-particle state are not spurious. In practice this sort of systematic study has been very difficult to carry out, being partially successful only for a number of materials such as with lithium (Borel and Millet, 1977) or for silver (Châtelain, Millet, and Monot, 1976; Monot, Narbel, and Borel, 1974; Monot and Millet, 1976), and for aluminum (Millet and Monot, 1975). All of the work referred to above is by the Lausanne group at the Ecole Polytechnique Fédérale, who have specialized in cryogenic inert gas matrix isolation of evaporated atoms and their subsequent growth by annealing. In spite of this care, there is a justifiable concern that impurities, free radicals, or localized surface states may be ESR active and be confused with the conduction electron resonance of the particles. In the ideal case one might like to have a material for which the bulk CESR (conduction electron spin resonance) is clearly identifiable at high temperatures, which restricts one's choice, unfortunately, to the lightest of the metallic elements. Then as the temperature is lowered the observed ESR intensity should remain temperature independent until $T \lesssim \delta/k_B$, where upon the onset of a Curie temperature dependence should be seen for odd valence elements. This would demonstrate convincingly that quantum effects were being observed. For ideally isolated particles of an even valence element the intensity should decrease for $T \lesssim \delta/k_B$.

Theoretical understanding for ESR in small metal particles has been established through the work of Kubo (1962), Holland (1967), Kawabata (1970), and Buttet, Car,

and Myles (1982). One of the most remarkable aspects of this subject has been the discovery that ESR of the conduction electrons in many elements is easily observed when the diameter of the particles is less than about 1000 Å. This may not seem surprising for the alkali metals. However, as Holland pointed out, it seems extraordinary that Smith and Ingram (1962) and subsequent workers were able to observe signals without difficulty from colloidal silver particles at room temperature. For silver the spin-orbit interaction is sufficiently large that observation of the resonance from bulk material is only possible at low temperatures (Schultz, Shanabarger, and Platzman, 1967). It is interesting then, to trace current understanding of how the ESR spectrum develops as particle size is decreased.

The peak-to-peak linewidth of the bulk derivative ESR spectrum can be expressed in terms of the electron spin relaxation time τ_s,

$$\Delta H_{\rm pp} \approx (\gamma_e \tau_s)^{-1} \tag{3.17}$$

for bulk metal or large particles, where γ_e is the electron gyromagnetic ratio and τ_s is given by the Elliott relation, Eq. (2.46): $\tau_s^{-1} = \tau_r^{-1} (\Delta g_\infty)^2$. The precise proportionality constant in Eq. (3.17) depends on the line shape. For a Lorentzian, as would be expected for conduction electron resonance, this has the value $2/\sqrt{3}$. The resistivity relaxation time τ_r has a monotonic temperature dependence which, in very pure materials, is associated with electron-phonon scattering, $\tau_r^{-1} = f(T)$. [For sodium, potassium, and aluminum, $f(T)$ is approximately linear in temperature above 77 K.] The Elliott relationship between the g shift and the linewidth appears to be generally valid for bulk material. Experiments confirming this have been reviewed by Beuneu and Monod (1978).

For particles with diameter d, smaller than an rf skin depth, one expects to see an effect of electron spin scattering from the particle surface (Dyson, 1955; Walker, 1971) contributing additionally to the resistivity scattering rate, τ_r^{-1}.

$$\tau_r^{-1} = v_F/d + f(T) \ . \tag{3.18}$$

The regime of size for which Eq. (3.18) holds is that for which the spin diffusion length is greater than the particle diameter,

$$d \ll d_s = [(v_F \lambda)\tau_s/3]^{1/2} \ .$$

Here λ is the electronic mean free path. [See the comments by Gordon (1976) concerning the CESR theory of Walker (1971).] For pure materials d_s may be typically a number of micrometers. This gives the picture suggested by Dyson (1955) where the conduction electron is scattered by the surface of a particle with the probability of a spin flip given simply by Δg_∞^2. Including both the bulk and surface terms the temperature dependent linewidth becomes

$$\Delta H_{\rm pp} \approx \gamma_e^{-1} [f(T) + v_F/d](\Delta g_\infty)^2 \ . \tag{3.19}$$

Consequently one may expect that the ESR line for small particles is broadened inversely in the particle diameter, a rather discouraging prospect. This effect, shown in Fig. 20 for particle diameters larger than 1500 Å, has been clearly identified experimentally in the alkali metals (Gen and Petinov, 1965; Saiki, Fujita, Shimizu, Sakoh, and Wada, 1972; Smithard, 1974b; Sako and Kimura, 1984). However, when the particle diameter becomes sufficiently small the classical scattering picture must be modified. The allowed electronic states should be chosen from a restricted basis set that directly incorporates the particle boundary conditions. This is just the situation described originally by Kubo (1962), where discreteness of the level spectrum comes into play. Holland (1967) and Kawabata (1970) have argued that it follows from this that the small-particle broadening phenomenon, Eq. (3.19), is quenched. This appears to be reasonable from the viewpoint that for well-separated energy levels it should be rather improbable to satisfy energy conservation for an electron-phonon scattering process. Kawabata found that the ESR linewidth in this situation is just that given above in Eq. (3.19), but now multiplied by the factor $\hbar\omega_z/\delta$. This takes the form

$$\begin{aligned} \Delta H_{\rm pp} &\approx \gamma_e^{-1} [f(T) + v_F/d](\Delta g_\infty)^2 \hbar\omega_z/\delta \\ &= \hbar\omega_z/(\gamma_e \delta \tau_s) \quad d \text{ small} \ . \end{aligned} \tag{3.20}$$

The conditions given by Kawabata under which d is suitably small are that

$$\left.\begin{aligned} &\hbar\omega_z/\delta \ll 1 \ , \\ &\hbar/(\tau_s \delta) \ll 1 \ . \end{aligned}\right\} \text{ Kawabata conditions (1970)} \tag{3.21}$$

In the first case one has a condition limiting spin-flip transitions to a particular electronic orbital state. For X-band and lower frequencies ($\nu \leq 9.3$ GHz) this requires that $\delta/k_B \gg 0.5$ K, necessitating that the particle sizes be much smaller than 100—200 Å, depending on the element. (See Fig. 1 or Table V for a more specific measure of this.) The second condition is usually less stringent for the light elements. If the first is satisfied then the second

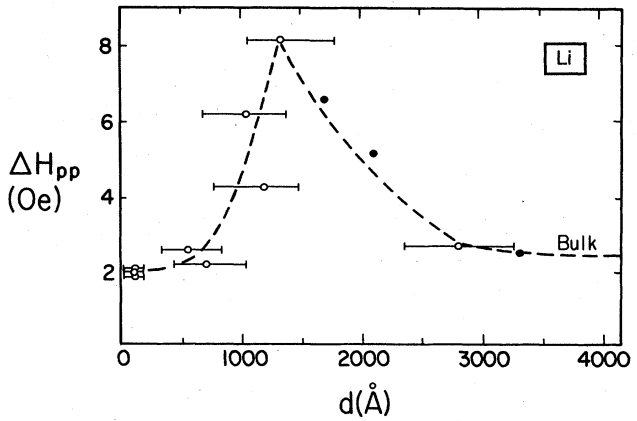

FIG. 20. Lithium ESR linewidths $\Delta H_{\rm pp}$ as a function of particle size showing evidence of quantum narrowing below 1300 Å, as reported by Saiki *et al.* (1972). (○) Saiki *et al.* (1972); (●) Gen and Petinov (1965).

TABLE V. In this table bulk properties of the metallic elements are presented. This is restricted to those elements discussed in this review. The Pauli susceptibility, χ_P; the NMR Knight shift at 300 K, K_{300}; the spin lattice relaxation time multiplied by the temperature, the Korringa constant, and the quadrupole moment of the most abundant nucleus Q, are taken from the compilation *Knight Shifts in Metals* by Carter, Bennett, and Kahan (1977). The Sommerfeld constant γ is obtained from the heat capacity measurements listed by Kittel (1976) and Ashcroft and Mermin (1976). The diameter of a particle that has an average electron level spacing of $\delta/k_B=1$ K is found from the expression, $d_{1K}=55.8(v/\gamma)^{1/3}$ Å. The density ρ and the molar volume v are listed in columns one and two. A graphical representation of these results is given in Fig. 1. The bulk metal conduction electron spin resonance g shift, $\Delta g(\infty)$, is taken from the review by Beuneu and Monod (1978) with the one exception indicated. The zero field superconducting transition temperatures T_c of known superconducting elements are included in this table in the last column.

	ρ (g/cm^3)	v (cm^3/mole)	γ (mJ/mole K^2)	d_{1K} Å	χ_P (10^{-6} emu/mole)	A	K_{300} (%)	T_1T (sec K)	Q (b)	$\Delta g(\infty)$	T_c (K)
Li	0.53	13.1	1.63	112	27	7	0.026	44	−0.04	-6.1×10^{-5}	
Be	1.85	4.9	0.17	171	1	9	−0.0025	1.8×10^4	0.05	$9(14)\times10^{-4}$ [d]	0.023
Na	0.97	23.7	1.38	144	29	23	0.113	4.6	0.14	-8×10^{-4}	
Mg	1.74	14.0	1.3	123	18[a]	25	0.112		0.22	$<10^{-2}$	
Al	2.70	10.0	1.35	109	30	27	0.161	1.81	0.15	-5×10^{-3}	1.196
K	0.86	45.5	2.08	156	50	39	0.26	25	0.055	-2.6×10^{-3}	
Ca	1.54	26.0	2.9	116	42[a]	43				-1.9×10^{-3} [e]	
V	6.1	8.35	9.26	54	255	51	0.58	0.79	−0.05		5.30
Cu	8.96	7.09	0.70	121	13.3	63	0.24	1.27	−0.211	3.1×10^{-2}	
Rh	12.4	8.30	4.90	67	103	103	0.43	9	0		0.000 325[f]
Pd	12.0	8.75	9.42	54	557	105	−3.05	0.7	0.8	0.24	
Ag	10.5	10.3	0.65	140	9.6	107	0.52	12	0	-1.9×10^{-2}	
In	7.31	15.7	1.69	117	33	115	0.82	0.08	0.83		3.40
Sn	7.30	16.3	1.78	117	29	119	0.72[b]	0.05	0		3.72
Os	22.6	8.42	2.4	85	33[a]	189	2.4[c]		0.8		0.655
Pt	21.4	9.12	6.8	62	192	195	−2.92	0.033	0		
Au	19.3	10.21	0.73	134	12	197	1.65	4.6	0.58	0.10	
Pb	11.2	18.17	2.98	102	43[a]	207	1.50	0.025	0		7.19

[a]Susceptibility calculated assuming free electron behavior, $\chi_P\approx3(\mu_B/\pi k_B)^2\gamma$.
[b]Isotropic Knight shift at 300 K.
[c]Estimated.
[d] $\|$ ($\perp$) configuration.
[e]From Damay *et al.* (1974).
[f]From Buchal *et al.* (1983).

requires that the bulk linewidth be $\Delta H_{pp}\ll5$ kOe. This is the case for most pure materials with weak spin-orbit coupling. Since δ varies as d^{-3} and $f(T)$ can be neglected at low temperatures, one finds from Eq. (3.20) that the linewidth should decrease as the square of the particle size. The results of Saiki *et al.* (1972) and Gen and Petinov (1965) for Li particles are shown in Fig. 20 indicating this behavior. It is commonly believed that this manifestation of the quantum size effect is the reason for facility of observation of CESR signals in heavy metal, small-particle samples, which would otherwise have very broad resonance lines. See, for example, the work on gold particles by Dupree, Forwood, and Smith (1967). The experimental work on lithium indicates that the condition for observation of quantum narrowing of the ESR line is that the size should be less than 1300 Å, Fig. 20. This is a factor of 10 less severe a constraint than that given by the Kawabata inequalities, Eq. (3.21). The reason for this discrepancy is not understood.

As the sample size is decreased below that determined by the conditions of Eq. (3.21), one should expect according to Kawabata (1970), that the g shift has the term $-\hbar/\delta\tau$, which disappears proportional to $-d^2$. This means that the g shift approaches the bulk metal value in the limit of small-particle size,

$$\Delta g=\Delta g_\infty-\hbar/\delta\tau_s \quad \text{(Kawabata 1970)}. \tag{3.22}$$

Consequently, in this theory the linewidth has the same dependence on size as the g shift and both of these are independent of the temperature, provided that $f(T)$ is sufficiently small. For a real system the particle-size distribution leads to a distribution of shifts and widths that produce inhomogeneous broadening of the ESR line. This can be thought of as a superposition of very narrow, easily saturated resonances with $T_1^{-1}<\gamma_e\Delta H_{pp}$. More recent work by Buttet, Car, and Myles (1982) takes issue with the g-shift calculation of Kawabata despite the excellent agreement shown in Fig. 7 for the spin-orbit matrix elements. They found from orthogonalized standing-wave calculations (OSW) for a sodium metal cube that the g shift is most significantly affected by surface contributions which approach the *atomic value* according to d^{-1}. Their calculation for sodium particles can be best summarized as

$$\Delta g=(1-f_s)\Delta g_\infty+f_s\Delta g_s \quad \text{(Buttet } et\ al.\text{, 1982)}, \qquad (3.23)$$

where f_s is the fraction of atoms at the surface (dispersion) and Δg_s is the contribution of a surface atom to the total g shift. This theoretical result is consistent with experiments on Mg particles (Millet and Borel, 1982) as will be discussed later. Buttet *et al.* (1982) also calculated the term contributing to the g shift that Kawabata had discussed but for the specific case of the sodium cube. They found that this term was small; however, the high degree of symmetry in their model particle produces a degeneracy of the electronic levels which in turn leads to larger energy intervals between states. For this reason their calculation of the Kawabata term is probably an underestimate for that appropriate to a particle with irregular surface conditions. The sodium cube calculation was extended to spherical particles by Myles (1982) finding results consistent with Eq. (3.23) from which it was concluded that a specific particle symmetry was not important.

The integrated intensity of the resonance is proportional to the susceptibility and can be expected to show the temperature dependence characteristic of the quantum size effect, Eqs. (2.28), (2.42), and (2.43). For even valence metals having negligible chemical interaction with the matrix, and small spin-orbit coupling, this should reduce to zero at low temperatures proportional to the temperature. For odd-electron-numbered particles, a Curie-type behavior is anticipated, growing out of a temperature-independent Pauli susceptibility as k_BT/δ becomes significantly less than 1. It should be emphasized that according to the theory (Kawabata, 1970), manifestation of the quantum size effect through observation of a narrow resonance line can take place at any temperature where the conditions of Eq. (3.21) hold. This condition is essentially independent of temperature except for such cases where $f(T)$ contributes significantly to the linewidth. Finally, we can expect that for either large magnetic fields or large spin-orbit interaction, the small-particle ESR intensity associated with quantum effects will be temperature independent, Eq. (2.18).

The experimental work has been performed on Li, Na, K, Mg, Ca, Al, Ag, Pt, and Au particles and will be reviewed in this order.

2. Alkali metals (Li, Na, K)

Early work on particles of Li, beginning with that of Gen and Petinov (1965) focused on documenting the small particle linewidth effects and measuring the g shift (Taupin, 1967; Saiki *et al.*, 1972; Borel, Borel-Narbel, and Monot, 1974). Later temperature-dependence studies of the integrated intensity of the ESR signal were performed by Borel and Millet (1977) who found a Curie law temperature dependence for very small particles, $d \leq 100$ Å. They interpreted this as evidence for the quantum size effect. Their samples were prepared by vacuum evaporation with cryogenic matrix isolation provided by either solid CO_2 or xenon. They found the interesting result that the use of a CO_2 matrix led to unexplained broadening of the ESR line as had been previously reported by Borel, Borel-Narbel, and Monot (1974). However, it was discovered that this could be avoided with the use of the rare gas Xe as a matrix material. With this ammendment, their Li ESR linewidths were consistent with the earlier measurements of Saiki *et al.* (1972), Fig. 20, whose samples had been prepared by inert gas evaporation followed by encapsulation in paraffin. It is interesting to note that recent ESR experiments on lithium films (Eigler and Schultz, 1985) show evidence for a significant conduction electron density at the site of surface adsorbed xenon indicating that this may not be an ideal, passive matrix either. For the smallest Li particle sizes at sufficiently low temperatures, Borel and Millet (1977) observed a significant departure from a temperature-independent ESR intensity. In the case of 32-Å particles this occurred below 20 K as is shown in Fig. 21. Unfortunately, they found that it was difficult to make reliable electron microscope measurements of the size distributions for Li particles with diameters less than 100 Å. They were forced to estimate the size of the particles in this range assuming that their observations could be accounted for by the quantum size effect. Consequently this work cannot be considered as an independent quantitative verification of details of the theory. It is, however, the only work reported to date which shows a clean evolution of the ESR intensity from a temperature-independent value at high temperatures to a Curie law dependence at low temperatures signaling the presence of the quantum effects on the electronic susceptibility as was predicted for odd particles. It is important to emphasize that during the heat treatment process that was used to promote particle growth, their small-particle signals grew, while at the same time the easily identified atomic hyperfine-split signals disappeared from the ESR spectrum. This means that it is very unlikely that the ESR they observed could come from any other source than the conduction electrons of

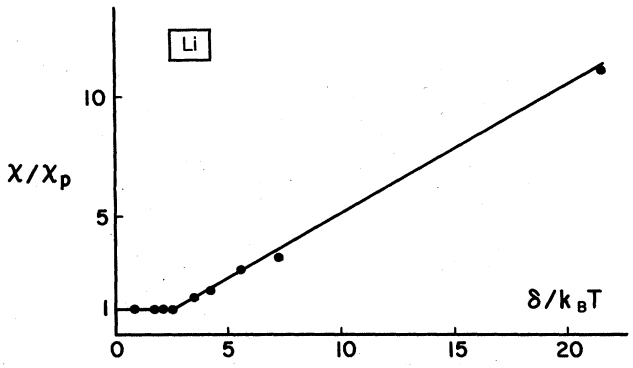

FIG. 21. The integrated intensity of the Li ESR line as a function of temperature measured by Borel and Millet (1977) for an average particle size estimated to be 32 Å for which $\delta/k_B=45$ K. The results are normalized to the temperature-independent value found above 20 K. The observed Curie-type dependence of the electronic susceptibility at low temperatures is clear evidence of the quantum size effect.

the Li particles themselves. For 100 Å and larger particles neither Saiki *et al.* (1972) nor Borel and Millet (1977) were able to observe a temperature dependence to the intensity down to 1.5 K (Saiki *et al.*). This negative result is consistent with the average level spacing being too small for these sizes to show the expected temperature-dependent behavior. The value of δ/k_B taken from Fig. 1 gives 1.4 K when $d=100$ Å so that quantum effects would be easily observable for this case only below ≈ 0.5 K, beyond the range of temperatures investigated.

In all cases the g shifts of the lithium resonances were found to be equal to the free-electron value within experimental accuracy. Since the bulk g shift is so small for this material, Table V, it is not practicable to use Li particles to test the theoretical g-shift calculations.

For sodium the situation is not nearly as clearcut. Both Smithard (1974b) and Gordon (1976) were unable to make any interpretation of their ESR intensity measurements in terms of the quantum size effect. Both of their samples were made by x-ray irradiation of crystalline NaN_3 (sodium azide) producing small metallic clusters that were increased in size by annealing. Unexplained broadening appeared at low temperatures in addition to that from scattering from the electron surface, Eq. (3.19). It was suggested (Gordon, 1976) that this might be attributed to exchange broadening from surface or matrix impurity spins. In other work, either larger particle samples were used (Petinov and Ardashev, 1969), or data were taken only at high temperatures where no anomalous broadening, or quantum size narrowing, has been reported (McMillan *et al.*, 1962). The one instance of interpretation of a sodium particle ESR signal in terms of the quantum size effect is that of Gordon (1976) who reported observing a broad (28 Oe), easily saturable signal that appeared in one of his irradiated NaN_3 samples at 4.2 K. He suggested this signal could be attributed to electron energy-level separation effects despite the presence of the broad line which clashes with the ideas advanced by Holland (1967) and Kawabata (1970). Gordon explained this source of broadening in terms of the nuclear-hyperfine contact interaction. However, there is contrary experimental evidence for this model from work with Li (Borel and Millet, 1977), where no such hyperfine effects were observed and so it seems that it is highly speculative to base interpretation of this one datum on quantum level size effects.

The fact that no evidence of quantum line narrowing has been reported for sodium particles may mean that the single fabrication method used so far is unsuitable. Perhaps, as Gordon (1976) suggests, the sodium azide irradiation technique introduces broadening from exchange coupling to impurity spins.

Very little work has been reported for small potassium clusters (McMillan, 1964) and none sufficiently extensive that a relationship with the predictions of the quantum size effect can be established.

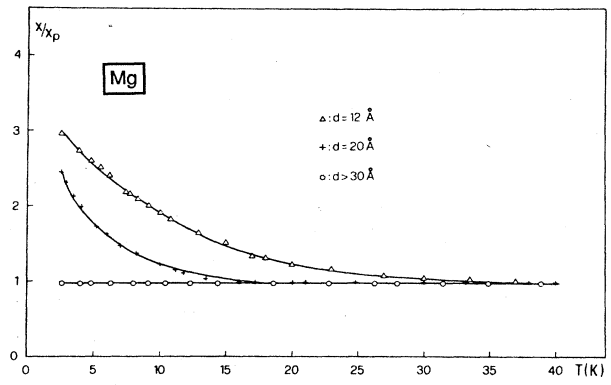

FIG. 22. The integrated intensity of the Mg ESR line as a function of temperature measured by Millet and Borel (1981) for three sample sizes. The results are normalized to the temperature-independent value found at high temperatures which was taken to be the Pauli susceptibility χ_P. This result is discussed in the text compared to the quantum size theory. Note, however, that this result is rather different from that of Kimura, Bandow, and Sako (1985) shown in Fig. 10.

3. Alkali earths (Mg, Ca)

Of the alkali earths, which are doubly valent, there have been studies of small particles of only Mg and Ca. Magnesium particles were investigated by Millet and Borel (1981,1982), and Sako and Kimura (1984,1985). The latter authors have also reported measurements on Ca. Millet and Borel (1981) used the atomic beam and solid-xenon, cryogenic-matrix isolation methods to obtain very small particles in three size groups $d=12$, 20, and ≥ 30 Å. Their results for the temperature dependence of the integrated intensity of the ESR line are presented in Fig. 22. The linewidths and g shifts of the resonance signals were described in detail in a later publication (Millet and Borel, 1982). As shown in the figure, they found that the intensity of the signals in the larger size group was temperature independent down to 2.6 K. However, the signals from the other samples indicated an increase in intensity below 35 and 20 K, respectively. They interpreted this in terms of a quantum effect involving odd-electron-numbered particles. This result is slightly surprising at first sight since the valence of Mg is even. Either charge neutrality of the metal particles is not maintained or the theory is inadequate in this case. It is useful to compare the temperature T_0 at which a point of departure from a temperature-independent intensity is observed, with the temperature given by the condition for observation of quantum effects, $\delta/k_B T \gtrsim 1$. For the three sizes quoted the latter gives 1100, 240, and 70 K, all very much larger than the departure temperature points, $T_0=35$, 20, <2.6K. By the same token, one expects from the quantum size theory much larger susceptibilities from odd particles than were observed, if indeed it is appropriate to suppose that a significant number of these Mg particles

had odd electron number. If a large majority of particles were even numbered the measured intensity would have been expected to decrease below the Pauli value at much higher temperatures, and this was not observed. It is unlikely that an ESR from impurities could account for the temperature dependence of the intensity since it would also be required to explain why the quantum size effect on the electronic susceptibility was suppressed by an order of magnitude below that which would have been otherwise expected. One possible explanation of these results is the following. The g shift of the bulk material, used in the fabrication of these particles, was found to be $g=2.06$ in contrast to presently accepted values for that of pure magnesium $g=2.00$ (Oseroff, Gehman, and Schultz, 1977; Beuneu and Monod, 1978), and that found by Sako and Kimura (1984) for small Mg particles, $g=1.997$. There is a possibility that this behavior of the g shift may be ascribed to some sort of an impurity effect. Millet and Borel (1982) analyzed the g-shift dependence on particle size in terms of the theory of Buttet *et al.*, Eq. (3.23). They found, as shown in Fig. 23 that the g shift varied as d^{-1} consistent with this theory. Without specifying what the origin might have been for the very large g shift in the bulk starting material, this measurement suggests the existence of an enhanced spin-orbit coupling in their samples. From Shiba's theory (1976) one can calculate a spin-orbit coupling parameter, $\rho=1.1$. This implies a very strong suppression of even-odd—electron-number anomalies and the attendant effect that the temperature dependence of the susceptibility would be washed out. This is approximately what is observed.

Sako and Kimura (1984) observed narrow, small-particle ESR signals from both Mg and Ca. For the Mg resonance the spectrum appeared to be a superposition of two contributions, a narrow signal ($\Delta H_{pp}\approx 14$ Oe) and a wide line ($\Delta H_{pp}\approx 500$ Oe), assumed to be that of the bulk metal. The relative amplitudes of the narrow signals, compared to the broad lines was always much less than 1%. For Ca only a narrow resonance was seen ($\Delta H_{pp}\approx 5$ Oe). Their preparation technique was to evaporate the metal in an inert gas required for nucleation of the particles. Isolation and encapsulation with a mixture of paraffin and Vaseline was found to be necessary for Ca, a material that is more easily oxidized than Mg. The samples had size distributions centered at values in the range 200—2500 Å. These sizes are relatively large compared to the Kawabata conditions for quantum effects, Eq. (3.22). These would only be satisifed with $d\lesssim 200$ Å for either Mg and Ca at 9.3 GHz. It should be recalled that a similar discrepancy was reported in the case of lithium. Sako and Kimura suggested that one interpretation of the narrow lines could be in terms of quantum effects on the ESR spectrum which arise from the smallest particles in the tail of their particle-size distributions. Another possible explanation that they brought forward related to the presence of the surface between metal and oxide that might have had ESR active sites. They reported a temperature dependence of the intensity of the ESR, weaker than Curie's law but showing up significantly at 200 K. This is just the opposite extreme from that reported by Millet and Borel (1981), where deviations from Curie's law were observed, but for $d\lesssim 20$ Å and at temperatures below 35 K. Despite this contrast in magnitude and a large difference in observed g shifts for their bulk material, Sako and Kimura point out that the nature of the narrow component of the Mg spectrum was quite similar in both cases, in that they exhibit a low-field shoulder and appear at approximately the same g value. It is however, not particularly fruitful to force a comparison of these measurements for which sizes are so radically different.

In summary some of the ESR results for Mg can be interpreted in terms of the size effect theory, but there remains ambiguities with this approach and other possible explanations have been suggested.

The results of ESR experiments with Ca particles by Sako and Kimura (1984) are similar to those they reported for Mg. The preparation techniques differed only insofar as the Ca particles were encapsulated in a mixture of paraffin and Vaseline in order to inhibit oxidation and the average size in this case was varied from 300 to 2000 Å. The Ca ESR line indicated several narrow components for which the linewidths were proportional to the frequency. The narrower one was $\Delta H_{pp}\approx 5$ Oe. A bulk metal contribution was not seen in contrast to their Mg spectra. The narrow lines for both metals appeared with larger negative g shifts than in the bulk. Sako and Kimura found that the narrow lines could be more easily saturated and that they increased in intensity somewhat more weakly than Curie's law as the temperature decreased, in very much the same way for Ca as for Mg. Their interpretation of these results in terms of the quantum size effect was equally as guarded for this material. Since only relatively large particles were investigated, quantum effects could be evident only for the smallest

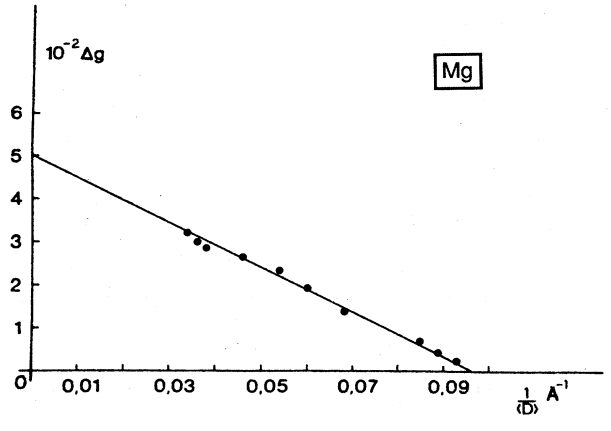

FIG. 23. The g shift for small Mg particles determined by Millet and Borel (1982), showing a size dependence consistent with the predictions of Buttet *et al.* (1982) given in Eq. (3.23).

particles in the size distribution about which only qualitative arguments could be made.

4. Aluminum

Millet and Monot (1975) have used the atomic beam methods to isolate aluminum atoms in cryogenic matrices of both benzene and carbon dioxide. The formation and growth of particles between 90 and 120 K was monitored simultaneous with the decline of the atomic ESR signal that could easily be identified from its characteristic hyperfine splitting. They found large positive g shifts for the metal particles, $\Delta g = 0.02$, which can be compared to accepted values for the bulk taken at 9.2 GHz, $\Delta g_\infty = -0.005$ (Schultz, Dunifer, and Latham, 1966). This effect on the g shift cannot be understood in terms of either the Kawabata (1970) or Buttet *et al.* (1982) theories. However, the bulk g values are known to have a significant frequency dependence, thought to be associated with many-body exchange effects (Lubzens *et al.*, 1972). How this mechanism might depend on particle size is not at all clear. The linewidths were found to scale with frequency for measurements at 35, 9.3, and 0.45 GHz. This is consistent with the theoretical quantum effect predictions, Eq. (3.20). No information about the temperature dependence of the integrated signal intensity is available nor were particle sizes varied in a systematic way.

5. The noble metals (Ag, Pt, Au)

Most of the ESR work on silver particles, for which the question of size effects is discussed, has been performed by the Lausanne group (Smithard, 1973; Monot, Narbel, and Borel, 1974; Châtelain, Millet, and Monot, 1976; Monot and Millet, 1976). On the other hand, narrow-line ESR has been reported by a number of other groups working with silver heterogeneous catalysts such as in the study by Abou-Kais, Jarjoui, Vedrine, and Gravelle (1977) performed at 77 K or the recent efforts by Grobet and Schoonheydt (1985) with very small silver clusters formed in the sodalite cages of a zeolite. In the former case, Abou-Kais *et al.* (1977) make contact with the quantum size theory incorrectly in their estimation of the signal intensity. At temperatures large compared to the average level spacing (≈ 20 K for their samples) the integrated ESR intensity should be proportional to the Pauli susceptibility and not the susceptibility of free ions with a concentration of one ion for every two particles, as was claimed.

Smithard (1973) made samples of silver particles by immersing thin glass plates in molten AgCl at 600 °C. Silver ions diffused into the glass where they were reduced to form colloidal metal particles. The exposure time to the AgCl, or stain time as Smithard called it, determined the particle size. This was analyzed using electron microscopy and optical absorption measurements interpreted with either the Mie theory (1908), see Sec. VI, or the quantum theory of Kawabata and Kubo (1966). Unfortunately no ESR was found by Smithard either at room temperature or 7.5 K despite good spectrometer sensitivity and for particles in the range 10—300 Å that could be expected to satisfy the Kawabata conditions, Eq. (3.22).

Monot, Narbel, and Borel (1974) were more successful in finding an ESR signal with silver particles prepared by two very different techniques. In one case a method was used that involved the reduction of Ag_2O with hydrogen, precipitating colloidal metal clusters that became dispersed on the container surface where they could be collected. The second approach was the atomic beam and cryogenic matrix isolation method mentioned earlier. With the latter technique larger concentrations of particles could be obtained. It was verified with electron microscopy, that small particles of silver with diameters between 10 and 60 Å were being produced, however no detailed information concerning particle size distributions was obtained. Consequently, to test the Kawabata theory, the g shift was plotted as a function of the linewidth for a large number of samples with the size of the particles an implicit, but unmeasured, variable. It will be recalled that the theoretical work, Eqs. (3.20) and (3.22), suggests that there should be a linear relation between these two parameters with the smallest particles having the narrowest lines and the bulk metal g shift. From their analysis it was deduced that the bulk g shift must be $\Delta g_\infty = 0.025$ for Ag samples prepared by either method. This is in poor agreement with the bulk metal results of Schultz, Shanabarger, and Platzman (1967), $\Delta g_\infty = -0.019$. Despite this discrepancy it was concluded that there was qualitative agreement with the Kawabata theory in so far as an approximately linear relation between linewidth and g shift was found. This unsatisfactory situation led Châtelain, Millet, and Monot (1976) to explore this comparison further. They tried different isolation matrices and performed numerical simulation of the ESR lines associated with various size distributions. Although the line shapes could be reproduced fairly well with appropriate size-distribution parameters, the difficulty in accounting for the g shift for silver particles was not clarified.

Up until this point there had been very little information concerning the intensity of the resonance for Ag particles. In another publication Monot and Millet (1976) specifically addressed this question. A sample of ≈ 10-Å particles was prepared by atomic beam methods in a benzene cryogenic matrix and size-distribution analysis was performed with electron microscopy. The ESR measurements were taken as a function of temperature from 8 to 190 K at the X band (9.3 GHz). They found that the g factor was 2.007 for this sample which cannot be directly compared with the earlier measurements of Monot, Narbel, and Borel (1974) since information about the linewidth is not given. In this work effort was directed at obtaining absolute measurements of the integrated ESR signal as a function of the temperature. This was found to be rather close to a Curie law for the one sample discussed in detail and for the temperature range investigat-

ed. The highest temperature was apparently limited by the choice of matrix and the requirement that the particles not grow larger during the measurement. Fitting the experimental results to the theory (Denton, Mühlschlegel, and Scalapino, 1973) gave an average level spacing of $\delta/k_B = 6600$ K. From Fig. 1 we can estimate that this corresponds to an average size of slightly more than 7 Å. This result is nicely consistent with the electron microscopy measurements. It would have been useful to conduct a more extensive analysis of this sort of experiment by varying the average particle size and, as was suggested by Monot and Millet, taking ESR spectra to higher temperatures where the temperature-independent Pauli susceptibility might have been recovered. Had they been successful in obtaining a measurement of a temperature-independent ESR intensity at high temperatures they would have had more convincing evidence for the origin of the Curie-type signal. In addition this would have provided an important calibration check of the absolute measurements of the intensity. They exercised considerable care in trying to eliminate the possibility of extraneous signals giving some confidence in the interpretation that odd-particle quantum effects on the susceptibility were in fact observed.

ESR signals from Pt particle samples have been investigated by Gordon, Marzke, and Glaunsinger (1977). Samples with an average size of 21 Å and a very narrow particle-size distribution were prepared by chemical reduction methods and then were embedded in a gelatin matrix. The magnetic susceptibility of these or similar samples was also studied by Faraday balance methods and has been discussed earlier in Sec. III.A. In the ESR work, Gordon *et al.* (1977) found that there was a free-electron-like signal at $g = 2.002$ with a width of 20 Oe having a Curie law temperature dependence in the range 17 K to room temperature. The amplitude of the signal was approximately an order of magnitude weaker than that which one might have expected if half of the particles had odd numbers of electrons. It was also observed that the resonance was quite easy to saturate and that the linewidth was the same at the two frequencies of 10 and 24 GHz that were used. This last result is not expected in the Kawabata (1970) theory, which finds that the resonance linewidth should be proportional to the observation frequency, $\Delta H_{\rm pp} = \hbar\omega_z/(\gamma_e \delta\tau_s)$, Eq. (3.20). The reduced intensity, however, might be a consequence of the large spin-orbit interaction in Pt giving rise to a reduction in the effective moment of the Pt particles according to the theory of Shiba (1976) or Sone (1977), expressed in Eq. (2.43). The essentially zero g shift is rather unexpected for Pt although there are neither atomic nor bulk metal ESR measurements with which one can compare. In light of these difficulties Gordon *et al.* (1977) have considered other possible sources for the signal suggesting that an Fe^{3+} impurity might be a more likely alternate candidate.

Measurements of ESR in gold particles have been performed by Dupree, Forwood, and Smith (1967) and Monot, Châtelain, and Borel (1971). In the work of Dupree *et al.*, Au particles were formed following evaporation in a relatively poor vacuum of 10^{-5} Torr on cleaved crystals of NaCl held at room temperature. Electron microscopy revealed particles of mean diameter of 30 Å separated by a distance of 200 Å. ESR measurements at 9.3 GHz were made over the temperature range from 180 K to room temperature. No ESR was observed for particles with larger average size than 40 Å, or for smaller sizes than 20 Å. A temperature-independent g shift in the range $0.22 < \Delta g < 0.27$ described all of the 20 samples that were investigated. A linewidth of order 200 Oe was found that varied by as much as 100 Oe from sample to sample. A modest decrease in the linewidth with decreasing temperature was noted. These results can be contrasted with those of the bulk metal obtained by Monod and Janossy (1977) using the reliable transmission technique through slabs of pure gold. They measured the g shift to be $\Delta g_\infty = 0.11$ and found that the linewidth was 800 Oe for a 100 μm-thick gold slab below 10 K, but increased rather sharply with increasing temperature. The discrepancy between the small-particle results and the bulk g shifts is not understood and does not fit in with any of the existing theories. The g value at room temperature measured for Au particles by Monot *et al.* (1971) was found to be identical to that of free electrons ($g = 2.0023$) and the linewidths were found to vary between 6 and 9 Oe. The samples were made by annealing ultrathin, 10-Å gold films deposited on quartz substrates. Heat treatment was shown to promote dislocation of the film and formation of small particles, generating crystals of well-defined shape and size with diameters in the range 20—80 Å. Here also it is difficult to account for the g shifts of the small-particle samples from the theory (Kawabata, 1970; Buttet, Car, and Myles, 1982) if indeed the observed resonances can be associated with the conduction electrons as was claimed. A rough estimate of the size of gold particles that might be necessary to satisfy the Kawabata conditions based on the relaxation time measurements of Monod and Janossy (1977) gives the requirement that $d \ll 5$ Å for temperatures below 10 K. Obviously this is not consistent with the experimental situation, but then a similar situation was found for lithium particles *vis-à-vis* the Kawabata conditions.

The experiments with small particles of platinum and gold are not sufficiently extensive that a quantitative comparison with theory can be made, particularly with regard to the ESR intensity and thence with the electronic susceptibility. Nonetheless it seems that quantum narrowing may be effective in allowing observation of the ESR at various temperatures and for particle sizes where it would be impossible to observe the resonance in the bulk. If this is the case, it must also mean that the application of the Kawabata conditions, Eq. (3.22), is excessively stringent in defining an upper bound on sample diameters for which ESR line narrowing may be observed, as was the case for Li particles. There, the line narrowing was reported for particles smaller than 1300 Å, Fig. 20. The Kawabata conditions for this to be observed in lithium particles require that their size be substantially smaller than 200 Å.

6. Summary of ESR experiments and the quantum size effect

Metal particle samples are inherently inhomogeneous. The presence of a matrix or oxide coating and its interface with the metal introduce additional variables in the problem. Consequently, it is quite difficult to be assured that the ESR of the metal particle samples is indeed conduction electron resonance and not associated with either the surface of the particle or of the matrix itself. Of course, it is helpful in principle that the bulk g shift varies from one material to another. In practice there is no clear general trend for the behavior of the g shift as a function of particle size although there are specific theoretical predictions. The measurements of Millet and Borel (1982) on the g shift of Mg particles, Fig. 23, appear to be the most comprehensive and in agreement with the theory of Buttet *et al.* (1982) despite reservations concerning the quality of their starting material.

The observation of line narrowing with decreasing size for small particles such as for lithium (Gen and Petinov, 1965; Saiki *et al.*, 1972) is consistent with theoretical expectations for quantum line narrowing (Kawabata, 1970). It is somewhat disconcerting that the theory stipulates conditions for observation of this effect that are at odds with the observations. For example in Li, narrowing of the ESR occur for particle sizes such that $\hbar\omega_z/\delta \leq 500$ in contrast with the theoretical constraint $\hbar\omega_z/\delta \ll 1$. There is a similar difficulty with the measurements on gold particles performed by Monot *et al.* (1971). It is interesting that in the case of Li it is the first of the Kawabata conditions that is in question, while for gold it is the second one that appears to be too strong by roughly 2—3 orders of magnitude. For Na particles no line narrowing was observed and this may be associated with an effect of impurity spins in the matrix (Smithard, 1974b; Gordon, 1976). Although narrow ESR lines have been observed for samples of other elements no systematic study of different sizes has been reported that is sufficiently comprehensive to indicate a transition of the linewidth from the classical to the quantum size regime.

The intensity of the ESR line is proportional to the electronic susceptibility. This has been studied carefully as a function of temperature, showing convincing evidence for odd-electron-number particles in the case of lithium (Borel and Millet, 1977), Fig. 21, magnesium (Millet and Borel, 1981), Fig. 22, and silver (Monot and Millet, 1976). Even in these cases, agreement with the theory is sketchy largely because measurements as a function of particle size have not been extensive. Only in the case of magnesium have measurements for different sizes been reported and this work shows that the signal intensity is much smaller than that expected for the particles to have odd-electron number, and inconsistent with there being a majority of even particles as might have been anticipated since the valence of magnesium is even. It may be possible to account for these observations if one postulates both that the majority of particles are odd in electron number, and that there is a large spin-orbit interaction, as suggested by the g-shift measurement.

In summary there are some puzzling features of the ESR data although evidence of quantum effects on the linewidth and intensity are unambiguous in a number of cases. In none of these, however, is there sufficient detail that one can extract information concerning the statistical distribution of energy levels.

IV. HEAT CAPACITY

There are essentially no measurements that have been performed of the heat capacity of small metal particles that show evidence for quantum electronic size effects. The one exception is a sample of platinum powder embedded in slica for which Stewart (1977) reported a reduced heat capacity at the lowest temperatures at which he was able to work. He argued that this result could be a manifestation of the quantum size effect, an interpretation which may not be unique. In all other cases only *enhancement* of the heat capacity has been reported and this has been attributed, either to quantum effects on the vibrational spectrum in small particles, or an increased electronic heat capacity most likely associated with the particle's surface states. Experiments have been conducted on Al, V, Pd, In, Sn, Pt, and Pb. Only two of these, Pd and Pt, are nonsuperconducting metals. In the case of the superconducting elements, we will focus on the normal metal behavior. The earlier discussion of Sec. II addresses the possible effects of discreteness of the electronic energy spectrum on the heat capacity. This should be kept in mind while reviewing the data, although, in fact, this theory turns out to be unnecessary for the interpretation of work reported so far. Consequently, this section begins with an introduction to other size effect theories.

A. Heat capacity theories for small particles

1. The vibrational spectrum

The application of the theory of lattice vibrations in an infinite medium to a particle with finite physical extent and restricted degrees of freedom produces two important effects. The first is that there are surface modes; new modes of lower frequency that contribute to the specific heat. The second is that the large wave-vector limit is truncated by the restricted geometry of the particle (Schafer, 1921; Planck, 1921). Following experimental work of Novotny, Meincke, and Watson (1972) and Novotny and Meincke (1973) on lead indium spherical particles there was stimulation for theoretical work to interpret the observed lattice enhancements in the heat capacity. The first of these more recent calculations was that of Baltes and Hilf (1973). These authors considered an improvement over previous calculations that were restricted to semi-infinite media leading to a quadratic temperature-dependent enhancement to the heat capacity

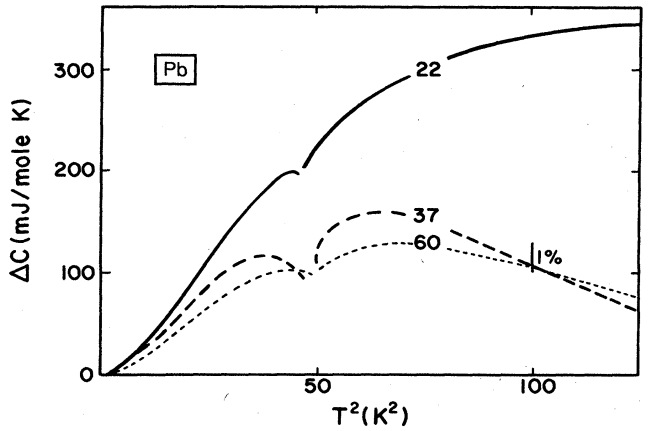

FIG. 24. The enhancement of the heat capacity of small lead particles of 22, 37, and 60 Å diameter measured by Novotny and Meinke (1973). The effect shown here can be principally associated with the vibrational spectrum of the metal. Electronic effects associated with the superconducting transition are evident near $T^2=50$ K^2. The bar indicates the relative size of ΔC to the total small-particle specific heat at one temperature.

associated with surface modes (Dupuis, Mazo, and Onsager, 1966; Maradudin and Wallis, 1966; Dickey and Paskin, 1970; Burton, 1970). These can be summarized as

$$C=BST^2+AVT^3 . \tag{4.1}$$

The surface contribution scales with the surface area S and the second term, the normal bulk contribution to the heat capacity, is proportional to the volume V, where A and B are constants. Baltes and Hilf (1973) avoided the use of a high-temperature expansion and explicitly carried out summation over the first 183 modes for a freely suspended homogeneous Pb sphere, 22 Å in diameter. The introduction of a cutoff in the spectrum owing to the finite particle size leads to a reduction in the surface-mode enhancement effect at sufficiently low temperatures. For 22-Å lead particles this corresponds to $T\ll 8$ K at which temperature a maximum enhancement was predicted. The experiment, Fig. 24, is qualitatively consistent with this. At extremely low temperatures one might expect only a single mode contribution. This would lead to an exponential decrease in the heat capacity precisely as expected for the electronic behavior of a metal particle and given by Eq. (2.5) (Baltes and Šimànek, 1981). A rough estimate of the energy of the lowest mode can be made setting the perimeter of the particle equal to a half-wavelength,

$$h\nu\equiv k_BT_0=\hbar v/(k_Bd) . \tag{4.2}$$

This gives $T_0=10$ K for a 25-Å particle where v is an average sound velocity taken to be 3×10^3 m sec^{-1}. One might speculate that the vibrational spectrum for a collection of many particles with different shapes and sizes would require a statistical description giving rise to a different sort of quantum size effect: a distribution of low-frequency modes having a weaker than exponential temperature dependence for the total heat capacity. This sort of theoretical approach has not yet been pursued.

One can account for the size effects in the vibrational spectrum of a freely suspended sphere (Neumann boundary conditions) giving an enhancement to the heat capacity from those eigenmodes that satisfy an appropriate wave equation (Lautenschläger, 1975; Baltes and Šimànek, 1981; Nishiguchi and Sakuma, 1981; Tamura, Higeta, and Ichinokawa, 1982)

$$C=\sum_l\sum_s\frac{3(2l+1)k_B\xi^2\exp\xi}{4\pi R^3[\exp(\xi-1)]^2} . \tag{4.3}$$

Here $\xi=\hbar va'_{l,s}/(k_BRT)$ and $a'_{l,s}$ is the sth zero of the derivative of the spherical Bessel function of order l. There are a number of ways proposed for limiting the summations above in order to account for both the discreteness in the vibrational spectrum and the finite number of possible modes. The latter is usually expressed by defining a maximum l for which $\sum(2l+1)=N$ where N is the number of atoms in the crystal. A different cutoff condition is used by Tamura *et al.* (1982). According to Baltes and Hilf (1973), the eigenfrequencies are $\omega_{l,s}=va'_{l,s}/R$ and $v=v(R,T)$ is the effective sound velocity that is both dependent on size R and temperature T. This is considered as an adjustable parameter in their theory. The size cutoff constraint mentioned earlier leads to a largest zero $a'_{\max}$ that in turn can be used to define an effective Debye temperature of the particle in terms of the effective sound velocity,

$$\theta_D(R,T)=\hbar a'_{\max}v(R,T)/k_BT . \tag{4.4}$$

Fitting to the experimental data of Novotny and Meincke (1973) leads to lower values of the Debye temperature and sound velocity than for the bulk as might be expected. Lautenschläger (1975) used the same scalar wave equation approach as Baltes and Hilf (1973), summing over the different longitudinal and transverse branches of the phonon spectrum, extending the work to higher temperatures, and considering clamped and free surface conditions. The results of both calculations clearly indicate enhancement effects for free surfaces demonstrated in the experimental work as shown in Fig. 24. However, they tend to underestimate the heat capacity at temperatures higher than that of the maximum enhancement. Both Nishiguchi and Sakuma (1981) and Tamura, Higeta, and Ichinokawa (1982) point out that the use of a scalar wave equation with separate longitudinal and transverse branches is incorrect and that one must use an approach first presented by Lamb (1882) to study the Helmholtz wave equation requiring consideration of both scalar and vector fields. The eigenfrequencies calculated in this way partly correct the difficiencies in the earlier theoretical work. The extensive discussion of these points by Tamura, Higeta, and Ichinokawa (1982) reveals that there remain two important difficulties in understanding the heat capacity. Their theoretical studies show that clamping of the boundary, as must be the case in the experiment to some yet undeter-

mined extent, leads to elimination of surface modes and a decrease of the vibrational heat capacity enhancement. Lautenschläger (1975) showed that under such conditions there could be, in fact, a negative enhancement. Second, surface relaxation gives rise to significant mode softening. Although the phenomenon of relaxation, or change in the lattice spacing at the surface, is well known in general, it is not known for the specific case of the samples used in heat capacity experiments. For these reasons there is no clear-cut demonstration of the validity of the details of the theoretical approaches through comparison with experiment.

2. Electronic contributions

The intention of separating electronic contributions from those discussed in Sec. II is just to emphasize the possible effects of the surface on the electronic heat capacity as distinct from that of the bulk. In fact it has been understood for some time that electronic surface states should increase the electronic heat capacity in proportion to the surface-to-volume ratio. That is to say that the surface density of states can be expected to be somewhat higher than that corresponding to the bulk. Kenner and Allen (1975) discuss surface effects on the density of states, heat capacity, and magnetic susceptibility for semi-infinite free-electron models. Both the heat capacity and the magnetic susceptibility are enhanced in proportion to the surface-to-volume ratio, expressed in terms of a phase shift. This parameter can be calculated and depends on the model potential that is used to incorporate exchange and correlation effects. Recently it has become possible to perform self-consistent electron band calculations of the total energy leading to a determination of the surface magnetic susceptibility and surface energy (see, for example, Fu *et al.*, 1985). This approach has been tested through comparison with experiment such as in the case of the surface Knight shift calculations for Pt (Weinert and Freeman, 1983) that have been discussed in Sec. III.B.1.

It is worthwhile recalling that the Kubo-Fröhlich effect on the bulk specfic heat of a metal particle is determined by an appropriate distribution function for the energies of the quasiparticle states and a single parameter: the average level spacing δ. This parameter may be estimated from the density of states determined from measurements of the heat capacity of the bulk metal. However, for small particles the surface contribution to the density of states may be quite significant, particularly for the smallest particles with a large fraction of atoms at the surface. We might, somewhat arbitrarily, delineate this case as that for particles which have dispersion $f_s \geq 0.2$ (corresponding very approximately to $d \lesssim 30$ Å). For such samples the estimate of δ from bulk measurements as listed in Table V or displayed in Fig. 1 is qualitative at best. Furthermore, the dependence on size of the thermodynamic properties of the metal particle must necessarily be weakened in this limit. The extent of the effect will vary from one material to another and cannot be easily determined from calculation since it depends on details of the surface electronic structure which in turn depend on possible alterations in the surface physical structure (relaxation and reconstruction). One might argue therefore that studies of the heat capacity (or of the magnetic susceptibility) to explore the quantum effects on the electronic spectrum should be conducted for the intermediate size of particles $d \gtrsim 100$ Å, at temperatures at least as low as 0.1 K in order to avoid this ambiguity of the role that is played by surface effects.

Finally, it should be noted that the electron-phonon interaction contributes significantly to the electronic density of states near the Fermi energy. This is reflected in an enhancement to the heat capacity of many metals more important than band effects, or effects of the electron-electron interaction (Ashcroft and Mermin, 1976). In the preceding section we have addressed the effects of finite size on the lattice excitations. It would be natural then to extend this discussion to include the effects of size on the electron-phonon interaction. This will have important consequences for the size dependence of the average level spacing δ which was otherwise taken to vary as d^{-3}. Since there is as yet no theoretical guidance in this direction the experimentalist might be advised to choose samples of particles for heat capacity measurements in the larger or intermediate size ($d \approx 100$ Å) to avoid possible untoward effects from small size on the electron-phonon interaction. Analysis of optical experiments suggests that this interaction is quenched in small silver particles of diameter less than 20 Å (Kreibig, 1974). As was noted earlier this is not a concern for measurements of the electronic susceptibility where the electron-phonon interaction does not play the same role.

B. Measurements of the small-particle heat capacity

One of the most difficult obstacles for the experimenter confronted with the task of measuring the heat capacity of metal particles is how to make thermal contact to the sample. There have been two approaches to this technical difficulty. One is to use a matrix with suitable thermal characteristics that is also appropriate from the viewpoint of ease of fabrication of the metal particles. Unfortunately, the effect of the matrix can be very substantial as has been found in measurements of the magnetic susceptibility. It is important to have samples with metal concentrations sufficiently high that the heat capacity background effects of the matrix are unimportant. Subtraction of the matrix heat capacity is a potentially complicated process. Measurements of the bulk matrix alone may not accurately reflect the background heat capacity in the metal-containing sample. This may be particularly true of the linear temperature-dependent contribution to the heat capacity generally found for noncrystalline dielectric solids (Zeller and Pohl, 1971) which may arise from the interface between matrix and metal or from the matrix

alone if it is amorphous. Another complication is that this background effect has the same dependence on temperature as that of the electronic heat capacity of the bulk metal.

The second method neatly avoids this difficulty with the matrix. This is to prepare particles that are self-supporting and which are subsequently packed into pellets. In this case there is the obvious disadvantage that the particles have both an undetermined boundary condition at their surfaces, and furthermore electrical isolation cannot be assumed. For instance, without assurance of electrical neutrality the quantum electronic size effects cannot be sensibly investigated. The poorly defined physical boundary conditions make interpretation of the heat capacity enhancements from the vibrational spectrum less straightforward to perform.

In order to interpret heat capacity measurements it is usual to plot the results, corrected for background contributions, as C/T vs T^2. The intercept at zero temperature is identified with the electronic heat capacity and the slope of the graph determines the vibrational part. This is appropriate for most solids at low temperatures giving a complete phenomenological description of the heat capacity within the framework of the Sommerfeld-Debye model,

$$C_{\text{bulk}}=\gamma T+BT^3 ,$$
$$\gamma=2\pi^2k_B^2/3\delta , \tag{4.5}$$
$$B=12\pi^4k_B/5\theta_D^3 .$$

The Sommerfeld constant γ shown here includes electron-phonon enhancement in the level spacing parameter δ as was noted in Sec. II. For heat capacity data analysis from small particles, a procedure similar to that for the bulk has been followed. To display the small-particle effects more clearly, the bulk heat capacity is subtracted leaving an enhancement ΔC that is also plotted in the same form as was described above in Eq. (4.5). An example of this is the data for Pb particles shown in Fig. 24 and for Pt particles in Fig. 25. A change in the electronic behavior is identified from the intercept at zero temperature with the tacit assumption that the electronic contributions are temperature independent, or at least less so than those from the lattice contributions that control the extrapolation toward zero temperature. By the same token it is presumed, in this sort of analysis, that there is no linear temperature-dependent contribution from the lattice heat capacity. Despite these shortcomings this is a reasonable basis for a first-order interpretation of experiment and can be summarized as

$$\Delta C/T=(C_{\text{meas}}-C_{\text{bulk}})/T\approx\Delta\gamma_{\text{elec}}+\Delta B_{\text{vib}}T^2 . \tag{4.6}$$

Compacts of palladium particles have been prepared by Comsa, Heitkamp, and Räde (1977). The particles were made by inert gas evaporation and characterized by electron microscopy and then were pressed into cylindrical pellets of 44% of the bulk density weighing about 30 mg. Particles of nominal initial diameters 30 and 66 Å, were

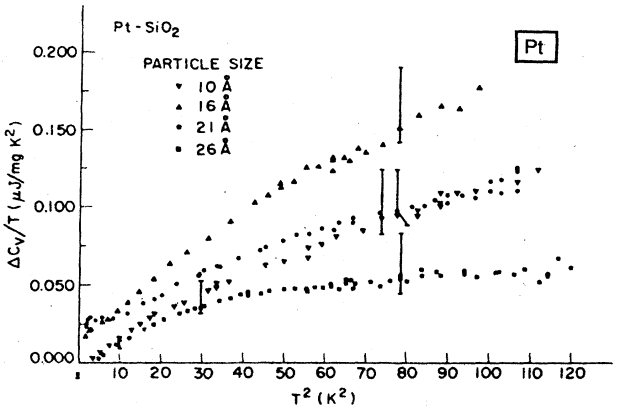

FIG. 25. The excess heat capacity of Pt particles embedded in SiO_2 measured by Stewart (1977). The majority of this enhancement was attributed to matrix effects although at the lowest temperatures a negative excess heat capacity was thought to be a consequence of discreteness in the electronic spectrum.

used and measurements were made over the range 1.4—30 K. These were compared to that of a standard bulk sample. No change in the electronic heat capacity was observed, $\Delta\gamma_{\text{elec}}=0$. However, an enhancement in the vibrational small-particle heat capacity over that of the bulk was found. This increased systematically with decreasing particle size. The results were interpreted with the homogeneous elastic theory of Baltes and Hilf (1973) from which a temperature-dependent effective sound velocity was determined by fitting the data. It is noteworthy that the electronic term appears unchanged whereas in contrast, substantial reduction of the electronic magnetic susceptibility has been reported for small Pd particles (Ladas *et al.*, 1978). To account for both results it may be necessary to postulate that the surface effect on the susceptibility is more a question of a reduction of the Stoner factor and not a decrease in the density of states at the surface.

Vanadium particles, prepared by the same methods as the palladium samples and pressed into pellets, have been studied by Comsa, Heitkamp, and Räde (1976) and more recently by Vergara, Heitkamp, and Löhneysen (1984). The samples had initial particle diameters of sizes 38 and 65 Å (Comsa *et al.*, 1976) and 29, 50, 82, and 132 Å (Vergara *et al.*, 1984). Measurements were taken from 1.3 to 12 K and, in the latter case, magnetic fields up to 3.5 T were applied in order to supress superconductivity allowing a more extended range of temperature over which the normal metal could be investigated. Comsa *et al.* (1976) found a dramatic increase in the electronic contribution to the heat capacity, as much as a factor of 3 over that of the bulk. This observation was confirmed by the measurements of Vergara *et al.* (1984) on similarly prepared samples. However, the latter authors were able to study the effect more systematically. They concluded that contributions to the electronic heat capacity from localized surface states or the enhancement in the surface density of states from narrowing of the *d* band were explanations

consistent with the observations. It was also pointed out that nonstoichiometric vanadium oxides could account for the extra heat capacity, although this was thought to be a less satisfactory explanation. Note that a similar interpretation was made in the case of magnetic susceptibility measurements on vanadium particles.

In the spirit of interpretation implicit in Eq. (4.5), both groups working with vanadium particles uncovered an enhancement in the vibrational heat capacity. Two viewpoints have been represented here. The phenomenological approach advanced by Baltes and Hilf (1973) and Lautenschläger (1975) allows data analysis in terms of a temperature-dependent sound velocity and Debye temperature. A second idea discussed by Vergara *et al.* (1984) is to constrain the elastic parameters to be temperature independent, and to analyze the additional contributions to the temperature-dependent heat capacity in terms of a collection of Einstein local oscillators of otherwise unspecified origin. For the vanadium particle pellets they found that the number of such oscillators scales accurately with the surface-to-volume ratio. This leads to the speculation that, if indeed such oscillators exist, they may be associated with edge and corner atoms of the particles. Another possibility for local modes could be linked to the more macroscopic character of the pressed pellets, that is to say cooperative effects and mode coupling between the particles. More work with this kind of sample may be necessary to understand the microscopic origins of the heat capacity enhancement in vanadium. Superconductivity was observed in all of the vanadium samples.

A novel technique of production of small particles by pressure intrusion of the molten metal into leached Vycor glass (porous glass) was developed by Watson (1966,1970). Samples of lead and indium were prepared in this way and the heat capacity measured from 1.5 to 15 K by Novotny, Meincke, and Watson (1972) and Novotny and Meincke (1973). The particle diameters were 22, 37, and 60 Å for the lead particles and 22 Å for indium. Typically these samples contained 1—2 g of metal and a similar amount of glass. The intruded metallic material can be described as a "three-dimensional system interconnected on the average over distances of several particle diameters" (Novotny and Meincke, 1973). Their results of measurement of the enhancement to the heat capacity ΔC are shown in Fig. 24 for Pb particles. This experiment predates much of the theory that was summarized earlier; however, the various theoretical efforts (Baltes and Hilf, 1973; Lautenschläger, 1975; Nishiguchi and Sakuma, 1981; Tamura, Higeta, and Ichinokawa, 1982) stimulated by these experiments, have all found at least qualitative agreement with these results. The maximum in the enhancement as a function of temperature shown in the figure appears to be more clearly defined for larger particle sizes, 37 and 60 Å. The effects of superconductivity are in evidence near the transition temperature, $T_c^2 = 50$ K^2. On the basis of this work it seems quite clear that a nonquadratic correction to the vibrational heat capacity enhancement is valid and that this can be understood in terms of quantum effects on the vibrational spectrum. Tamura, Higeta, and Ichinokawa (1982) have found in their calculations that the physical structure of the surface is important in determining the surface mode and that second, the degree to which the physical surface is clamped at points of contact to the particle can significantly decrease the surface mode contributions to the heat capacity. This leaves the detailed theoretical calculations in a difficult form with which to compare with experiment since a precise experimental determination of the metal particle's surface conditions is hard to achieve.

Stewart (1977) has prepared samples of platinum particles imbedded in SiO_2, co-sputtering the two materials. Typically the composite films (cermets) weighed 15 mg with from 15% to 30% Pt by weight as determined by microprobe analysis. Measurements on four samples with average diameters 10, 16, 21, and 26 Å were performed in the range 1—12 K. The technique Stewart used was to subtract published values for the bulk heat capacity of Pt and vitreous silica from his data. The results for his excess heat capacity are shown in Fig. 25. This has a disadvantage that inaccuracy in the measured amount of each constituent can produce error in the calculated excess heat capacity and there is no guarantee that the heat capacity of sputtered SiO_2 is the same as that of vitreous silica. These points have been discussed by Stewart. He finds, in fact, that it is necessary to postulate that there are additonal or enhanced Einstein modes in the matrix beyond that already widely accepted as being characteristic of bulk silica. Analysis of the data for three of the samples, 10, 16, and 21 Å, gave convincing evidence for this type of behavior that Stewart has associated with the presence of Pt particle inclusions. It is in rather stark contrast to the other heat capacity work, that no size effects of the vibrational contributions to the heat capacity from Pt were identified or discussed. In the last sample, 26 Å, it was found that the excess heat capacity actually becomes negative. In Fig. 25 this is clearly evident with there being a strong tendency for similar behavior in the 10-Å sample as well. It is this observation that he attributed to the quantum size effect. Other possible explanations might include quenching of the electron-phonon interaction, clamping of surface modes in the vibrational spectrum [see Lautenschläger (1975)], an incorrect subtraction of the silica background heat capacity and, to a lesser extent, inaccuracy in the determination of the amount of platinum. It is clear, nonetheless, that further heat capacity measurements are warranted on Pt particles with emphasis on the low-temperature region and that these may serve to elucidate the provocative result Stewart has obtained.

V. MAGNETIC RESONANCE RELAXATION

A. Effects of particle size

Generally speaking if there is a gap Δ in the electron spectrum at the Fermi energy one expects that the probability for a nuclear magnetic transition via the electron-

nuclear dipolar or contact interaction will be substantially suppressed; the number of suitable, available electron states being reduced by the Boltzmann factor $\exp(-\Delta/k_BT)$. From this point of view it would seem that the nuclear spin-lattice relaxation rate in a small metal particle should have a temperature dependence of $\exp(-\delta/k_BT)$ in the limit $\delta \gg k_BT$. However, there does not appear to be evidence for this from experiment. Many of the small-particle experiments have been performed with particular emphasis on the Knight shift and these have frequently used continuous-wave techniques that are unsuitable for measurement of the spin-lattice relaxation. A notable exception to this is the work of the University of Tokyo group (Kobayashi, Sasaki, and colleagues). They have extensively investigated relaxation effects in Cu, Al, and Sn. However, copper is the only nonsuperconducting metal that has been looked at by them and interpretation of these results are somewhat clouded by the very large quadrupolar line broadening in small particles of this element, not to mention possible effects of the spin-orbit interaction. The spin-lattice relaxation in superconducting materials is strongly affected by superconducting order parameter fluctuations. In addition to these mechanisms, it has been argued qualitatively that electronic level discreteness must play some role as well. For other nonsuperconducting metals such as Pt no variation from the bulk metal relaxation rate has been observed (Yu and Halperin, 1981b).

The case of electron spin resonance (ESR) relaxation times has already been discussed in Sec. III.C. An additional point, not emphasized there, is that as a consequence of a size-dependent g shift and a nonuniform particle-size distribution, one expects that the small-particle, low-temperature ESR line will be inhomogeneously broadened. This spectrum might be viewed as being composed of a manifold of narrower lines from different particle sizes where the latter have widths given by the Kawabata theory (1970). Apart from this, and in the absence of impurity relaxation, there is no theoretical basis for expecting that the longitudinal relaxation time T_1 should be larger than the inverse ESR linewidth. There exists some experimental literature that reports saturation studies of the small-particle resonance from which T_1 has been deduced for Li particles and found to be as much as an order of magnitude longer than that deduced from the linewidth (Borel, Borel-Narbel, and Monot, 1974). Although this appears to be consistent with the hand-waving arguments given above, there is no further evidence from work with other elements for this behavior. Consequently, we return the discussion to that of the spin-lattice relaxation rate, for which a number of experimental results can be compared.

The nuclear spin-lattice relaxation rate can be written in terms of transition probabilities $W_{m,n}$ from one nuclear state n to another m (Slichter, 1978)

$$T_1^{-1}=\frac{1}{2}\sum_{m,n}\frac{W_{m,n}(E_m-E_n)^2}{\sum_n E_n^2} . \tag{5.1}$$

For this sort of description it is most convenient to assume that spin-spin coupling allows the definition of a well-defined nuclear spin temperature. Consequently, the energy states E_n and E_m cannot be strictly considered as exact eigenstates of the nuclear spin Hamiltonian, although they are normally treated as such. The transition probabilities can be written as

$$W_{n,m}=\frac{2\pi}{\hbar}\sum_{ks,k's'}|\langle mks\,|\,V\,|\,nk's'\rangle|^2 P_{ks}(1-P_{k's'}) \times\delta(E_m-E_n+E_{ks}-E_{k's'}) , \tag{5.2}$$

where V is the electron-nuclear hyperfine-contact interaction operator, the probabilities of occupation of the electron states ks and $k's'$ are given by the P functions, and the δ function ensures energy conservation. For bulk metal the P functions are given by the Fermi function but for the small particle this is, of course, inappropriate. In the equal-level spacing approximation these two factors together should be proportional to $\exp(-\delta/k_BT)$ at low temperatures. Furthermore, the energy conservation condition, always easy to satisfy in the bulk limit, is no longer applicable. This latter constraint may be expected to substantially restrict the nuclear spin relaxation rate. Equations (5.1) and (5.2) presume that the notion of well-defined electronic states relative to the nuclear Zeeman levels is clearly established. Consequently the inverse lifetime of each such state should be much less than the nuclear resonance splitting $E_m-E_n=\hbar\omega_Z$ for spin $I=\frac{1}{2}$,

$$\hbar/\tau_s \ll \hbar\omega_Z . \tag{5.3}$$

Equality in the above relation may be expected at temperatures of order 4.2 K and a magnetic field of 10 kOe. At much lower temperatures or larger fields the inequality of Eq. (5.3) may be expected to hold ($\tau_s^{-1}\propto T^2$; $\hbar\omega_Z\propto H$). In this case the energy conservation condition embodied in the δ function in Eq. (5.2) imposes a constraint independent of the temperature while strongly temperature-dependent effects arise from the P functions. Then one might expect that the relaxation rate would be quenched. Indeed the recovery of the magnetization from an excitation pulse ($\pi/2$ pulse, for example) will be inhomogeneous over the sample since we assume negligible interparticle nuclear spin coupling. In fact the few experiments conducted so far suggest that the small-particle relaxation rate is reduced only by as much as an order of magnitude over that of the bulk.

It has been shown by Gates and Potter (1976) that a mechanism for spin-lattice relaxation in small insulating particles involves nuclear spin diffusion. Diffusion of nuclear Zeeman energy to the surface is followed by surface relaxation in the presence of paramagnetic centers such as adsorbed oxygen. Similar surface relaxation processes may mask the quantum effects that one might otherwise expect to observe in metal particles.

B. NMR spin-lattice relaxation experiments

Early measurements of the spin-lattice relaxation time T_1 for copper small particles (Kobayashi, Takahashi, and Sasaki, 1972) showed that the relaxation rate was substantially increased over that of the bulk metal as the size of particles became smaller (90 and 40 Å). Nonetheless the temperature dependence was still found to be that of bulk copper in each case: $T_1T=1.27$ ksec. The fact that the susceptibility of these particles was found to be strongly paramagnetic led these authors to conclude that surface oxides were contributing to the magnetic susceptibility and providing a mechanism for relaxation as well. In later measurements reported by Kobayashi (1977), special care was exercised to make particles embedded in SiO to protect them from oxidation following the procedure of Yee and Knight (1975). In these spin-lattice relaxation experiments a complex echo amplitude recovery was observed significantly deviating from an exponential in three of the four samples investigated (15, 25, 50, 110 Å). Although it was argued in this case that oxides at the surface were not providing relaxation centers, the rates were still not strongly suppressed at 1.4 K as might have been expected from Eq. (5.4). However, it was observed that the small-particle linewidths were severely broadened ($\Delta H_{pp}\approx 100$ Oe) most likely owing to the quadrupolar interaction. There can be some difficulty in uniformly irradiating such a sample using rf pulses. The change in nuclear magnetization deduced from the spin-echo height depends on spectral diffusion in this case and does not reliably give the spin-lattice relaxation time. Work with other normal metal elements with $I=\frac{1}{2}$, might be better suited for studying this problem.

An element that satisfies both of these characteristics is Pt. Extensive measurements of the spin-lattice relaxation of small Pt particles (33—200 Å) have been conducted by Yu and co-workers (Yu, Gibson, Hunt, and Halperin, 1980; Yu and Halperin, 1981a,1981b) and on smaller particles (9, 27, and 39 Å) supported on alumina by Slichter and co-workers (Slichter, 1981a,1981b; Rhodes, Wang, Makowka, Rudaz, Stokes, Slichter, and Sinfelt, 1982). The spin-lattice relaxation of Pt at temperatures as low as 1.7 K has been found to be accurately the same as that of the bulk metal (Yu *et al.*, 1980; Yu and Halperin, 1981a,1981b). At least this is consistent with their observation that the Knight shift is also unchanged from that of the bulk, and thus that neither experiment indicates effects of discreteness from the electronic level spectrum. For the Knight shift this may be understood as a manifestation of strong spin-orbit interaction.

Although Al and Sn are superconducting elements some of the work on these very small particles shows effects that cannot be interpreted in terms of superconductivity alone. This will be discussed next.

The results for spin-lattice relaxation of 100-Å Al particles obtained by Nomura, Kobayashi, and Sasaki (1980) are shown in Fig. 26 as a function of temperature and for various magnetic fields. This is the most recent of a series of experiments on Al particles performed by this group in substantial magnetic fields $H>2$ kOe and is probably the best representation of such enhancement effects. Before discussing this in detail let us outline some of the earlier work. This includes the first, albeit qualitative, report of enhancement of the relaxation time in small Al particles well above the transition temperature performed by Fujita, Ohshima, Wada, and Sakakibara (1970). Kobayashi, Takahashi, and Sasaki (1971) found that the relaxation time at temperatures higher than the critical temperature was actually smaller than the bulk value for particles below 100 Å in size. This effect is similar to what had been seen by this group in copper as was discussed above. It is not clear, however, whether this may be attributed to a similar mechanism, where spectral diffusion within a quadrupolar broadened NMR line takes place. This work was extended to lower temperatures by Kobayashi (1974) and a more extensive report of a systematic study for a wider range of larger particle sizes was given by Kobayashi, Takahashi, and Sasaki (1974,1975) and Takahashi, Kobayashi, and Sasaki (1975). In the last two papers comparison was made with the theory of Sone (1976) that *assumes* a continuum of electron states. Good agreement was found with the results for particles larger than 150 Å. Here the relaxation and its field dependence is determined primarily by superconducting order parameter fluctuations. For smaller parti-

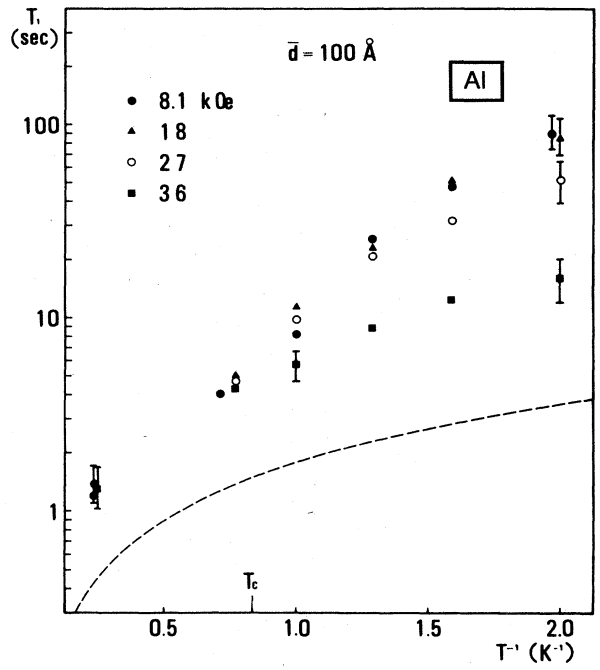

FIG. 26. The temperature dependence of the ^{27}Al nuclear spin-lattice relaxation time from a 100-Å aluminum sample as reported by Nomura, Kobayashi, and Sasaki (1980). The dashed line shows the expected behavior for bulk aluminum in the normal state. Note that the decrease in T_1 with increasing magnetic field indicates that the superconducting fluctuations are quenched in large magnetic fields.

cles, $d \leq 100$ Å, it was discovered that the relaxation time was substantially increased at temperatures both above and below the critical temperature. The continuum assumption is presumably no longer justified in this case and the experimental results can be best summarized as

$$T_1 \propto \exp(\Delta/k_B T) , \tag{5.4}$$

where Δ is larger than Δ_{BCS}.

It should be possible to deconvolve the effects of superconductivity from those inherent to small metal particles by increasing the magnetic field sufficiently to quench superconductivity. Using magnetic fields as high as 36 kOe, Kobayashi, Nomura, and Sasaki (1978) showed that T_1 first increased with increasing field and then dramatically decreased. The latter is evident from the data in Fig. 26 taken from the work of Nomura, Kobayashi, and Sasaki (1980). This reduction in T_1 at large fields can be accounted for by superconducting pair-breaking effects from both the orbital and Zeeman interactions (Kobayashi *et al.*, 1978). It was Nomura *et al.* who discovered that the NMR lines for Al particles were actually much broader than had been previously thought, $\Delta H \approx 200$ Oe. This may be a consequence of electric field gradients near the surface coupling to the quadrupole moment of the aluminum nucleus. This leads to two technical difficulties. First, there is the problem that, without care, an NMR experiment will be mostly sensitive to the larger particles in a size-distributed sample for which the line broadening from surface effects is minimal. Second, the measurements of the echo recovery may not accurately reflect T_1. If the NMR line from a single particle is very broad and is only inhomogeneously irradiated then the recovery following a pulse may be attributed to cross relaxation or spectral diffusion. In the case of severe broadening of quadrupolar origin one normally expects to see only the central $\frac{1}{2} \rightarrow -\frac{1}{2}$ transition which has the smallest coupling to electric field gradients appearing only in second order in the quadrupolar interaction and decreasing inversely with increasing magnetic field. Thus, Nomura *et al.* have argued that their higher magnetic field experiments were probably the more reliable. Indeed Nomura *et al.* found that their Al Knight shifts, Fig. 16, were very much smaller than had been previously thought (Kobayashi, Nomura, and Sasaki, 1978), and that the relaxation time T_1 was enhanced by as much as a factor of 2. The relaxation time enhancement was also found to be temperature independent. Although an enhancement is expected from the quantum size effect it should be strongly dependent on temperature in contrast to that observed in this case. Since Nomura *et al.* have raised the point that as much as half of their particle's volume could be aluminum oxide there is also the possibility that they are measuring some of the ^{27}Al resonance from the oxide as well as from the metal. This could push the apparent Knight shift to lower values and would also enhance T_1 to some extent. It would be likely in this case that there would be sufficient cross relaxation such that the temperature dependence of T_1 of the aluminum nuclei in the oxide and the metal would be the same. This question of possible oxide contributions to the aluminum resonance experiments is not discussed by Nomura *et al.* (1980).

The results for tin are not nearly so extensive as for aluminum. This element, although a superconductor, has the decided advantage of $I = \frac{1}{2}$, for which the quadrupole moment is zero. One disadvantage is that there is a significant spin-orbit interaction in Sn. Relaxation time measurements have been reported by Kobayashi, Takahashi, and Sasaki (1974), and Fukugawa, Kobayashi, and Sasaki (1982). In the last article it was found that for particle sizes above 230 Å the relaxation time measurements were in reasonable agreement with Sone's theory (1976,1983) provided they included the effects of the real particle-size distribution. According to the theory the distribution affects the results in two ways. There is an explicit effect on the level spacing parameter. However, there is also an implicit effect from the critical temperature and critical magnetic field dependence on size. For tin particles smaller than 230-Å deviation from the fluctuation theory was observed and it was suggested that this difference could be associated with discreteness in the electron level spectrum. These results are displayed in Fig. 27. Since there is no theory that accounts for both discrete level effects and fluctuation contributions to the relaxation, it remains for future work to quantitatively interpret the additional enhancements in the relaxation time observed by Fukugawa *et al.* (1982) and presented in this figure.

VI. OPTICAL AND INFRARED ABSORPTION

Metals have unique optical properties compared to other materials. One obvious example is that metallic reflectivity is characteristically very high. Although most metals are silvery in color, copper appears reddish and gold is yellow. These are optical manifestations of the conduction electrons. It is natural then to ask how this behavior might be modified on reducing physical size. In fact, for particle diameters substantially smaller than a wavelength of light, samples prepared without a matrix generally appear quite black. When the particle concentration is low and they are isolated in a matrix, such as glass, they can have rich colors. An example of this is the ancient technology where colored stained glass is prepared by diffusion of metal ions into the matrix with subsequent formation of metal clusters that selectively absorb light into the particle's surface plasmon mode.

The Mie theory (1908) allows a reasonably clear description of many of the experimental observations. A small particle has a well-defined surface plasmon mode positioned in the visible range of wavelengths with a width that varies approximately inversely with particle size, and an intensity that is proportional to the metal concentration. Since small particles must be supported in some way, by oxide coatings or a matrix, it is necessary to take the optical properties of the supporting medium into account at the same time as that of the metal. Effective medium theories (Maxwell-Garnett theory, 1904,1906; Bruggeman, 1935) combined with the Drude model for

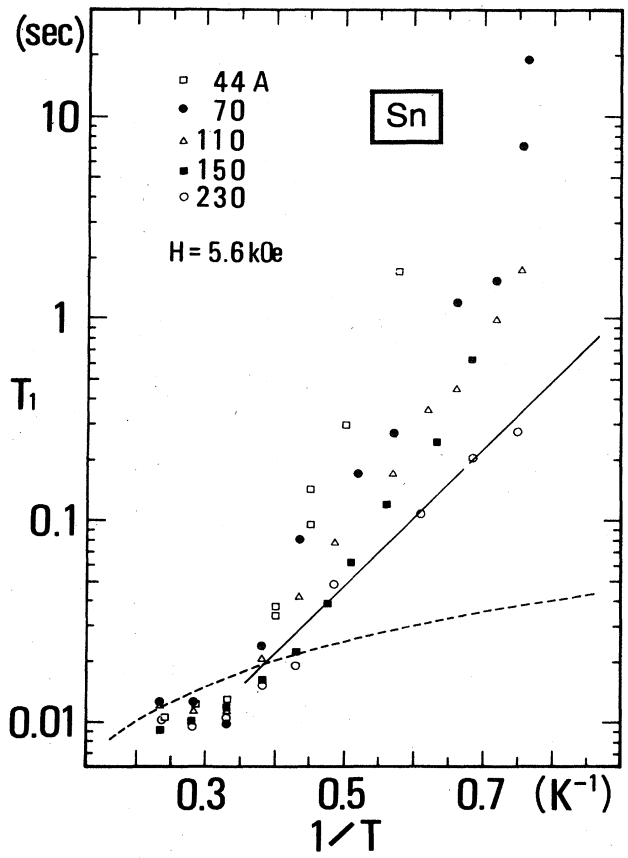

FIG. 27. The temperature dependence of the ^{119}Sn nuclear spin-lattice relaxation time from a series of small-particle samples measured by Fukagawa, Kobayashi, and Sasaki (1982). The dashed line shows the expected behavior for bulk tin in the normal state. The solid line is calculated from the fluctuation theory of Sone (1976) for $d=150$ Å. The dip of the data below that of the dashed line can be attributed to the superconducting transition but the enhancement of the data at low temperatures was suggested to be a manifestation of the discreteness in the electronic energy spectrum, despite the absence of a detailed theory with which comparison could be made.

conduction electrons, have been successful in describing almost all measurements and so we will give an account of the classical aspects first. Next, it is appropriate to ask in what way quantum effects become important. This was discussed first by Kawabata and Kubo (1966) showing that a completely different theory is necessary when the electronic level spectrum is discrete. The surface plasmon mode of course persists, however the mechanism for its damping can no longer be attributed to the same frequency-dependent conductivity as one might expect to invoke in a classical description. The results of a quantum theory (Kawabata and Kubo, 1966) show that the width of the plasmon mode has the same dependence on particle size as before but reduced in strength by about a factor of 2. Furthermore, one can expect (Kubo, 1969) that the temperature dependence of the damping, normally associated with the electron-phonon interaction, might be severely inhibited owing to quantization effects in both the electronic and vibrational spectra of the small particle. This later aspect, although intuitively reasonable, remains a conjecture with some support from experiment (Kreibig, 1974).

From the experimental side there are several outstanding advantages of optical methods such as the high precision with which experiments can be conducted. They have sufficient sensitivity to detect very small metal concentrations in a matrix, which can ensure their electrical isolation and minimize the effect of electric dipole-dipole interactions between the particles. On the other hand, there are some practical difficulties as well. Depending on the matrix used, the dependence of the surface plasmon damping on inverse particle size can be very significantly altered (Kreibig and Genzel, 1985). Collective behavior can become very important depending on both metal concentraton and particle-shape distributions (Granqvist and Hunderi, 1977). These geometric effects change the intensity, position, and width of the mode, particularly when the metal concentration is sufficiently large making it difficult to distinguish between classical and quantum characteristics.

A. Surface plasmon mode

Consider a single, representative, spherical particle of diameter d with complex dielectric constant,

$$\varepsilon=\varepsilon_1+i\varepsilon_2 , \tag{6.1}$$

embedded in a dielectric medium of dielectric constant ε_m. In the presence of an oscillating electric field, and for sufficiently small diameter, the build-up of surface charge provides a restoring force that leads to resonant density oscillations of the conduction electrons at a suitable frequency. This is the surface plasmon mode. For very large particle sizes the bulk plasmon mode becomes clearly defined as well. This evolution is neatly indicated in jellium calculations (Ekardt, 1984). Experimental results for Ag particles are shown in Fig. 28 (Kreibig, 1974).

For homogeneous materials the complex dielectric coefficient is written as $\varepsilon=(\eta+ik)^2$ when η is the refractive index and k the absorption coefficient. In the case of the hypothesized inhomogeneous medium the total absorption coefficient, K is given by Mie (1908),

$$K=\frac{18\pi f\varepsilon_m^{3/2}}{\lambda}\frac{\varepsilon_2}{(2\varepsilon_m+\varepsilon_1)^2+\varepsilon_2^2} , \tag{6.2}$$

where the volume-filling fraction of metal is f and the photon wavelength is λ. The absorption coefficient has a maximum value at a resonance frequency where

$$\varepsilon_1=-2\varepsilon_m . \tag{6.3}$$

One may take the dielectric constant of the metal to be of the Drude-Sommerfeld form (Ashcroft and Mermin, 1976),

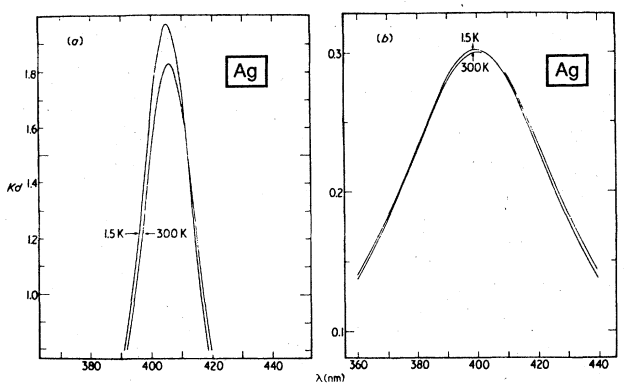

FIG. 28. The optical absorption spectra of Ag particles prepared in a glass matrix showing the surface plasmon mode measured by Kreibig (1974). Results are for experiments at 1.5 and 300 K on particles of diameter (a) 115 and (b) 34 Å. The absorption coefficient K multiplied by the sample thickness d is plotted as a function of the wavelength of light.

$$\varepsilon(\omega)=\varepsilon_0(\omega)+4\pi i\sigma(\omega)/\omega \ , \tag{6.4}$$

where $\varepsilon_0(\omega)$ is the dielectric constant of the metal associated with bound charges and the frequency-dependent conductivity for the free charges of density n is given in terms of the Drude relaxation time τ,

$$\sigma(\omega)=\frac{ne^2\tau/m}{1-i\omega\tau} \ . \tag{6.5}$$

From Eqs. (6.4) and (6.5) one finds in the high-frequency limit ($\omega\tau\gg 1$),

$$\begin{aligned}\varepsilon_1&=\varepsilon_0-\omega_p^2/\omega^2 \ ,\\ \varepsilon_2&=\omega_p^2/\omega^3\tau \ ,\end{aligned} \tag{6.6}$$

where the usual expression for the bulk plasma resonance frequency is used,

$$\omega_p^2=4\pi ne^2/m \ . \tag{6.7}$$

Using the condition Eq. (6.3), that determines the surface plasmon resonance frequency, ω_{sp}, we have

$$\omega_{sp}/\omega_p=(\varepsilon_0+2\varepsilon_m)^{-1/2} \ , \tag{6.8}$$

and from Eq. (6.2) we find that the absorption spectrum has a Lorentzian shape that, after linearization in the vicinity of ω_{sp} can be expressed as

$$K=\frac{9}{4}\frac{f\varepsilon_m^{3/2}}{c(\varepsilon_0+2\varepsilon_m)^3}\frac{\omega_p^2/(\omega^2\tau)}{(\omega_{sp}-\omega)^2+(2\tau)^{-2}} \ . \tag{6.9}$$

The full width Γ at half-height of this spectrum is just the inverse of the Drude scattering time τ. Classically, we can write this for a sphere (Kreibig, 1974) as

$$\tau=d/2v_F \tag{6.10}$$

assuming that the electron mean free path is entirely limited by boundary scattering. Consequently one might expect that the width of the surface plasmon mode Γ should be proportional to d^{-1}. In the interest of simplicity we neglect intrinsic contributions to the scattering as may be appropriate for sufficiently small particle size and we have, from Eq. (6.9),

$$\Gamma=\tau^{-1}=2v_F/d \ . \tag{6.11}$$

In Fig. 29 the inverse linewidth for silver particles prepared in glass is shown, taken from Kreibig (1974). This includes some of the first experimental work, that of Doremus (1964,1965) that has been reanalyzed by Kreibig (1974), Kreibig and Fragstein (1969), and Smithard (1973). Taking the Fermi velocity for silver to be $v_F=1.4\times10^8$ cm sec^{-1} one easily calculates that the classical theory of the linewidth summarized in Eq. (6.11) falls precisely through this data as indicated by the dashed line in the figure. Although this is a rather nice agreement it is probably fortuitous for several reasons: in principle, a quantum theory should be used and in later work matrix effects have been found to be overwhelmingly important, affecting the constant of proportionality between Γ and d^{-1} (Kreibig and Genzel, 1985).

First, the calculation itself is naive. Kawabata and Kubo (1966) argued that for small-size particles the electronic wave functions are themselves determined by the boundary conditions and cannot be viewed as a superposition of Bloch waves. Consequently the Drude theory is inappropriate. A more careful approach was used by both Holland (1967) and Kawabata (1970) in order to account for the ESR properties of small particles as outlined in Sec. III.C. The semiclassical theory used by Kawabata and Kubo (1966) expresses the frequency-dependent conductivity in terms of current-current correlation functions and makes use of the fluctuation-dissipation theorem. Integration over the energy is carried out assuming that particle sizes are large enough that effects of different level

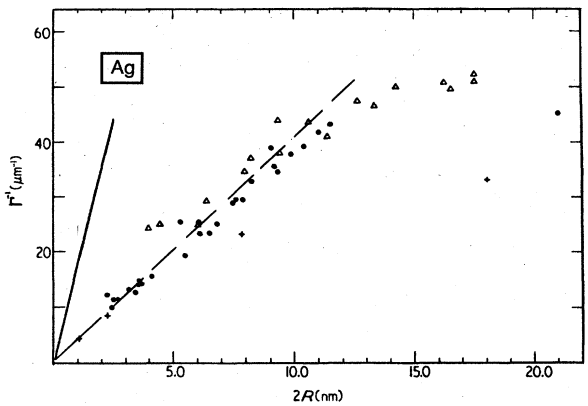

FIG. 29. The inverse halfwidth of the surface plasmon mode, Γ^{-1} as a function of particle diameter $2R$ taken from Kreibig (1974). These results include (△), work by Doremus (1965) reanalyzed by Kreibig (1974); (+) Smithard (1973); and (●) work by Kreibig (1974). The dashed curve follows the predictions of the classical theory while the solid curve gives the quantum theory calculation of Kawabata and Kubo (1966).

distribution functions are insignificant. They find that for silver particles the full width of the plasmon mode can be expressed as

$$\Delta\lambda = 0.0063 + 0.58/d + 4.32\times 10^{-9}/d^3 , \quad (6.12)$$

where $\Delta\lambda$ is in micrometers and the diameter d is in angstrom units. The leading-order behavior for small d from Eq. (6.12) is displayed as a solid line in Fig. 29 and it is clear that for particles less than 100 Å the results are significantly different from the classical theory (dashed line). As far as experiment is concerned the silver-glass samples appear to be in good agreement with the classical theory, while, on the other hand, very recent work (Charlé, Frank, and Schulze, 1984) on rare-gas isolated silver particles gives evidence for much narrower plasmon resonances and appears to be more consistent with the Kawabata and Kubo theory (1966). These experiments are reviewed by Kreibig and Genzel (1985) and clarification of the theoretical picture has been presented by Tran Thoai and Ekardt (1982). Work with metals other than silver include measurements on gold particles (Granqvist and Hunderi, 1976,1977) where effects of aggregation were successfully explained in the context of effective medium theory; and, with sodium particles produced by x-ray irradiation and annealing of sodium azide (Smithard, 1974a). A further complication arises when one considers deviations from spherical particle shape. A change in the depolarization factor for ellipsoidal particles shifts the plasmon mode. For either a distribution of shapes or orientations of ellipsoidal particles the combined plasmon absorption will be spread over a wider frequency range masking the intrinsic contributions to the width of the mode (Granqvist and Hunderi, 1977; Kraus and Schatz, 1983). It is interesting to note that there may be some indication of quantum effects on the plasmon mode taken from measurements of the temperature dependence of the width indicated in Fig. 28 (Kreibig, 1974). It appears that the difference in the width at 300 and 1.5 K depends inversely on the particle diameter extrapolating to zero at about $d=20$ Å for silver. This result may be consistent with quenching of the electron-phonon interaction as a consequence of discreteness in the electronic and vibrational spectra of the smallest particle sizes.

Other nonclassical theories have been advanced such as the work of Genzel, Martin, and Kreibig (1975) and Kraus and Schatz (1983). These are based on calculations with a free-electron-in-a-box model and explicitly compute the matrix elements of the dipole operator. For spherical boundary conditions Kraus and Schatz (1983) find that the width of the plasmon mode is actually 16% larger than the classical value, Eq. (6.11).

A general formalism based on a random-phase approximation has been presented by Wood and Ashcroft (1982). This has been applied to the box model leading to predictions for the width and frequency of the surface plasmon mode. These authors question the evidence for a statistical description of the energy level structure. Naturally, the high symmetry of the model considered leads to larger level spacings for which the corresponding electron states are multiply degenerate. A recent review of theories and experiments on this subject has been prepared by Kreibig and Genzel (1985). Of particular note, Ekardt (1984) has calculated self-consistently the absorption spectrum of a single particle treated within the framework of the local density approximation and applied to a spherical jellium model. Both surface and bulk plasma resonances were found as well as other collective modes.

It is generally accepted that the calculation of the shift in the plasmon resonance as a function of particle size is a difficult task and that meaningful comparison with experiment is somewhat uncertain at this time (Cini, 1981; Kreibig and Genzel, 1985).

B. Anomalous polarizability

Of the significant number of important new ideas developed by Gor'kov and Eliashberg (1965) concerning quantum effects in metal clusters, several have since been reinvestigated. One of these is the now ill-fated prediction of an enhanced, nonlinear electric polarizability.

Following usual definitions we write the two response functions to the applied field. First, the polarizability α relates the induced dipole moment p on a particle to the externally applied electric field E_0,

$$P=\alpha E_0 . \quad (6.13)$$

Second, we have the electric susceptibility χ, expressing the polarization $P=p/V$ in terms of the local or internal field $E_{\rm int}$,

$$P=\chi E_{\rm int} , \quad (6.14)$$

the internal and applied fields being interrelated by $E_{\rm int}=E_0-4\pi DP$, where D is the depolarization factor, and $V=\pi d^3/6$ is the volume of the particle. The intrinsic small particle's response to an applied electric field is given by the susceptibility and has been calculated by Gor'kov and Eliashberg (1965) with some errors later corrected by Devaty and Sievers (1980). However, the most experimentally accessible parameter is the polarizability α, and this can be expressed as

$$\alpha=\chi V/(1+4\pi D\chi) \quad (6.15)$$

and can be determined directly from low-frequency capacitance measurements of the dielectric constant $\epsilon(0)$,

$$\varepsilon(0)=\varepsilon_m \frac{1+\frac{2}{3}f\alpha/V}{1-\frac{1}{3}f\alpha/V} . \quad (6.16)$$

The volume-filling fraction of metal is represented by f and the dielectric constant of the matrix as ε_m. (The classical polarizability of a metal sphere is $\alpha_c=3V$.) Consequently for small filling fractions, measurements of capacitance of the metal-in-a-matrix, normalized to that of the matrix alone can be expected to have the form

$$C/C_0=1+3f , \quad f\ll 1 , \quad (6.17)$$

according to the classical theory.

A quantum-mechanical calculation of the susceptibility χ_{QM} was first carried out by Gor'kov and Eliashberg (1965) for weak applied electric fields, $eEd \ll \delta$. This can be illustrated in perturbation theory (Baltes and Šimànek, 1981) with the result.

$$\chi_{QM} \propto d^2/\delta \propto d^5 .$$

Gor'kov and Eliashberg incorrectly identified this as the polarizability and consequently found a dramatic enhancement of the polarizability over the classical result with an enhancement factor A that can increase as d^2 to be more than 2 orders of magnitude, until the condition $eE_0 d \approx \delta$ is reached. At this point, it was suggested that the polarizability would fall back to its classical value α_c, for further increases in size. Equation (6.17) would then be ammended to read

$$C/C_0 = 1 + A\,3f .$$

Such an effect could be looked for either as a function of the strength of E_0 or as a function of particle size. Negative results were reported by both Meier and Wyder (1972) and Dupree and Smithard (1972) using small particles of gold and silver in glass matrices. The correction to the Gor'kov and Eliashberg theory was pointed out shortly thereafter by Strässler and Rice (1972) and extended by Rice, Schneider, and Strässler (1973) showing that depolarization must be taken into account. However, there is still active theoretical discussion as to whether the actual polarizability is depressed or enhanced relative to the classical value (Ekardt, 1984). In any case the magnitude of the effect is probably rather small ($\approx 20\%$) and might be difficult to observe.

C. Absorption in the far-infrared

Another important observation of Gor'kov and Eliashberg (1965) was that quantum effects in optical absorption could be expected in the far-infrared range of frequencies. In the equal-level spacing approximation one has the picture of a well-defined set of electronic levels between which electronic transitions might be induced at the radiation frequency $\nu = \delta/h$. If $\delta \approx 10$ K ($d \approx 30$ Å) this corresponds roughly to radiation at 7 cm^{-1}. Consequently one might expect to see spikes in the infrared absorption spectrum corresponding to direct observation of these transitions between the discrete levels. These δ-function responses result from the requirement for energy conservation on the transition probability from one state to another with the absorption of a photon of energy $h\nu$. Obviously the equal-level spacing picture is highly artificial. More realistically we should consider a statistical distribution of levels. Calculating the transition rate now requires converting the sums over all possible electron states to an integral over the energy difference ΔE between initial and final electron states with the important multiplicative factor $R^a(\Delta E)$ that expresses the probability of finding two energy levels with separation ΔE. This function is graphed in Fig. 5 for the various statistical distributions. The larger the statistical ensemble index a the more the quasiparticle states are mutually repulsive. For the orthogonal ensemble ($a = 1$), this is weakest. For the symplectic ensemble ($a = 4$), the two-energy-level correlation function $R^a(\Delta E)$ oscillates most strongly, and one might expect to see some sort of corresponding oscillatory structure in the far-infrared absorption coefficient. Numerical calculations have been performed by Granqvist (1978) and Devaty and Sievers (1980), Fig. 30.

More specifically, Devaty and Sievers (1980) have written the absorption coefficient,

$$K(\nu) = 2\pi\nu[2(\varepsilon_1^2+\varepsilon_2^2)^{1/2} - 2\varepsilon_1]^{1/2} , \tag{6.18}$$

using the Maxwell-Garnett (1904,1906) effective medium model for the dielectric constant,

$$\varepsilon = \varepsilon_1 + i\varepsilon_2 = \varepsilon_m \frac{1 - f + 3\sum_j \frac{f_j \varepsilon_j}{2\varepsilon_m + \varepsilon_j}}{1 - f + 3\varepsilon_m \sum_j \frac{f_j}{2\varepsilon_m + \varepsilon_j}} . \tag{6.19}$$

This is given in terms of the dielectric constant of the matrix ε_m, the filling fraction $f = \sum_j f_j$ where f_j is the volume fraction for particles of each size within the size distribution having dielectric constant $\varepsilon_j = 1 + 4\pi\chi_j$ expressed in terms of the electric susceptibility χ_j. Gor'kov and Eliashberg (1965) have calculated the electric susceptibility as an integral over the two-level correlation function,

$$\chi_j = \chi_{j0} + B_j \int_{-\infty}^{+\infty} \frac{R^a(z)\,dz}{z^2 - (h\nu + i0^+)^2} ,$$

$$\chi_{j0} = \frac{m^*}{m} \frac{k_F d_j^2}{20\pi^2 a_B} , \tag{6.20}$$

$$B_j = \frac{m^*}{m} \frac{139(h\nu)^2}{300\pi^2 a_B k_F \delta_j} ,$$

and this has been reevaluated for each of the ensembles a by Devaty and Sievers (1980) correcting errors made in the earlier work (Gor'kov and Eliashberg, 1965). In the above expressions a_B is the Bohr radius and k_F the Fermi wave vector. The results of their numerical calculation of the absorption coefficient for aluminum particles using the symplectic ensemble are shown in Fig. 30. In the calculation, a log-normal size distribution, Eq. (2.50), was assumed (Granqvist and Buhrman, 1976a) defined by the average particle diameter d_0 ($d_0 = 25$ Å) and various values of the width parameter σ:

$$\frac{dn}{N} = \frac{1}{\sqrt{2\pi}\ln\sigma} \exp\left[-\frac{\ln^2(d/d_0)}{2\ln^2\sigma}\right] d\ln(d/d_0) . \tag{6.21}$$

Even a narrowly distributed sample of particles might realistically have a width parameter larger than 1.3; consequently it is clear that the oscillatory character of the far-infrared absorption spectrum associated with discreteness in the level spectrum will be essentially impossible to resolve for the symplectic energy level distribution. The

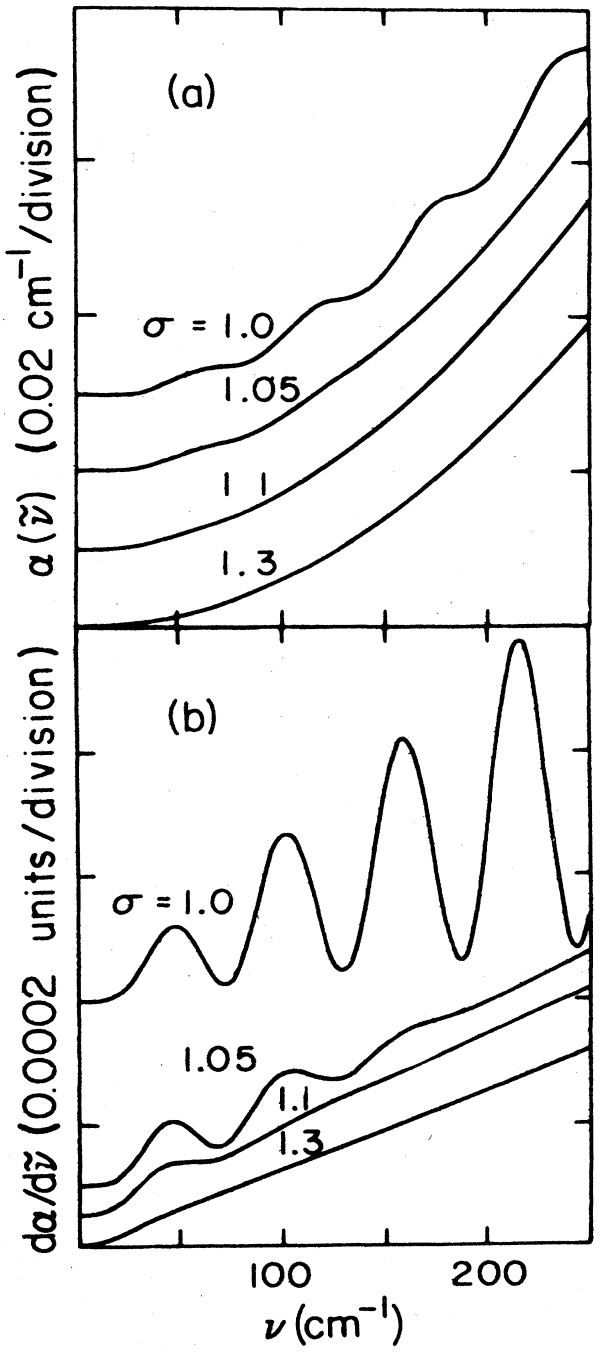

FIG. 30. Calculated far-infrared absorption coefficients and their derivatives with respect to frequency for 25-Å-diam Al particles by Devaty and Sievers (1980). The numerical calculations follow a corrected theory of Gor'kov and Eliashberg (1965) applied to log-normal particle-size distributions with width parameter σ. These calculations were performed for the symplectic distribution function of electronic levels which, although the most favorable for observation of quantum effects, still shows that the quantum effect oscillations as a function of frequency are washed out by a reasonable choice of the size-distribution parameter, $\sigma = 1.3$.

situation is even worse for the other statistical distributions where the oscillations are less pronounced. Earlier numerical calculations have been performed with the original Gor'kov and Eliashberg results for the susceptibility (Granqvist, Buhrman, Wyns, and Sievers, 1976; Granqvist, 1978). The conclusions from this work were also pessimistic from the viewpoint of observation of quantum effects.

Compounding these difficulties, large anomalous absorption in the far-infrared has been found to be a ubiquitous characteristic of small-particle absorption spectra. This background absorption would cloak the quantum effects discussed above by about 3 orders of magnitude (Tanner, Sievers, and Buhrman, 1975; Granqvist, Buhrman, Wyns, and Sievers, 1976; Carr, Henry, Russell, Garland, and Tanner, 1981). The high absorptivity can be summarized phenomenologically in the range 10—150 cm^{-1} as

$$K/f = Cv^2 , \tag{6.22}$$

where the coefficient C depends weakly on particle size, frequency, and material. It now appears that this effect can be explained in part by collective interactions among the particles (Devaty and Sievers, 1984; Curtin *et al.*, 1985). To investigate this absorption, Devaty and Sievers performed measurements as a function of the degree of aggregation among silver particles produced by a hydrosol technique. Clustering was induced by the addition of sodium citrate to the sol. Enhanced far-infrared absorption correlated quite well with the amount of aggregation induced between particles. Under the best conditions of minimum particle clumping and dilute metal concentration, it was found that the matrix dominated the absorptivity preventing an accurate measure of intrinsic effects. Nonetheless, Devaty and Sievers established a new lower bound on the possible enhancement effects of the absorption that still remains 2 orders of magnitude above that calculated from the classical Drude theory. Curtin *et al.* (1985) confirm this thesis with experiments on tin particles, either oxide free or coated with oxide prepared by inert gas evaporation and embedded in a KBr matrix. These authors speculate that oxide free particles in the "as-prepared" state can be represented as a percolation cluster which they calculated has anomalously large electric dipole absorption. After heat treating these samples the enhancement in absorption decreases significantly by a factor of 2 consistent with the view that the cluster topology may be broken up. Central to this explanation of enhanced absorption is the existence of clustering between particles during preparation. Niklasson and Granqvist (1986) have pursued this further, finding evidence that the particle clusters have a fractal structure (as does the backbone of the percolation cluster). They use this toplogy as a basis for a calculation of absorption in semiquantitative agreement with experiment. Although interparticle interactions may be pinpointed as being responsible for enhanced absorption, the phenomenon still remains an important technical problem to be solved before there can be further progress in understanding quantum effects on

the far-infrared spectrum.

Other modifications and additions to the Gor'kov-Eliashberg (1965) theory have been suggested during the past twenty years with the apparent intention of providing a more detailed basis with which comparison to experiment might be made, and to account for the anomalous absorptivity. Šimànek (1977) has taken into account effects of surface oxides as well as particle aggregation. Granqvist (1978) used effective medium theories, generalized to include a discussion of dipole-dipole interaction between particles and the possible role of oxide coatings on the metal surface. Lushnikov, Maksimenko, and Simonov (1978) have included the Coulomb interaction between conduction electrons in the particle with a reported agreement with experimental particle size dependence of the absorption coefficient. The question of excitation of phonon modes by the electromagnetic fields coupling to surface ions has been discussed by Glick and Yorke (1978). The effect of aggregates and oxide layers has been extended by Ruppin (1979) and Šimànek (1981). Using a phenomenological approach to represent a smoothed dielectric constant, matched to quantum-mechanical calculations, Genzel and Kreibig (1980) have found a new quantum size effect where the absorption in the infrared should be enhanced by comparison with the classical Drude theory. They predict that for $d \gtrsim 100$ Å there is a shallow peak in the absorption between 100 and 1000 cm^{-1} that depends on size and which has its origin in magnetic dipole contributions associated with eddy currents. Observation of this enhancement effect (of order a factor of 3) will require a detailed understanding of other possible absorption processes that have so far masked the intrinsic small-particle absorption by 2 or 3 orders of magnitude. Mechanisms for the enhancement of the far-infrared absorption by metal particle composites including magnetic and electric dipole absorption, and effects of coatings has been discussed further by Sen and Tanner (1982) and Wood and Ashcroft (1982). Although the prospects appear to be dim for using far-infrared techniques to obtain information about the statistical distribution of the electronic level structure nonetheless, one might expect to see anomalously low absorption at very low frequencies ($h\nu < \delta$). This idea has been explored by Devaty and Sievers (1985) and would require that the extrinsic enhancements in absorption discussed above be eliminated.

VII. PARTICLE PREPARATION TECHNIQUES

A wide variety of methods have been used to prepare the samples for which results have been discussed in this paper. It is apparent that there is not a universally good method for production of particles applicable to every element. In many cases the preparation methods must be chosen according to constraints imposed by the experimental measurement techniques themselves. For instance, the measurement of the heat capacity requires good thermal contact between particles and large amounts of material while optical absorption experiments can be most easily interpreted if the particles are widely dispersed in a matrix. Another illustration of this point is the unique experiment of Ladas *et al.* (1978) on the susceptibility of palladium particles which takes advantage of the change of electronic structure following absorption of hydrogen. This experiment is best conducted with samples presented in a form typical of heterogeneous catalysts. Above all, the experimenter is concerned with background contributions to the small-particle experiment that arise from the support matrix or from chemical or electronic modifications at the surface. Some experiments are very much more sensitive to such problems than others. As an example compare the measurement of the electronic susceptibility by NMR Knight shift methods with that from the SQUID magnetometer. The magnetization of the entire sample is measured with the SQUID including the matrix, the particle surface, diamagnetic contributions, as well as the Pauli susceptibility. It is only the latter that is the quantity of interest in the study of quantum effects. On the other hand, the NMR technique is selectively sensitive to the Pauli susceptibility and consequently the matrix does not affect this measurement. In brief, one finds a necessary diversity in the marriage of methods for preparation of metal particles and the measurement of their properties.

In the following summary, information on the preparation techniques referred to earlier is collected together. In some cases references will be made to work not previously discussed where it is particularly relevant to preparation methodology. An excellent and comprehensive discussion of this topic has been given in an earlier review article by Perenboom *et al.* (1981a).

A. Hydrosols

The preparation of a hydrosol requires the following important steps. An acid solution of the appropriate metallic element is prepared. A reducing agent, usually sodium citrate, is rapidly mixed with the solution to produce a suspension of particles. Dialysis can be used to remove the remaining ions and then a protective agent such as gelatine is normally introduced to ensure that the particles do not clump together. The sample can then be dehydrated leaving the particles embedded in the gelatine matrix. Noble-metal particles have been prepared in this way including silver (Carey Lea, 1889; Frens and Overbeek, 1969), gold (Zsigmondy, 1906; Turkevich *et al.*, 1951) and platinum (Wilenzick *et al.*, 1967; Marzke and Glaunsinger, 1984). One advantage of the hydrosol approach is that control over the chemical purity of the ingredients can be maintained in order, for example, to discriminate against introducing specific kinds of magnetic impurities. It is also apparent that relatively narrow size distributions can be achieved at least for samples with average diameters of order 20 Å. For platinum particles considerable success has been achieved by Marzke, Glaunsinger, and Bayard (1976) and Marzke and Glauns-

inger (1984). In their most recent work they have reported using reducing agents other than sodium citrate. These include sodium borohydride, dimethylamine borane, and hydroxylamine hydrochloride. It was found that particles without a protective agent could be prepared as well. It is interesting that their ESR experiments revealed that a significant signal could be associated with the particle surface. van der Klink *et al.* (1984) also prepared platinum sols for NMR measurements; however, they used a silica gel support as a protective agent during the drying process. One disadvantage of the hydrosol technique is that it is difficult to make narrow size distributions of particles of larger diameter than 100 Å.

B. Impregnation/chemical reduction and ion exchange/chemical reduction

Another powerful chemical method uses a support matrix with very high specific surface area (of the order of 100 m^2/g) and a restricted pore size (typically less than 100 Å) within which chemical reduction of a metallic salt can be performed. Customarily the reduction is effected with hydrogen gas at elevated temperature. In this method an aqueous solution containing the metallic element is prepared and impregnated into the pore space of the support. (Usually this is SiO_2 or Al_2O_3.) For instance, in the case of Pt this could be a solution of H_2PtCl_6 (Dorling *et al.*, 1971; Uchijima *et al.*, 1977; Butt, 1985) or for Pd one might use $PdCl_2$ or $Pd(NH_3)_4Cl_2$ (Ladas *et al.*, 1978). Similarly particles of many other metallic elements have been made such as Na, K, Ca, Cu, Mo, Ru, Rh, Ag, Ta, W, Re, Os, Ir, Au, and Tl, to name a few. The support material, impregnated with solution, is usually dried and then heated in air, a process referred to as calcination. Then it is chemically reduced to the metallic state in flowing hydrogen at a temperature between 250 °C and 450 °C. A final step of heat treatment in a flowing helium gas stream at a somewhat higher temperature is frequently used to ensure that the metal surface is cleansed of chemisorbed hydrogen. This technique yields small, generally spherical particles of size necessarily less than the pore space dimension of the support.

A preparation approach based on ion exchange can be used where one exposes the support (silica) to a solution of the desired metallic salt presented in the form of a cation, for example $Pt(NH_3)_4^{2+}$ in the presence of OH^- coming from NH_4OH at a pH of ≈ 9.5. After washing the cation remains electrostatically bound to the support. The samples are then dried and reduced in the normal way (Cinneide and Clarke, 1972).

There are only phenomenological relationships between average particle size, the initial metal concentration in the aequous solution, the heat treatment schedule, and the physical characteristics of the support material. This has been studied extensively by many workers and can be found in the catalysis journals and conference proceedings. An important case in point is the extensive work of the Northwestern University group on the fabrication of Pt particles (Sashital *et al.*, 1977; Uchijima *et al.*, 1977; Kobayashi *et al.*, 1980). The vast literature on preparation of heterogeneous catalysts concerns many variations on a theme that involves the production of metallic particles. Some aspects of this methodology are reviewed by Andrew (1981), Cinneide and Clarke (1972), Lee and Aris (1985), and Bond (1985).

The method of impregnation (or ion exchange) followed by chemical reduction is very general. Many elements can be prepared in this way in metallic particle form. For some measurements of their physical properties there are advantages in having finely dispersed samples. This is naturally realized with this preparation approach. In fact some form of matrix isolation is necessary if one is to be assured that the particles are not in electronic contact, a condition for observation of the Kubo-Fröhlich quantum effects. Without altering the size distribution in the sample the particle surfaces can be cleaned by reduction and oxidation cycles in flowing gases, followed by flushing with helium at an elevated temperature. Finally, it is possible to determine the cleanliness and directly measure the area of the exposed metal surface by hydrogen or oxygen chemisorption experiments in many cases. Particle growth can be promoted on the support itself by extensive heating in order to systematically increase particle size (Rhodes, Wang, Stokes, Slichter, and Sinfelt, 1982). It is also possible to completely remove the support material if it is a silica gel (SiO_2), by dissolving it in a solution of NaOH as was done by Yu and Halperin (1981b) in their preparation of Pt particles. One can easily make more than 10^3 cm^3 of heterogeneous catalyst at one time producing $\gtrsim 0.5$ cm^3 of metal powder. This means that large amounts of material can be prepared under essentially identical conditions using these methods.

There are, however, some disadvantages of this approach. Magnetic impurities in the support material may be combined with the metal of the particles during preparation, their valence state, and hence their magnetic properties, being determined by combinations of the heat and gas treatment conditions that may not be easy to control independently. Some elements do not form spherical particles with these techniques but are reported to form "rafts" covering the surface of the support material. The loading of the as-prepared catalyst normally is less than 5% by weight ($\approx 0.5\%$ by volume). Despite the capability of cleaning the particle surface, as noted before, there is still an electronic interaction between the support and the particle which may be sufficiently strong as to significantly alter the electronic properties of the particle from that expected from the ideal unsupported situation. Realistically a matrix of some sort is necessary, but one which should be chemically inert. A close approximation to this may be the rare-gas cryogenic matrices used extensively by the Lausanne group which will be discussed later. Although a wider range of samples with different average particle diameters can be fabricated with the impregnation method as compared with the hydrosol technique, nonetheless, it is not easy to make these well-separated

particles much larger than 100 Å. This constraint is lifted with the use of the evaporation methods that are described next.

C. Inert gas evaporation

Perhaps the most commonly used sample preparation technique for the work reviewed in this paper, is that of inert gas evaporation. The presence of an inert gas during the process of evaporation of a metal provides sites for nucleation of small crystals and their subsequent growth from the atomic vapor. The resulting smoke can be collected from the walls of the evaporation chamber and has an average particle size that can be easily controlled between 30 and 1000 Å depending on the temperature of the metal vapor source, pressure, and type of gas used (such as helium, argon, or xenon). Addition of oxygen during the evaporation process has been attempted in order to systematically oxidize the particle surfaces and thereby electronically isolate them from each other (Buhrman and Halperin, 1973; Tanner, Sievers, and Buhrman, 1975; Nomura, Kobayashi, and Sasaki, 1980). This points out that there is a difficulty in collecting the particles for later experiments such that they remain electrically isolated, one of the principal disadvantages of the method.

The method of inert gas evaporation was introduced by Pfund (1930,1933) and Burger and van Cittert (1930) and was significantly developed by researchers at Nagoya University (Wada, 1967,1968; Kimoto and Nishida, 1967a,1967b,1967c; and Uyeda and collaborators). [See the summary by Uyeda (1974) and references therein.] This includes the extensive measurements by Yatsuya *et al.* (1972,1973) on the evaporation of aluminum in helium. They observed that there were several distinct regions in the evaporation chamber. Near the source in what they call the inner zone, the particles were of uniform size becoming larger farther away. Finally, the particles ceased to increase in size at some limiting distance from the source that depended on the inert gas pressure. This limiting distance was found to decrease with increasing gas pressure which also increased the limiting size of the particles. An analytical review of this method including extensive new work was presented by Granqvist and Buhrman (1976a) with some emphasis on the idea that the size distribution of particles produced by this and other methods is best described by the log normal distribution function, Eqs. (2.50) and (6.21). In their work, Granqvist and Buhrman set up a particle production system, shown schematically in Fig. 31, capable of making samples with large amounts of material up to 1 g at a time. An important adjunct to the method is the use of a temperature-regulated oven in order to produce the narrowest size distributions. Care must also be taken to avoid coalescence of the particles on the collection surface by adequately shielding them from the radiation of the source. Many elements have been successfully prepared as small particles in this way. These include Be, Mg, Al, Cr, Mn, Fe, Co, Ni, Cu, Zn, Ga, Se, Ag, Cd, In, Sn, Te, Au, Pb, and

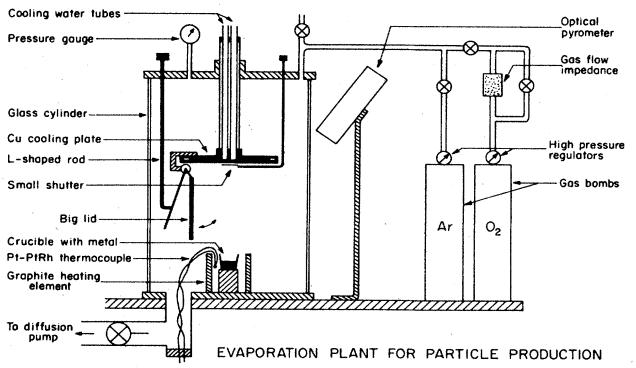

FIG. 31. The particle-production system of Granqvist and Buhrman (1976a). Inert gas evaporation of a variety of elements has been used to produce large quantities of very fine particles with this arrangement.

Bi (Kimoto and Nishida, 1967); Li (Gen and Petinov, 1965; Saiki *et al.*, 1972); Be, Mg, Al, V, Cr, Mn, Co, Ni, Cu, Ag, Au, Fe, Zn, Ge, Ga, Se, Cd, In, Te, Pb, and Bi (Uyeda, 1974); Mg, Al, Cr, Fe, Co, Ni, Cu, Zn, Ga, and Sn (Granqvist and Buhrman, 1976a); Mg and Ca (Sako and Kimura, 1984); Mo and W (Iwama and Hayakawa, 1985); and W (Yatsuya *et al.*, 1985). This list does not give a comprehensive account of all work, rather the intention is to indicate the variety of elements that have been fabricated this way. Extensive use of this method has been used by Kobayashi, Sasaki and colleagues at the University of Tokyo to study the NMR characteristics of Cu, Al, and Sn particles. [See for example, Kobayashi, Takahashi, and Sasaki (1971,1972) and Nomura, Kobayashi, and Sasaki (1980).] This and other related work (Fujita *et al.*, 1970; Ido and Hoshino, 1975) has been discussed earlier in the section on measurement of the Pauli susceptibility using NMR experiments.

There are several drawbacks of the gas evaporation technique, the most serious of which may be the difficulty of dispersing the particles so as to be assured that there is no electrical interparticle contact. Even with oxidation of the surface there remains the possibility of electron tunneling from one particle to another when they are clumped together (Cavicchi and Silsbee, 1984). This is emphasized by Fukagawa *et al.* (1982) from the viewpoint of interpretation of NMR results. Even without electrical contact the aggregates of such particles, or necklaces as they have frequently been referred to, are not suitable samples for investigation of quantum effects on the far-infrared absorption spectrum (Devaty and Sievers, 1984). However, the separation of the particles can be achieved by a suitable recovery method such as encapsulation in a matrix. A number of workers have set up continuous evaporation systems capturing the particles in paraffin oil as in the case of Li (Gen and Petinov, 1965) and In (Meier and Wyder, 1973). Ag particles have been evaporated in vacuum where nucleation and growth takes place on a surface with running oil or solvent (Yatsuya *et al.*, 1974,1985). This allows rather good definition of the

size distributions for smaller sizes. There are also some restrictions on the metallic elements that may be used. Although it is, in principle, possible to use similar methods to prepare particles of the refractory elements such as Nb, Mo, Rh, W, Re, Os, and Ir this is very much more difficult since their melting temperature is substantially in excess of 2000 °C. In these cases sputtering or electron beam techniques are necessary. Iwama and Hayakawa (1985) have used a combination of inert gas and electron beam heating to produce small particles of Mo and W. Sputtering methods in Ar gas have been successfully tried recently by Yatsuya, Yamauchi, Kamakura, Yanagida, Wakayama, and Mihama (1985) to produce particles of W. Even in the case of Pt and Pd it is not a simple matter to make gas-evaporated particles. Although the total yield can be made reasonably large, as had been noted before (Granqvist and Buhrman, 1975), the efficiency is much less than 100% in contrast to the use of chemical methods. Consequently the material costs may prohibit producing large quantities of particles of some of the rarer elements using inert gas evaporation techniques.

A new gas evaporation technique has been investigated by Yatsuya, Yamauchi, Kamakura, Yanagida, Wakayama, and Mihama (1985) where hydrogen was used instead of an inert gas. This has been applied to produce Al particles with the discovery of new growth habits. Other approaches have been developed using cluster beam methods with either an inert gas carrier and condensation medium (Abe, Schulze, and Tesche, 1980; Sattler, Mühlbach, and Racknagel, 1980; Frank *et al.*, 1985) or a seeding method (Kappes, Kunz, and Schumacher, 1982).

D. Vacuum evaporation

It is generally found during vacuum evaporation of a metallic element such as gold ($P < 10^{-6}$ Torr) that the early stages of evaporation produce islands on the evaporation substrate. These islands eventually coalesce to form discontinuous films. However, prior to this later stage of development halting the evaporation gives just the small islands which can be used for investigation of small-particle effects. A large number of articles have been published to account for the observed early stages of evaporation. Of these, the work of Schmeisser (1974) and Granqvist and Buhrman (1975,1976a) are representative. These discuss the various mechanisms leading to cluster growth including island coalescence and single-atom processes often referred to as Ostwald ripening.

For ESR measurements of small-particle quantum effects large amounts of material are not crucial. Consequently a slow evaporation technique onto a clean crystalline substrate is quite appropriate having the advantage that the evaporation can proceed in high vacuum in order to maintain purity of the sample. Dupree, Forwood, and Smith (1967) have used this method to prepare samples of gold particles of average diameter 30 Å on cleaved single crystals of NaCl. With a slightly different approach Monot, Châtelain, and Borel (1971) have found that evaporation of gold on high-purity quartz plates permitted a heat treatment procedure that allowed controlled growth of the gold islands in the range of 20—80 Å. Despite the advantages of the vacuum evaporation method it suffers from the drawback of not providing large quantities of material and flexibility over the possible sizes that can be produced. The problem of quantity can be addressed, however, by sequential evaporation of the metal alternated with the evaporation of a suitable insulating support. This procedure has been followed by Knight's group (Androes and Knight, 1961; Wright, 1967; Hines, 1971; Hines and Knight, 1971; Yee and Knight, 1975) as well as the Tokyo University group, Fukagawa, Kobayashi, and Sasaki (1982), using nylon and silicon monoxide as insulating layers. All of these efforts were directed at obtaining samples on which NMR measurements were to be performed. The micrographs of three of the particle samples of Fukagawa *et al.* are shown in Fig. 32. Quite uniform particle diameters can be produced in a compact form and the separation of the particles prepared this way is much better defined than for inert-gas-evaporated particles. The larger particles tend to have an oblate shape, described by Wright (1967) as platelets. The aspect ratio may be as large as 1:2 for particles larger than 200 Å. This systematic variation in particle shape with increasing particle size can produce difficulties in accounting for the results of physical measurements of electronic properties in terms of a simple size distribution, as was assumed in our earlier discussion, Sec. II.

The multiple vacuum evaporation method, with SiO insulating layers, appears to be the best compromise in terms of obtaining a suitable metal particle filling factor and ensuring that the particles are well separated. This can be compared favorably to inert-gas-evaporation methods that do not have matrix isolation introduced explicitly into the procedure. However, it may be that this technique is most useful in the preparation of the smaller particle sizes, less than 200 Å, as was demonstrated by Yee and Knight (1975).

In order to avoid difficulties of coalescence and growth limiting the production of very small particles by the evaporation methods discussed above, Yatsuya, Mihama, and Uyeda (1974) and Yatsuya, Tsukasaki, Mihama, and Uyeda (1978) developed a new method. Their technique employs vacuum evaporation onto a running oil substrate (VEROS). The nucleation and growth of particles takes place in oil driven by a supporting rotating disc. The fluid also serves as a collection medium. It was found that a rather narrow size distribution with mean size in the range 20—80 Å could be prepared in this way. They also recognized that this method is easily adapted to large-scale production that may be of technical or commerical interest. In a more recent improvement of the technique they have made stable distributions of small Ag particles (≈ 50 Å) on a cooled ethyl alcohol substrate that can be evaporated at a later time to give a higher concentration of metal (Yatsuya, Tsukasaki, Yamauchi, and Mihama, 1985). According to these reports the particle

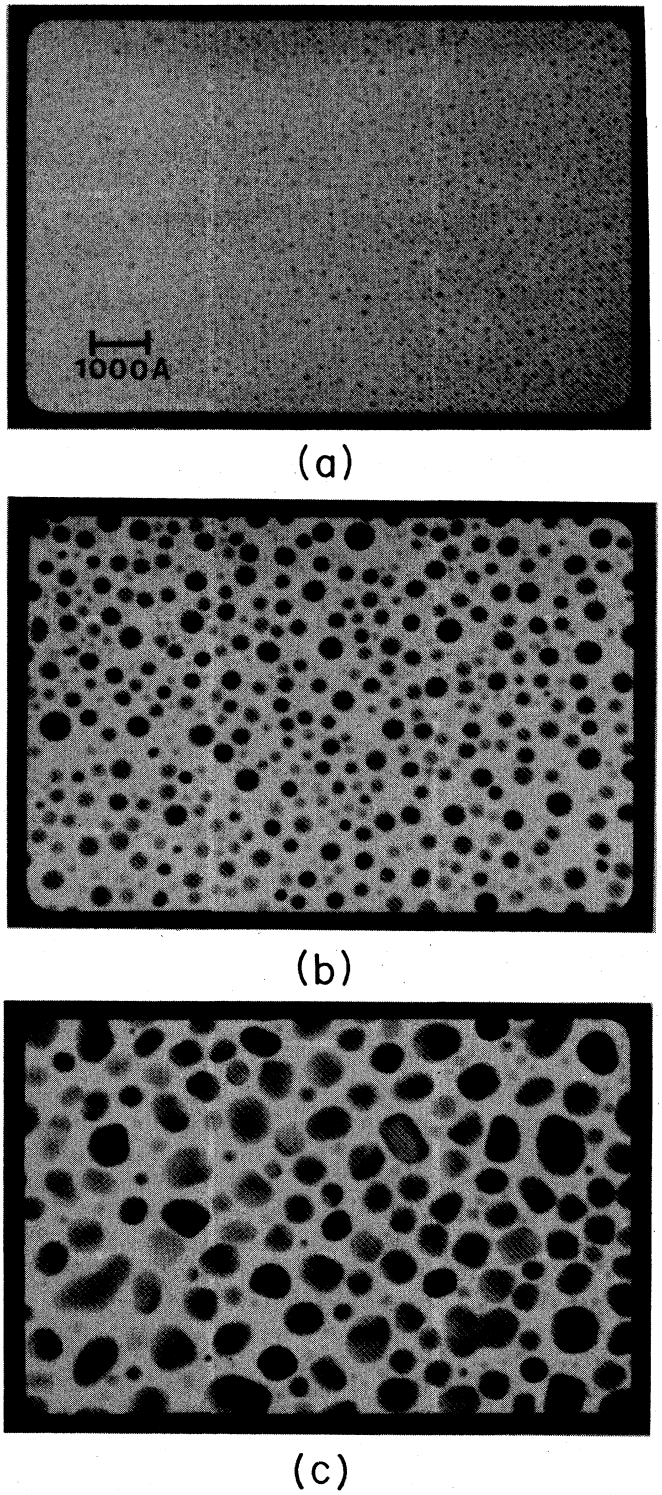

FIG. 32. Electron micrographs of three samples of Sn particles produced by the method of vacuum evaporation and subsequent island formation on Mylar substrates by Fukagawa, Kobayashi, and Sasaki (1982). The average diameters of these samples d' and the average cube root of the third moment of the size distributions $d=(6\bar{\Omega}/\pi)^{1/3}$, were found to be (a) $d'=75$ Å, $d=70$ Å; (b) $d'=330$ Å, $d=280$ Å; and (c) $d'=610$ Å, $d=450$ Å. In the above, $\bar{\Omega}$ is the average volume of a particle.

size is controlled by the viscosity of the fluid that is used, the rotation speed of the disc supporting the fluid, and the evaporation rate. This appears to be one of the more promising of the evaporation techniques.

Some of the motivation for the development of the VEROS methods was derived from the perceived need to supply samples suitable for observation of quantum effects. The stated requirement (Yatsuya, Mihama, and Uyeda, 1974) for very small particles ($d<100$ Å) is not a rigorous condition. In fact, for the smallest particles the surface properties play an important role that can confuse interpretation of measurements. This has been found to be the case in preceding sections of this paper. The difficulties with separation of surface and volume effects are exacerbated depending on the chemical reactivity between the metal and its support. On the other hand, it is possible to study quantum effects without this ambiguity in larger particles if the measuring temperature is adequately low and if the spin-orbit interaction is not too strong. Reduction of the metal support interaction can be achieved using cryogenic methods for isolation of the particles in a rare gas solidified matrix. This subject is discussed next.

E. Vacuum evaporation and cryogenic matrix isolation

ESR experiments on the quantum effects of metals can be expected to measure the properties of roughly one conduction electron per particle. It was recognized more than ten years ago by the Lausanne group that at this level of sensitivity the ESR measurement could be confused with background signals arising from free radicals or ESR active sites located at the interface between the metal particle and its support. It is precisely this interface which may have ill-defined chemical character. Their approach was to minimize the alterations in electronic environment at the interface by embedding it in a chemically nonreactive medium at cryogenic temperatures. This procedure calls for the evaporation of the desired element in the presence of a jet of a suitable condensable matrix medium near the cryogenically cooled collection surface. Normally this is held at liquid-nitrogen temperature (77 K). In early work with Li particles Borel, Borel-Narbel, and Monot (1974) used CO_2 matrices. Generally, the characteristic signature of the atomic state of the element is observed directly after the evaporation. This can be identified from the known hyperfine splitting of the ESR spectrum. Heat treatment of the sample at temperatures up to 140 K gives rise to the formation of small particles by diffusive aggregation of the evaporated atoms. This annealing can be controlled systematically to produce desired particle sizes. Subsequent work with other elements (Al, Ag, Mg) and matrices (C_8H_8, $C_{18}H_{38}$, and Xe) led to the discovery that the rare gas matrix consisting of solidified Xe was more suitable, having less chemical interaction with the metal. This is confirmed in the case of Li particles, from the ESR spectrum (Borel and Millet, 1977).

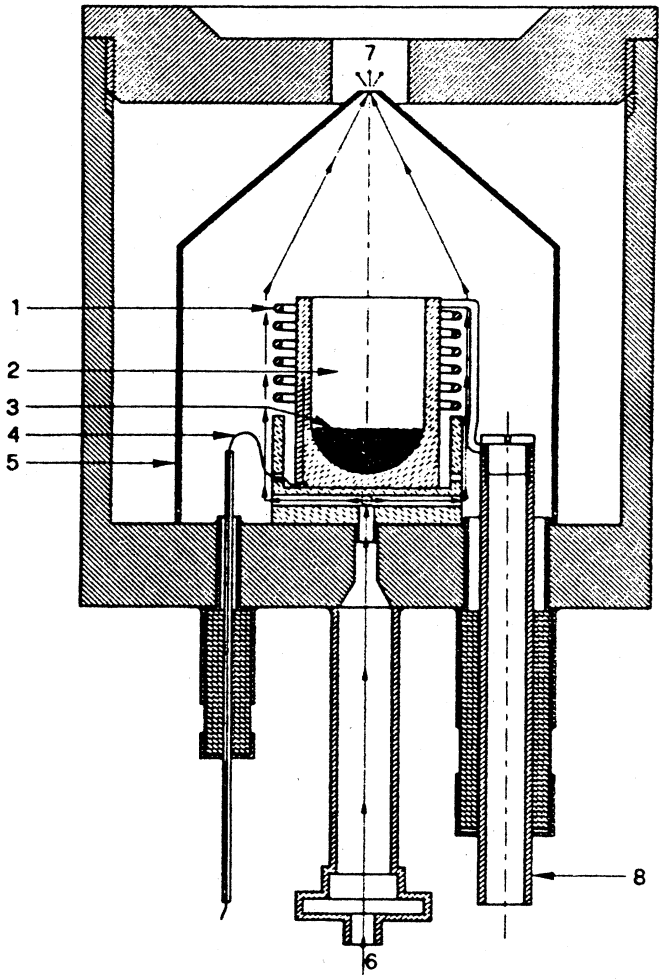

FIG. 33. Schematic of the source for preparation of particles by a cluster beam method where nucleation takes place in a high purity cold helium gas stream as reported by Millet and Borel (1981,1982). The metal clusters of Mg produced by this source were subsequently trapped in a xenon cryogenic matrix, collected and sealed into quartz ampoules without venting the evaporation chamber. Shown above are (1) filament, (2) crucible, (3) charge of starting material, Mg in this case, (4) thermocouple, (5) screen, (6) helium inlet, (7) nozzle, and (8) electrical heater lead.

More recent refinements in technique have produced an apparatus for which the particle source is sketched in Fig. 33 used in the production and study of Mg particles (Millet and Borel, 1981,1982). In this case nucleation of the particles is provided by the He gas carrier as shown in the figure. These clusters were embedded in xenon at the collection surface. A scraper could be activated *in situ* causing the collected sample to drop down into a high-purity quartz tube containing liquid argon. The tubes were flame sealed and the samples maintained at cryogenic temperatures.

A similar approach has been used by Kimura, Bandow, and Sako (1985) where the Mg particles were prepared in helium gas, providing an environment for nucleation, and where condensed hexane was used as the matrix.

F. Cermets

A modification of vacuum evaporation and matrix isolation involves the simultaneous deposition of metal and insulator by sputtering or electron beam evaporation. This results in a granular metal film whose properties depend quite strongly on the fraction of metal to insulator. Ceramic materials such as SiO_2 or Al_2O_3 are commonly used as insulators from which the generic term cermet is derived. In the limit of small metal fractions isolated metal particles are obtained with typical sizes in the range 10—40 Å depending on the specific materials and conditions. [See for example Abeles *et al.* (1975), Stewart (1977), or Filler *et al.* (1980).] These authors report applications with the metallic elements Ni, Pt, Au, and Al producing particles with fairly broad size distributions. These composite materials are well suited to heat capacity studies (Stewart, 1977; Filler *et al.*, 1980) since reasonable amounts of material can be prepared [$\approx$20 mg, Stewart (1977)]. However, a lack of definition of the interfacial conditions between metallic element and ceramic matrix leads to ambiguous interpretaton of thermodynamic measurements for particles that are this small (Filler *et al.*, 1980). Extensive measurements of the conductivity of cermets have been reported by Abeles *et al.* (1975) with theoretical interpretation of their work proposed by Mostefa and Olivier (1985) involving discreteness of the electron level distribution in each of the metal particles.

G. Cluster beams

The application of atomic beam techniques to the production of metal clusters has been developing steadily. In the pioneering effort of Knight and collaborators (Knight, Monot, Dietz, and George, 1978) this technology was used to observe Stern-Gerlach deflection of small particles. One might expect that the magnetic quantum effects associated with even- or odd-electron-number clusters would be manifest in their effect on the deflection of a cluster beam. This was the phenomenon observed by Knight *et al.* Magnetic properties of cluster beams have been discussed further by Knight (1983).

A significant advance was made by Sattler, Mühlbach, and Recknagel (1980) in preparing a cluster beam using an inert gas atmosphere to nucleate the formation of clusters. Time-of-flight measurements allowed the determination of the masses produced. Evidence for clusters up to 400 atoms was found. Recent reviews of the properties of such cluster beams have been prepared by Stein (1985) and Schaber and Martin (1985). The combination of cluster beam technology and cryogenic matrix isolation of the clusters was developed by Millet and Borel (1981,1982) to study size effects on the ESR of Mg particles.

The application of cluster beams to observe quantum effects directly through their magnetic susceptibility or

optical properties without a matrix interaction at all appears to be still speculative at this stage. Another possible implication of the cluster beam technology for the understanding of quantum effects is the filtering of the cluster beam to obtain monodispersed cluster masses for use in the investigation of their electronic properties. Direct observation of even-odd electron structure effects on the photoion yield in cluster beams has been reported by Saunders *et al.* (1985).

H. Pressure impregnation of a porous material

A rather interesting and unique particle preparation method involves the impregnation with molten metal of the pore space of leached Vycor glass. The principle is much the same as that upon which mercury porosimetry is based. When the pressure on the molten metal is relieved and the sample is cooled the liquid metal retracts and forms small spherical particles with some evidence for interparticle contact, although not more extensive than approximately three particle diameters. This technique was developed by Watson (1966,1970). Novotny and Meincke (1973) investigated the specific heat of small size lead and indium particles prepared by this method and Charles and Harrison (1963) performed NMR measurements on lead particles made this way. Despite the difficulty of there being some amount of interparticle contact there are real advantages of this approach. An impressive amount of sample can be prepared with a relatively narrow distribution in size since the porosity of the glass is usually at least 20%. Naturally it can be expected that there will be some effect of the interaction between metal and the glass matrix on electronic properties. The method is restricted to those metals with low melting temperatures which, apart from the chemically reactive alkalis, are all superconductors (Pb, In, Sn, Ga, Cd, Zn, and Hg).

I. Nucleation of metal clusters by irradiation

The earliest investigations of electron spin resonance in small metal clusters were performed on samples prepared using a radiation technique. The effect of the radiation in sodium azide NaN_3 was to nucleate atomic sodium that would later grow into metal clusters following an annealing treatment (McMillan, King, Miller, and Carlson, 1962). Later work with this material included studies by Smithard (1974b) and Gordon (1976). When sodium azide is irradiated with ultraviolet or x-ray radiation with dosages in the order of 10 Mrad, decomposition results from which sodium metal particles form during a subsequent heat treatment. Samples have been prepared in both powder and single crystal form. The latter were found to be mechanically unstable if they were annealed sufficiently to produce sodium metal content greater than 0.2% (Gordon, 1976). Particle size determinations were based on the optical absorption work of Smithard (1974a), interpreted in terms of the classical Mie theory discussed in Sec. VI. Difficulty in understanding the effect of the matrix compromises the effectiveness of this preparation technique. Since the resulting particle concentrations are limited to a few tenths of a percent there is too small an amount of material for susceptibility, NMR, and specific heat experiments, although quite an adequate amount for ESR and optical work. A similar method for producing potassium particles from KN_3 has been used by McMillan (1964) for the purpose of performing ESR experiments.

Precipitation of either gold (Meier and Wyder, 1972) or silver (Doremus, 1965; Dupree and Smithard, 1972; Smithard, 1973) particles in glass has been used to prepare samples for optical investigation of their electronic properties. This basic procedure produces silver atoms from a photosensitive glass by ultraviolet irradiation. Heat treatment allows cluster growth and further reduction of silver oxides in the glass. The particle size can be controlled to some extent depending on the heat treatment although the volume-filling fraction of metal is generally substantially less than 10^{-3}. Such samples are useful particularly for optical and ESR experiments where large amounts of material are not required. Matrix effects may be significant as it now appears from recent optical work comparing the surface plasmon linewidth for glass matrix samples with those prepared in an inert gas cryogenic matrix (Kreibig and Genzel, 1985).

A variation on this theme is a stain glass process that permits higher volume fractions of metal to be obtained. Here silver ions are diffused into the glass and exchanged for sodium ions at high temperatures. Reduction of the silver ions and their diffusion-driven aggregation produces a colorful sample with particles of the order of 40 Å (Dupree and Smithard, 1972).

Some of the most provocative experiments stimulating work on quantum effects in metal clusters were the early ESR and NMR results of Charvolin *et al.* (1966) and Taupin (1967) on Li platelets produced from LiF crystals by neutron irradiation. Although these workers did not directly determine the particle sizes they have nonetheless determined that there tend to be both small (10 Å) and larger (200 Å) particles in these samples. Of particular note for Li is that this method leaves the clusters out of contact with oxygen and other potential contaminants. On the other hand, the local environment of the cluster is not chemically inert and the matrix may affect the ESR experiments.

J. Microlithography

Considerable advances have been made in recent years in the development of techniques for producing microelectronic circuitry by electron and photolithographic methods. It is natural to speculate how these capabilities could be applied to the production of well-defined particles having not only a specific size but also a particular shape. Ideally such particles should be considered identical to the extent that each provides the same boundary conditions for the electronic wave functions. Control of

the samples at this level could allow one to experiment with samples without recourse to Kubo's basic statistical ansatz of random boundary conditions. At Cornell University, Hammel and Richardson (1981) have initiated an attempt to prepare particles this way. From their preliminary work it seems clear that the definition of particle size and shape is an achievable goal. Control of geometry at the atomic level, however, appears to be unrealistic.

VIII. SUMMARY AND CONCLUSIONS

There are two issues that thread through the present review and should be focused upon in this summary. First, have quantum size effects in the electronic behavior of metal particles been observed? It is obvious that the conduction electronic levels must indeed be discrete and consequently, at sufficiently low temperatures, effects of this discreteness ought to be apparent in some way. This first question really asks if the technical problems of working with large numbers of nonidentical particles have been solved and the appropriate experiments been done that demonstrate this fundamental aspect of single-particle properties. The answer to this question is unambiguously yes and can be found in almost all classes of experiment summarized in Tables VI–X. This is most clearly demonstrated in the temperature dependence of the electronic susceptibility, including direct measurements with Faraday balance methods (Mg), ESR intensity measurements (Li, Ag), and Knight shift experiments (Cu, Sn). The ESR linewidth experiments for Li, Al, and Ag and ESR g-shift results (Mg, Ag) show effects of a discrete electronic spectrum. An inhibited magnetic relaxation rate (Li, Cu) is also consistent with these ideas. There are notable absences of observation of quantum effects in the heat capacity and optical behavior.

Second, we would like to determine if the energy level spacings are correlated as indicated by an appropriate energy level distribution function. Certainly a statistical theory is necessary since real samples have on the order of 10^{15} particles. What is at issue is whether the electronic level spacings are randomly distributed over the sample or not. If not, then by what statistics? The Kubo theory (Kubo, 1962) and its ammended versions (Gor'kov and Eliashberg, 1965; Denton *et al.*, 1973) state that random particle shapes and surface structures require a statistical theory for the level spacings that depends only on the symmetry of the electron Hamiltonian. So then the second question is: what is the experimental evidence for random or nonrandom statistics of the energy level distribution functions? Here the answer must be more guarded based on the current experimental situation for the magnetic susceptibility summarized in Table VI. There is a good indication that Poisson statistics are inappropriate since its prediction for the even particle susceptibility (Fig. 4) is quite inconsistent with the Knight shift observations for Cu and Sn presented in Fig. 19 and the magnetization measurements on Mg, Fig. 10. According to Poisson statistics the electronic susceptibility for even particles does not decrease at low temperatures, rather it increases above the Pauli value. On the other hand, the measurements clearly show a decrease. It is not possible to proceed much further than this in selecting a correct statistical description from these experimental results. The Knight shift measurements for Cu and Sn decrease linearly with the temperature suggesting that an orthogonal ensemble is appropriate. However, Perenboom *et al.* (1981a) argue that this is necessarily the expected result for all even electron particle measurements, such as for the Knight shift, independent of the electron Hamiltonian symmetry.

The experiments on Cu and Sn demonstrate that there is a nonzero electronic susceptibility at $T=0$ in these materials, as is expected theoretically for elements with a substantial spin-orbit interaction. This residual susceptibility depends on particle size but is not found to be proportional to the square of the particle size as the theory predicts.

The only quantitative information comes from the electronic susceptibility experiments. There are several directions that could be pursued that could clarify this picture further. Both the NMR Knight shift and ESR intensity experiments have been used successfully to probe the quantum size regime. The NMR method looks predominantly at the susceptibility of the even-electron-numbered particles. This complements the ESR experiments for which the ESR signal intensity is proportional to the total electronic susceptibility. A definitive experiment might combine the two measurement techniques for the same samples. Second, the magnetic field dependence of the Knight shift at low temperatures allows a direct measurement of the two-level correlation function. These experiments might be tried in Li or Ag where spin-orbit interactions are less important than in Cu or Sn.

It is unfortunate that there are no heat capacity results that allow a quantitative statement to be made concerning electronic size effects. The heat capacity is the most important probe of the thermodynamical behavior of the metal particle system, but is also the most difficult to measure. It is necessary to find a solution to technical problems for sample production which guarantee thermal contact but maintain particle-to-particle isolation. One possibility may be to use the cluster beam methods and inert gas nucleation of the particles in combination with a cryogenic rare gas matrix.

There are clear indications of quantum effects in the ESR line width (Li, Al, Ag) and g shift (Mg, Ag). However, neither the experiment nor the theory is sufficiently refined that information on level distribution statistics can be obtained.

The magnetic relaxation situation is in an even more primitive state. There is no theory and the experiments are qualitative at best. As a practical matter it may be difficult to distinguish between the surface and bulk relaxation processes.

The identification of quantum size effects on the surface plasmon mode linewidth is an interesting and promising subject. However, it is unlikely that electron-

TABLE VI. Summary of theory and experiment for quantum size effects on the magnetic susceptibility.

QSE theory	Magnetic Susceptibility	References
For elements with small spin-orbit interaction odd-number-electron particles have a Curie law susceptibility at low temperatures and low magnetic fields. Even-number-electron particles have a susceptibility that goes to zero at low temperatures and low fields according to a (linear) power law. At high temperatures the susceptibility is equal to the Pauli susceptibility for both cases.	$\chi_{odd}=\mu_B^2/k_BT$ $\chi_{even}=7.63\mu_B^2k_BT/\delta$ $K(T)/K(\infty)=\chi_{even}(T)/\chi_{Pauli}$	Eq. (2.28); Denton *et al.* (1973); Perenboom *et al.* (1981a).
For small spin-orbit interaction the NMR Knight shift goes to zero at low temperatures, and small magnetic fields, linear in the temperature since the only observable contribution to the NMR line is from even particles in this limit.	$k_BT \ll \delta$ $2\pi\mu_BH \ll \delta$ $\overline{\langle H_{so}\rangle} \ll \delta$ $K(0),\chi_{even}(0) \propto d^2$	Sec. III.B
The field dependence of the magnetic susceptibility is given by the two-level correlation function $R(x)$. For large fields and/or large spin-orbit interaction the susceptibility is equal to the Pauli susceptibility. For intermediate values of the spin-orbit interaction the even-particle susceptibility and the Knight shift have residual values at $T=0$ that scale as the square of the particle size.		Eqs. (2.33) and (2.34) and Denton *et al.* (1973). Shiba (1976); Sone (1977)
The ESR integrated intensity from conduction electrons is proportional to the electronic susceptibility described above.		

	Experiment			
Li	20 Å, 100 Å; NMR Knight shift; 10 kOe; 300–370 K	The NMR line appears at the zero Knight shift position for Li at room temperature.	weak evidence for QSE	Charvolin *et al.* (1966); Taupin (1967)
	32 Å; ESR intensity; 0.2–3.3 kOe; 2–120 K	The ESR intensity shows a temperature independent value at high temperatures and a Curie-type dependence at low temperatures.	clear evidence for QSE	Borel and Millet (1977)
Be	30 Å; Faraday balance, 10 kOe; 2–150 K	The susceptibility increases slightly with decreasing temperature.	no evidence for QSE	Kimura *et al.* (1985)
Na	10–1000 Å; ESR intensity; 3.3 kOe; 4.2–300 K	No temperature dependence of the intensity was observed. The intensity was consistent with the bulk Pauli susceptibility.	no QSE	Smithard (1974)
	24,52,≈200 Å, 1350 Å; ESR intensity; 3.3–8.6 kOe; 4.2–450 K	The ≈200-Å sample appeared to have an increase in intensity at 4.2 K, other samples did not.	no clear evidence for QSE	Gordon (1976)

TABLE VI. (*Continued*).

	Magnetic Susceptibility			
	Experiment			References
Mg	12, 20, >30 Å; ESR intensity; 3.3 kOe; 2.6–150 K	A slight increase in intensity with decreasing temperature was observed at the lowest temperatures for the two smallest samples. Those larger than 30 Å were temperature independent.	possibly QSE but why is the g shift so large?	Millet and Borel (1981)
	200–2300 Å; ESR intensity; 3.3–8.6 kOe; 4.2–250 K	An increase in intensity was measured with decreasing temperature.	particles seem too big for QSE	Sako and Kimura (1984,1985)
	20 Å; Faraday balance, 10 kOe; 2–150 K	An approximately constant susceptibility was observed down to $\approx$25 K where it decreased abruptly toward zero.	clear evidence for QSE	Kimura *et al.* (1985)
Al	70, 90, 110 Å; NMR Knight shift; 1.3–78 K	No temperature dependence to the Knight shift was observed.	no QSE seen	Fujita *et al.* (1970)
	45–200 Å; NMR Knight shift; 3.7–10 kOe; 0.5–4.2 K	The Knight shift moves toward zero with decreasing temperature.	how much is QSE and how much is superconductivity?	Kobayashi *et al.* (1970, 1971, 1972, 1974) Ido and Hoshino (1975); Ido (1976)
	80, 100, 160 Å; NMR Knight shift; 8.1, 27, 36 kOe; 0.5–4.2 K	The Knight shift moves toward zero with decreasing temperature. Superconductivity is quenched in the largest fields but surprisingly the QSE on the susceptibility is not quenched.	evidence for QSE	Kobayashi *et al.* (1978); Nomura *et al.* (1980)
Cu	40–150 Å; NMR Knight shift; 4.5–8.9 kOe; 0.5–77 K	Temperature-dependent inhomogeneous NMR line broadening. No even-particle Knight shift was observed.	no clear evidence for the QSE	Hines (1971); Kobayashi *et al.* (1971, 1972); Kobayashi (1974)
	25–450 Å; NMR Knight shift; 2–9 kOe; 0.4–77 K	The Knight shift moves toward zero approximately linearly with decreasing temperature indicating a nonzero residual shift at $T=0$. The residual shift decreases with decreasing particle size qualitatively according to theory.	clear evidence for the QSE, see Fig. 19	Yee and Knight (1975)
	15–110 Å; NMR Knight shift; 10 kOe; 0.66–1.4 K	The Knight shift moves toward zero approximately linearly with decreasing temperature indicating a nonzero residual shift at $T=0$. The residual shift decreases with decreasing particle size qualitatively according to theory.	clear evidence for the QSE, see Fig. 19	Kobayashi (1977)

TABLE VI. (*Continued*).

	Magnetic Susceptibility			
	Experiment			References
Ag	10 Å; ESR intensity; 3.3 kOe; 8–190 K	Temperature-dependent ESR intensity consistent with a Curie law susceptibility.	evidence for QSE	Monot and Millet (1976)
Sn	150–850 Å; NMR Knight shift; 1.2–8.8 kOe; 1.5–77 K	Knight shifts were observed that can be understood in terms of effects of interplay of superconductivity and a large spin-orbit interaction.	particles too large for QSE	Androes and Knight (1961); Wright (1967); Hines and Knight (1971); Kobayashi *et al.* (1974)
	22–450 Å; NMR Knight shift; 5.7–30 kOe; 1.3–4.2 K	Evidence for partial quenching of superconductivity in the largest fields was found from spin-lattice relaxation data. The Knight shift moves toward zero approximately linearly with decreasing temperature indicating a nonzero residual shift at $T=0$. The residual shift decreases with decreasing particle size qualitatively according to theory.	clear evidence for QSE, see Fig. 19	Nomura *et al.* (1977); Fukagawa *et al.* (1982)
Os	10 atom cluster; Faraday balance; 4.2–300 K	A Curie law susceptibility was observed.	possibly QSE	Benfield *et al.* (1982)
Pt	22 Å; Faraday balance; 2–13 kOe; 1.5–200 K	Curie-Weiss temperature dependence of the susceptibility was observed that in the later work was shown to be most likely a surface effect.	no QSE	Marzke *et al.* (1976, 1983); Marzke and Glauninger (1984)
	33 Å; SQUID; 1 Oe; 0.02–0.6 K	Curie-Weiss temperature dependence of the susceptibility was observed.	no clear evidence for QSE	Yu and Halperin (1981b)
	21 Å; ESR intensity; 3.5, 8.5 kOe; 17–291 K	Curie-Weiss temperature dependence of the ESR intensity was observed.	likely not QSE	Gordon *et al.* (1977)
	33–200 Å; NMR Knight shift; 6–12 kOe; 1.6–77 K	The Knight shift was independent of temperature. Given the large spin-orbit interaction in Pt this is consistent with the QSE theory.	no evidence for QSE	Yu *et al.* (1980); Yu and Halperin (1981a,1981b)

TABLE VII. Summary of theory and experiment for quantum size effects on the heat capacity

QSE theory		Heat capacity		References
The Kubo theory ammended by Denton *et al.* (1973) predicts that the low-temperature dependence of the heat capacity on temperature should be a power law in the temperature. The coefficients of the power law will depend on the relative proportions of even- and odd-electron-numbered particles. This quantitative aspect would be difficult to determine experimentally. The predicted power law depends on the statistics of the level distribution function.		$C \propto (k_B T/\delta)$ $\propto (k_B T/\delta)^2$ $\propto (k_B T/\delta)^5$ for $(k_B T/\delta) \ll 1$	Poisson Orthogonal Symplectic	Kubo (1962); Denton *et al.* (1973) Eq. (2.27)
	Experiment			
V	29–132 Å; 0–35 kOe; 1.3–12 K	Enhancements in both electronic and lattice contributions to the heat capacity were observed. The samples were compacted from the metal powder. Superconductivity was observed.	no QSE	Comsa *et al.* (1976); Vergara *et al.* (1984)
Pd	30, 66 Å; 1.4–30 K	No change in the electronic heat capacity but an increase in the lattice contribution over the bulk was reported. The enhancement increased with decreasing particle size. The samples were compacted from the metal powder.	no QSE	Comsa *et al.* (1977)
In	22 Å; 1.5–15 K	Enhancement in the lattice contribution to the heat capacity was observed as well as the transition to superconductivity. The samples were contained in porous glass.	no QSE	Novotny *et al.* (1972); Novotny and Meincke (1973)
Pt	10, 16, 21, 26 Å; 1–12 K	Enhancement in the lattice heat capacity was found with a decrease in the electronic heat capacity for 26- and 10-Å sizes. Samples were Pt/SiO_2 sputtered cermets.	possible QSE	Stewart (1977)
Pb	22, 37, 60 Å; 1.5–15 K	Enhancement in the lattice contribution to the heat capacity was observed as well as the transition to superconductivity. The samples were contained in porous glass.	no QSE	Novotny *et al.* (1972); Novotny and Meincke (1973)

TABLE VIII. Summary of theory and experiment for quantum size effects on the ESR linewidth and g shift.

ESR linewidth and g shift			References
QSE theory			
According to the classical theory the effect of small particle size is to increase the ESR linewidth inversely with the size d. For sufficiently small particles (Kawabata conditions) a quantum theory must be used whereupon the linewidth should decrease as the square of the particle size, becoming inhomogeneous.	$\Delta H_{pp}=\hbar\omega_z/(\gamma_e\delta\tau_s)$ $\hbar\omega_z/\delta \ll 1$ (I) $\hbar/(\delta\tau_s) \ll 1$ (II)	(Kawabata conditions)	Kawabata (1970) Eq. (3.20) Eq. (3.21)
The ESR g shift has been predicted by Kawabata to approach the bulk g shift with decreasing particle size linearly with the term $-\hbar/\delta\tau_s \propto d^2$. In contrast, the theory of Buttet *et al.* (1982) predicts that the g shift approaches the surface atom g shift with a term proportional to the fraction of atoms at the surface f_s.	$\Delta g=\Delta g_\infty-\hbar/\delta\tau_s$	(Kawabata)	Kawabata (1970) Eq. (3.22)
	$\Delta g=(1-f_s)\Delta g_\infty+f_s\Delta g_s$	(Buttet *et al.*)	Buttet *et al.* (1982) Eq. (3.23)

	Experiment			
Li	6000–100 Å; ESR linewidth and g shift; 3.3 kOe; 77–300 K	With decreasing particle size the linewidth was found to increase, and then for sizes below 1300 Å it decreased. The turn-over size is an order of magnitude larger than expected from the Kawabata condition (I). A narrow line was seen at 77 K that was not understood. The g shift was equal to the free-electron value.	Quantum line narrowing is expected from the QSE	Gen and Petinov (1965); Saiki *et al.* (1972)
	7–18 Å; ESR linewidth and g shift; 0.053–3.3 kOe; 77–300 K	A frequency-dependent ESR linewidth was observed. This is expected in the quantum size regime as indicated above. Results are consistent with Saiki *et al.* (1972). The g shift was equal to the free-electron value. Important matrix effects on the linewidths were found.	consistent with QSE	Borel *et al.* (1974); Borel and Millet (1977)
Na	10–1000 Å; ESR linewidth and g shift; 3.3 kOe; 4.2–300 K	Classical behavior for the linewidth was observed with increasing linewidth on decreasing size. The g shift was that of the bulk metal. Note other work on Na by Petinov and Ardashev (1969) and Gordon (1976) who saw some evidence for QSE in one sample.	no QSE despite satisfying (I) and (II)	Smithard (1974b)
Mg	10–30 Å; ESR linewidth and g shift; 3.3 kOe; 3–77 K	The linewidth was found to vary with the particle-size distribution. The g shift depended on size consistent with the theory of Buttet *et al.* (1982). The bulk g shift was 2.06 inconsistent with values of other workers. Note other Mg work by Sako and Kimura (1984, 1985) and Kimura *et al.* (1985).	consistent with theory of Buttet *et al.* (1982)	Millet and Borel (1982)
Al	10–200 Å; ESR linewidth and g shift; 0.16–12 kOe; 90–120 K	A linewidth proportional to frequency was observed consistent with the theory. The g shift was independent of size and frequency and larger than accepted values for bulk Al. This is not understood.	consistent with QSE theory for linewidth not for the g shift	Millet and Monot (1975)
Ag	10–100 Å; ESR; 3.3 kOe; 7.5–300 K	No ESR signal was observed.		Smithard (1973)

TABLE VIII. (*Continued*).

	ESR linewidth and g shift			
	Experiment			References
	≈10 Å?; ESR linewidth and g shift; 0.16–3.3 kOe; 77 K	A correlation between linewidth and g shift was observed with the presumed implicit variable being the particle size in qualitative agreement with the Kawabata theory (1970). The extrapolation to the bulk g shift was different from accepted values. Note also line-shape analysis of Chatelain *et al.* (1976).	qualitative agreement with Kawabata (1970)	Monot *et al.* (1974)
Pt	22 Å; ESR linewidth and g shift; 3.3 kOe; 17–291 K	The linewidth (20 Oe) and g shift (equal to the free-electron value) are independent of temperature and frequency.	inconsistent with QSE theory	Gordon *et al.* (1977)
Au	30 Å; ESR linewidth and g shift; 3.3 kOe; 300 K	The linewidths were roughly 200 Oe varying from sample to sample. The g shifts were in the range 0.22–0.27 significantly larger than that accepted for bulk material, 0.11.	no clear evidence for QSE	Dupree *et al.* (1967)
	20–80 Å; ESR linewidth and g shift; 3.3 kOe; 300 K	The linewidths varied between 6 and 9 Oe with a g shift equal to the free-electron value.	no clear evidence for QSE	Monet *et al.* (1971)

TABLE IX. Summary of theory and experiment for quantum size effects on magnetic resonance relaxation.

	Magnetic resonance relaxation		
	QSE theory		References
It is understood at a qualitative level that the ESR longitudinal relaxation time should become very long in the limit specified by the first Kawabata condition. In this case there is a decoupling of the conduction electron states from the electronic Zeeman energy reservoir. The ESR line narrows and is limited by inhomogeneous broadening. However, there is no detailed theory for the longitudinal relaxation time.		$T_L \to \infty$, $\hbar\omega_e/\delta \ll 1$	Kawabata (1970,1977)
The NMR spin lattice relaxation rate should be inhibited as well. However, there is no theory for this effect apart from an estimation by Kawabata of the effect of interparticle electron tunneling.		$T_1 \to \infty$, $\hbar\omega_n/\delta \ll 1$	Kawabata (1970,1977)
	Experiment		
Li	7, 12, 15 Å; ESR 0.16 kOe; 77 K	Progressive saturation allowed measurement of the longitudinal relaxation time almost 2 orders of magnitude larger than the inverse linewidth. This effect clearly increased with decreasing particle size.	likely a QSE	Borel *et al.* (1974)
Na	≈150 Å; ESR; 3.2 kOe; 4.2 K	This sample appeared to have a broad easily saturable signal.	no clear evidence for QSE	Gordon (1976)

TABLE IX. (*Continued*).

Magnetic resonance relaxation				
	Experiment			References
Al	80, 100, 160 Å; NMR; 3–36 kOe; 0.5–4.2 K	Some evidence for an enhanced spin-lattice relaxation time although this is due in large measure to effects of superconductivity.	no clear evidence for QSE	Nomura *et al.* (1980)
Cu	15–100 Å; NMR; 10 kOe; 0.66–1.4 K	Clear evidence for enhanced spin-lattice relaxation times was found, however the recovery was nonexponential and a quantitative analysis was difficult.	evidence for QSE	Kobayashi (1977)
Sn	70–450 Å; NMR; 5.6–30 kOe; 1.3–4.2 K	Some evidence for an enhanced spin-lattice relaxation time although this is due in large measure to effects of superconductivity.	no clear evidence for QSE	Fukagawa *et al.* (1982)
Pt	22 Å; ESR; 3.3 kOe; 138–291 K	The ESR signal was found to be very easily saturable but it was not concluded that this signal originated from conduction electrons.	no clear evidence for QSE	Gordon *et al.* (1977)
	33–200 Å; NMR; 6–12 kOe; 1.6–77 K	The spin-lattice relaxation was equal to the bulk metal value in all cases.	no evidence for QSE	Yu and Halperin (1981a)

TABLE X. Summary of theory and experiment for quantum size effects on optical and infrared absorption.

Optical and infrared absorption			
QSE theory			References
The classical and quantum theories for the surface plasmon mode predict that the linewidth should vary inversely with the particle diameter with a linewidth narrower by approximately a factor of 2 for the quantum case.	$\Gamma_{cl}=2v_F/d$ $\Gamma_{qm}\propto v_F/d$	classical quantum	Kawabata and Kubo (1966); Genzel *et al.* (1975); Genzel and Kreibig (1980); Kraus and Schatz (1983)
There is not yet a clear consensus as to what is expected for the plasmon mode frequency shift in the quantum theory.			Cini (1981); Kreibig and Genzel (1985)
The same is true for the polarizability.			Ekardt (1984); see Sec. IV
The far infrared absorption should have an oscillatory dependence on wave number that will likely be washed out by size-distribution effects. At very small wave numbers it was suggested that one might see anomalously low absorption. Enhanced absorption from particle clusters is expected.			Devaty and Sievers (1980,1985) Curtin *et al.* (1985); Niklasson and Granqvist (1986)

TABLE X. (*Continued*).

	Optical and infrared absorption			
	Experiment			References
Al	50–400 Å; Far-infrared abs.; 1.2–20 K	Enhanced absorption was observed.	no QSE	Tanner *et al.* (1975) Granqvist *et al.* (1976)
Cu	100–270 Å; Far-infrared abs.; 1.2–20 K	Enhanced absorption was observed.	no QSE	Tanner *et al.* (1975);
Ag	10–200 Å; Surface plasmon absorption; 1.5–300 K	Classical behavior for the surface plasmon mode width was observed.	no QSE	Doremus (1964,1965); Kreibig and Fragstein (1969); Smithard (1973); Kreibig (1974); Kreibig and Genzel (1985)
	≈50 Å; Surface plasmon absorption	Narrower surface plasmon modes were observed possibly consistent with QSE.	possibly QSE	Charlé *et al.* (1984)
	30–120 Å; Polarizability; 4.2–300 K	No enhanced polarizability was observed.	no QSE	Dupree and Smithard (1972)
	100 Å; Far-infrared abs.; 0–60 kOe; 1.2–25 K	Enhanced absorption due to particle clumping was observed. See also Carr *et al.* (1981,1983).	no QSE	Devaty and Sievers (1984)
Sn	50–400 Å; Far-infrared abs.; 1.2–30 K	Enhanced absorption was observed.	no QSE	Tanner *et al.* (1975); Carr *et al.* (1983)
Au	25–60 Å; Polarizability; 0.3 K	No enhanced polarizability was observed.	no QSE	Meier and Wyder (1972)
Pb	≈100 Å; Far-infrared abs.; 1.2–30 K	Enhanced absorption was observed.	no QSE	Tanner *et al.* (1975); Carr *et al.* (1983)

level statistics play an important role here. Comparison of experiment with the single-particle theory for the polarizability or far-infrared absorption coefficient will be extemely difficult. In the latter case enhanced absorption from particle clustering seems to mask the predicted quantum effects. Even so, model calculations have shown that a realistic distribution of particle sizes will wash out the effects of discrete electron levels anyway.

In general, these measurements will have contributions from the surface of the particle as well as from the bulk quantum effects that are the central theme in this review. The surface effects are themselves a very interesting subject. Some might be clearly delineated as in the NMR identification of a surface Pt atom in the work of Slichter and colleagues (see Fig. 15 and Rhodes, Wang, Makowka, Rudaz, Stokes, Slichter, and Sinfelt, 1982; Stokes *et al.*, 1982) and van der Klink *et al.* (1984). Others have been evident in the size dependence of magnetization measurements on V particles by Akoh and Tasaki (1977); Pd particles (Ladas *et al.*, 1978); and Pt (Marzke and Glaunsinger, 1984). Surface electronic effects have been observed in the NMR linewidth of Pt particles by Yu *et al.* (1980) and Yu and Halperin (1981b). In order to separate the volume quantum size effects from these surface effects it may be necessary to work with larger particles. This will obviously require lower temperatures to study the quantum effects.

The results that have been obtained on the heat capacity of particle compacts points out that the discreteness of the lattice vibrational modes plays an important role. In addition, there are surface modes and possibly modes associated with collections of particles. The inherent statistical nature of this problem which might be evident in experiments in the low-temperature limit has not been investigated theoretically. It is also not understood what are the effects of reduced particle size on the electron-phonon interaction.

ACKNOWLEDGMENTS

In preparing this review the author has benefited from helpful commentary and discussion from R. Burwell Jr., J. Buttet, C. Granqvist, S. Kobayashi, R. Monot, J. Wilkins, and I. Yu. The hospitality of the Centre de Recherche sur les Très Basses Températures, CNRS, Grenoble is gratefully acknowledged where the preparation of this manuscript was initiated. Partial support was obtained from the NSF DMR-8318614.

REFERENCES

Abe, H., W. Schulze, and B. Tesche, 1980, Chem. Phys. **47**, 95.
Abeles, B., P. Sheng, M. D. Coutts, and Y. Arie, 1975, Adv. Phys. **24**, 407.
Abou-Kais, A., M. Jarjoui, J. C. Vedrine, and P. C. Gravelle, 1977, J. Catal. **47**, 399.
Abrikosov, A. A., and L. P. Gor'kov, 1960, Zh. Eksp. Teor. Fiz. **39**, 480 [Sov. Phys.—JETP **12**, 337 (1961)].
Adawi, I., 1966, Phys. Rev. **146**, 379.
Akoh, H., and A. Tasaki, 1977, J. Phys. Soc. Jpn. **42**, 791.
Anderson, P. W., 1959, Phys. Rev. Lett. **3**, 325.
Andrew, S. P. S., 1981, Chem. Eng. Sci. **36**, 1431.
Androes, G. M., and W. D. Knight, 1961, Phys. Rev. **121**, 779.
Appel, J., 1965, Phys. Rev. **139**, A1536.
Ashcroft, N. W., and N. D. Mermin, 1976, *Solid State Physics*, 1st ed. (Holt, Rinehart and Winston, New York).
Baltes, H. P., and E. R. Hilf, 1973, Solid State Commun. **12**, 369.
Baltes, H. P., and E. Šimànek, 1981, in *Aerosol Microphysics II*, Topics in Current Physics Vol. 29 (Springer, Berlin), p. 7.
Barojas, J., E. Cota, E. Blaisten-Barojas, J. Flores, and P. A. Mello, 1977, Ann. Phys. (N.Y.) **107**, 95.
Benfield, R. E., P. P. Edwards, and A. M. Stacy, 1982, J. Chem. Soc. **10**, 525.
Bennett, L. H., R. E. Watson, and G. C. Carter, 1970, J. Res. Natl. Bur. Stand. Sect. A **74**, 569.
Beuneu, F., and P. Monod, 1978, Phys. Rev. B **18**, 2422.
Bond, G. C., 1985, Surf. Sci. **156**, 966.
Borel, J.-P., C. Borel-Narbel, and R. Monot, 1974, Helv. Phys. Acta **47**, 537.
Borel, J.-P., and J.-L. Millet, 1977, J. Phys. (Paris) Colloq. **38**, C2-115.
Brody, T. A., J. Flores, J. B. French, P. A. Mello, A. Pandey, and S. S. M. Wong, 1981, Rev. Mod. Phys. **53**, 385.
Bruggeman, D. A. G., 1935, Ann. Phys. (Leipzig) **24**, 636.
Buch, V., R. B. Gerber, and M. A. Ratner, 1982, J. Chem. Phys. **76**, 5397.
Buchal, C., F. Pobell, R. M. Mueller, M. Kubota, and J. R. Owers-Bradley, 1983, Phys. Rev. Lett. **50**, 64.
Buhrman, R. A., and W. P. Halperin, 1973, Phys. Rev. Lett. **30**, 692.
Burger, H. C., and P. H. van Cittert, 1930, Z. Phys. **66**, 210.
Burton, J. J., 1970, J. Chem. Phys. **52**, 345.
Butt, J. B., 1985, Appl. Catal. **15**, 161.
Buttet, J., 1981, in *Entre l'atome et le cristal: les agrégats*, 4ième École d'Été Méditerranéene (Les Editions de Physiques, Paris), 287.
Buttet, J., R. Car, and C. W. Myles, 1982, Phys. Rev. B **26**, 2414.
Bylina, E. A., V. B. Evidokimov, and N. I. Kobozev, 1962, Russ. J. Phys. Chem. **36**, 1392.
Carey Lea, M., 1889, Am. J. Sci. **37**, 476.
Carr, G. L., J. C. Garland, and D. B. Tanner, 1983, Phys. Rev. Lett. **50**, 1607.
Carr, G. L., R. L. Henry, N. E. Russel, J. C. Garland, and D. B. Tanner, 1981, Phys. Rev. B **24**, 777.
Carter, G. C., L. H. Bennett, and D. J. Kahan, 1977, Prog. Mater. Sci. **20**, 295.
Cavicchi, R. E., and R. H. Silsbee, 1984, Phys. Rev. Lett. **52**, 1453.
Charlé, K.-P., F. Frank, and W. Schulze, 1984, Ber. Bunsenges. Phys. Chem. **88**, 350.
Charles, R. J., and W. A. Harrison, 1963, Phys. Rev. Lett. **11**, 75.
Charvolin, J., C. Froidevaux, C. Taupin, and J. M. Winter, 1966, Solid State Commun. **4**, 357.
Châtelain, A., J.-L. Millet, and R. Monot, 1976, J. Appl. Phys. **47**, 3670.
Cini, M., 1981, J. Opt. Soc. Am. **71**, 386.
Cinneide, A. D. O., and J. K. A. Clarke, 1972, Catal. Rev. **7**, 213.

Clogston, A. M., V. Jaccarino, and Y. Yafet, 1964, Phys. Rev. **134**, A650.
Colbert, T., A. Zangwill, M. Strongin, and S. Krummacher, 1983, Phys. Rev. B **27**, 1378.
Comsa, G. H., D. Heitkamp, and H. S. Räde, 1976, Solid State Commun. **20**, 877.
Comsa, G. H., D. Heitkamp, and H. S. Räde, 1977, Solid State Commun. **24**, 547.
Curtin, W. A., R. C. Spitzer, N. W. Ashcroft, and A. J. Sievers, 1985, Phys. Rev. Lett. **54**, 1071.
Damay, P., T. David, and M. J. Sienko, 1974, J. Chem. Phys. **61**, 4369.
Delley, B., D. E. Ellis, A. J. Freeman, E. J. Baerends, and D. Post, 1983, Phys. Rev. B **27**, 2132.
Denton, R., B. Mühlschlegel, and D. J. Scalapino, 1971, Phys. Rev. Lett. **26**, 707.
Denton, R., B. Mühlschlegel, and D. J. Scalapino, 1973, Phys. Rev. B **7**, 3589.
Devaty, R. P., and A. J. Sievers, 1980, Phys. Rev. B **22**, 2123.
Devaty, R. P., and A. J. Sievers, 1984, Phys. Rev. Lett. **52**, 1344.
Devaty, R. P., and A. J. Sievers, 1985, Bull. Am. Phys. Soc. **30**, 307.
Dickey, J. M., and A. Paskin, 1970, Phys. Rev. B **1**, 851.
Doremus, R. H., 1964, J. Chem. Phys. **40**, 2389.
Doremus, R. H., 1965, J. Chem. Phys. **42**, 414.
Dorling, T. A., B. W. J. Lynch, and R. L. Moss, 1971, J. Catal. **20**, 190.
Dupree, R., C. T. Forwood, and M. J. A. Smith, 1967, Phys. Status Solidi **24**, 525.
Dupree, R., and M. A. Smithard, 1972, J. Phys. C **5**, 408.
Dupuis, M., R. Mazo, and L. Onsager, 1966, J. Chem. Phys. **33**, 1452.
Dyson, F. J., 1955, Phys. Rev. **98**, 349.
Dyson, F. J., 1962, J. Math. Phys. **3**, 140.
Efetov, K. B., 1982a, J. Phys. C **15**, L909.
Efetov, K. B., 1982b, Zh. Eksp. Teor. Fiz. **83**, 833 [Sov. Phys.—JETP **56**, 467 (1982)].
Eigler, D. M., and S. Schultz, 1985, Phys. Rev. Lett. **54**, 1185.
Ekardt, W., 1984, Phys. Rev. Lett. **52**, 1925.
Elliott, R. J., 1954, Phys. Rev. **96**, 266.
Ferrell, R. A., 1959, Phys. Rev. Lett. **3**, 262.
Filler, R. L., P. Lindenfeld, T. Worthington, and G. Deutscher, 1980, Phys. Rev. B **21**, 5031.
Frank, F., W. Schulze, B. Tesche, J. Urban, and B. Winter, 1985, Surf. Sci. **156**, 90.
Frens, G., and J. Th. G. Overbeek, 1969, Kolloid. Z. Z. Polym. **233**, 922.
Fröhlich, H., 1937, Physica (Utrecht) **4**, 406.
Fu, C. L., S. Ohnishi, H. J. F. Jansen, and A. J. Freeman, 1985, Phys. Rev. B **31**, 1168.
Fujita, T., K. Ohshima, N. Wada, and T. Sakakibara, 1970, J. Phys. Soc. Jpn. **29**, 797.
Fukagawa, Y., S. Kobayashi, and W. Sasaki, 1982, J. Phys. Soc. Jpn. **51**, 1095.
Gates, J. V., and W. H. Potter, 1976, Phys. Rev. B **13**, 8.
Gen, M. Y., and V. I. Petinov, 1965, Zh. Eksp. Teor. Fiz. **48**, 29 [Sov. Phys.—JETP **21**, 19 (1965)].
Genzel, L., and U. Kreibig, 1980, Z. Phys. B **37**, 93.
Genzel, L., T. P. Martin, and U. Kreibig, 1975, Z. Phys. B **21**, 339.
Glick, A. J., and E. D. Yorke, 1978, Phys. Rev. B **18**, 2490.
Gordon, D. A., 1976, Phys. Rev. B **13**, 3738.
Gordon, D. A., R. F. Marzke, and W. S. Glaunsinger, 1977, J. Phys. (Paris) Colloq. **38**, C2-87.
Gor'kov, L. P., and G. M. Eliashberg, 1965, Zh. Eksp. Teor. Fiz. **48**, 1407 [Sov. Phys.—JETP **21**, 940 (1965)].
Granqvist, C. G., 1978, Z. Phys. B **30**, 29.
Granqvist, C. G., and R. A. Buhrman, 1975, Appl. Phys. Lett. **27**, 693.
Granqvist, C. G., and R. A. Buhrman, 1976a, J. Appl. Phys. **47**, 2200.
Granqvist, C. G., and R. A. Buhrman, 1976b, J. Catal. **42**, 477.
Granqvist, C. G., R. A. Buhrman, J. Wyns, and A. J. Sievers, 1976, Phys. Rev. Lett. **37**, 625.
Granqvist, C. G., and O. Hunderi, 1976, Solid State Commun. **19**, 939.
Granqvist, C. G., and O. Hunderi, 1977, Phys. Rev. B **16**, 3513.
Greenwood, D. A., R. Brout, and J. A. Krumhansl, 1960, Bull. Am. Phys. Soc. **5**, 297.
Grobet, P. J., and R. A. Schoonheydt, 1985, Surf. Sci. **156**, 893.
Hammel, P. C., and R. C. Richardson, 1981, Physica B **107**, 611.
Hammond, R. H., and G. M. Kelly, 1967, Phys. Rev. Lett. **18**, 156.
Hines, W. A., 1971, in *Proceedings of the 12th International Conference on Low Temperature Physics,* Kyoto, 1970, edited by Eizo Kanda (Academic Press of Japan, Tokyo), p. 591.
Hines, W. A., and W. D. Knight, 1971, Phys. Rev. B **4**, 893.
Holland, B. W., 1967, in *Proceedings of the 14th Colloque Ampère,* Ljubljana, 1966, edited by R. Blinc (North-Holland, Amsterdam), p. 468.
Hurault, J. P., K. Maki, and M. T. Béal-Monod, 1971, Phys. Rev. B **3**, 762.
Ido, M., 1976, J. Phys. Soc. Jpn. **41**, 412.
Ido, M., and R. Hoshino, 1975, J. Phys. Soc. Jpn. **38**, 898.
Iwama, S., and K. Hayakawa, 1985, Surf. Sci. **156**, 85.
Kappes, M., R. Kunz, and E. Schumacher, 1982, Chem. Phys. Lett. **91**, 413.
Kawabata, A., 1970, J. Phys. Soc. Jpn. **29**, 902.
Kawabata, A., 1977, J. Phys. (Paris) Colloq. **38**, C2-83.
Kawabata, A., and R. Kubo, 1966, J. Phys. Soc. Jpn. **21**, 1765.
Kenner, V. E., and R. E. Allen, 1975, Phys. Rev. B **11**, 2858.
Kimoto, K., and I. Nishida, 1967a, Jpn. J. Appl. Phys. **6**, 1047.
Kimoto, K., and I. Nishida, 1967b, J. Phys. Soc. Jpn. **22**, 744.
Kimoto, K., and I. Nishida, 1967c, J. Phys. Soc. Jpn. **22**, 940.
Kimura, K., S. Bandow, and S. Sako, 1985, Surf. Sci. **156**, 883.
Knight, W. D., 1983, Helv. Phys. Acta **56**, 521.
Knight, W. D., R. Monot, E. R. Dietz, and A. R. George, 1978, Phys. Rev. Lett. **40**, 1324.
Kittel, C., 1976, *Introduction to Solid State Physics,* 5th ed. (Wiley, New York).
Kobayashi, M., Y. Inoue, N. Takahashi, R. L. Burwell, Jr., J. B. Butt, and J. B. Cohen, 1980, J. Catal. **64**, 74.
Kobayashi, S., 1974, *Proceedings of the 13th Low Temperature Conference on Low Temperature Physics,* University of Colorado, 1972, edited by K. D. Timmerhaus, W. J. O'Sullivan, and E. F. Hammel (Plenum, New York), Vol. 4, p. 315.
Kobayashi, S., 1977, J. Phys. (Paris) Colloq. **38**, C2-121.
Kobayashi, S., K. Nomura, and W. Sasaki, 1978, J. Phys. (Paris), Colloq. **39**, C6-663.
Kobayashi, S., T. Takahashi, and W. Sasaki, 1970, Phys. Lett. A **33**, 429.
Kobayashi, S., T. Takahashi, and W. Sasaki, 1971, J. Phys. Soc. Jpn. **31**, 1442.
Kobayashi, S., T. Takahashi, and W. Sasaki, 1972, J. Phys. Soc. Jpn. **32**, 1234.
Kobayashi, S., T. Takahashi, and W. Sasaki, 1974, J. Phys. Soc.

Jpn. **36**, 714.
Kobayashi, S., T. Takahashi, and W. Sasaki, 1975, *Proceedings of the 14th International Conference on Low Temperature Physics,* Otaniemi, 1975, edited by M. Krusius and M. Vuorio (North-Holland, Amsterdam), Vol. 2, p. 372.
Kraus, W. A., and G. C. Schatz, 1983, J. Chem. Phys. **79**, 6130.
Kreibig, U., 1974, J. Phys. F **4**, 999.
Kreibig, U., and C. V. Fragstein, 1969, Z. Phys. **224**, 307.
Kreibig, U., and L. Genzel, 1985, Surf. Sci. **156**, 678.
Kubo, R., 1962, J. Phys. Soc. Jpn. **17**, 975.
Kubo, R., 1969, in *Polarization, Matière et Rayonnement,* livre jubilé en l'honneur du Professeur A. Kastler (Presses Universitaires de France, Paris), p. 325.
Kubo, R., 1977, J. Phys. (Paris) Colloq. **38**, C2-69.
Kubo, R., A. Kawabata, and S. Kobayashi, 1984, Annu. Rev. Mater. Sci. **14**, 49.
Kunz, A. B., 1980, in *Theory of Chemisorption,* edited by J. R. Smith (Springer, Berlin), p. 115.
Ladas, S., R. A. Dalla Betta, and M. Boudart, 1978, J. Catal. **53**, 356.
Lamb, H., 1882, Proc. Math. Soc. London **13**, 187.
Lautenschläger, R., 1975, Solid State Commun. **16**, 1331.
Lee, S. Y., and R. Aris, 1985, Catal. Rev. **27**, 207.
Lubzens, D., M. R. Shanabarger, and S. Schultz, 1972, Phys. Rev. Lett. **29**, 1387.
Lushnikov, A. A., V. V. Maksimenko, and A. Y. Simonov, 1978, Fiz. Tverd. Tela (Leningrad) **20**, 505 [Sov. Phys.—Solid State **20**, 292 (1978)].
MacLaughlin, D. E., 1976, Solid State Phys. **31**, 1.
Makowka, C. D., C. P. Slichter, and J. H. Sinfelt, 1982, Phys. Rev. Lett. **49**, 379.
Maradudin, A. A., and R. F. Wallis, 1966, Phys. Rev. **148**, 945.
Marzke, R. F., 1979, Catal. Rev. Sci. Eng. **19**, 43.
Marzke, R. F., and W. S. Glaunsinger, 1984, Proceedings of the Symposium on the Characterization of Materials with Submicron Dimensions, Philadelphia, 1983 (unpublished).
Marzke, R. F., W. S. Glaunsinger, and M. Bayard, 1976, Solid State Commun. **18**, 1025.
Marzke, R. F., W. S. Glaunsinger, K. B. Rawlings, P. Van Rheenen, M. McKelvy, J. H. Brewer, D. Harshman, and R. F. Kiefl, 1983, in *Electronic Structure and Properties of Hydrogen in Metals,* edited by P. Jena and C. B. Satterthwaite (Plenum, New York).
Mason, M. G., 1983, Phys. Rev. B **27**, 748.
Maxwell-Garnett, J. C., 1904, Philos. Trans. R. Soc. London **203**, 385.
Maxwell-Garnett, J. C., 1906, Philos. Trans. R. Soc. London **205**, 237.
McMillan, R. C., 1964, J. Phys. Chem. Solids **25**, 773.
McMillan, R. C., G. J. King, B. S. Miller, and F. F. Carlson, 1962, J. Phys. Chem. Solids **23**, 1379.
Mehta, M. L., 1967, *Random Matrices and the Statistical Theory of Energy Levels* (Academic, New York).
Meier, F., and P. Wyder, 1972, Phys. Lett. A **39**, 51.
Meier, F., and P. Wyder, 1973, Phys. Rev. Lett. **30**, 181.
Messmer, R. P., 1979, in *The Nature of the Surface Chemical Bond,* edited by Th. Rhodin and G. Ertl (North-Holland, Amsterdam), p. 51.
Messmer, R. P., 1981, Surf. Sci. **106**, 225.
Mie, G., 1908, Ann. Phys. (Leipzig) **25**, 377.
Millet, J.-L., and J.-P. Borel, 1981, Surf. Sci. **106**, 403.
Millet, J.-L., and J.-P. Borel, 1982, Solid State Commun. **43**, 217.
Millet, J.-L., and R. Monot, 1975, in *Proceedings of the 18th Ampère Congress,* Nottingham, 1974, edited by P. S. Allen, E. R. Andrew, and C. A. Bates (North-Holland, Amsterdam), Vol. 2, p. 319.
Monod, P., and A. Janossy, 1977, J. Low Temp. Phys. **26**, 311.
Monot, R., 1983, *Second Symposium on the Physics of the Latent Image in Photography,* Trieste, Italy (unpublished).
Monot, R., A. Châtelain, and J.-P. Borel, 1971, Phys. Lett. A **34**, 57.
Monot, R., and J.-L. Millet, 1976, J. Phys. (Paris) **37**, L-45.
Monot, R., C. Narbel, and J.-P. Borel, 1974, Nuovo Cimento B **19**, 253.
Morokhov, I. D., V. I. Petinov, L. I. Trusov, and V. F. Petrunin, 1981, Usp. Fiz. Nauk **133**, 653 [Sov. Phys.—Usp. **24**, 295 (1981)].
Morozov, Yu. G., 1980, Fiz. Tverd. Tela Leningrad **22**, 196 [Sov. Phys.—Solid State **22**, 113 (1980)].
Mostefa, M., and G. Olivier, 1985, J. Phys. C **18**, 93.
Mühlschlegel, B., D. J. Scalapino, and R. Denton, 1972, Phys. Rev. B **6**, 1767.
Myles, C. W., 1982, Phys. Rev. B **26**, 2648.
Niklasson, G. A., and C. G. Granqvist, 1986, Phys. Rev. Lett. **56**, 256.
Nishiguchi, N., and T. Sakuma, 1981, Solid State Commun. **38**, 1073.
Nomura, K., S. Kobayashi, and W. Sasaki, 1977, Solid State Commun. **24**, 81.
Nomura, K., S. Kobayashi, and W. Sasaki, 1980, J. Phys. Soc. Jpn. **48**, 37.
Novotny, V., and P. P. M. Meincke, 1973, Phys. Rev. B **8**, 4186.
Novotny, V., P. P. M. Meincke, and J. H. P. Watson, 1972, Phys. Rev. Lett. **28**, 901.
Ohnishi, S., C. L. Fu, and A. J. Freeman, 1985, J. Magn. Magn. **50**, 161.
Oseroff, S., B. L. Gehman, and S. Schultz, 1977, Phys. Rev. B **15**, 1291.
Pechukas, P., 1983, Phys. Rev. Lett. **51**, 943.
Perenboom, J. A. A. J., P. Wyder, and F. Meier, 1981a, Phys. Rep. **78**, 173.
Perenboom, J. A. A. J., P. Wyder, and F. Meier, 1981b, Phys. Rev. B **23**, 279.
Petinov, V. I., and A. Y. Ardashev, 1969, Fiz. Tverd. Tela (Leningrad) **11**, 3 [Sov. Phys.—Solid State **11**, 1 (1969)].
Pfund, A. H., 1930, Phys. Rev. **35**, 1434.
Pfund, A. H., 1933, J. Opt. Soc. Am. **23**, 375.
Planck, M., 1921, *Theorie der Wärmestrahlung,* 6th ed. (Joh. Ambrosius Barth, Leipzig).
Porter, C. E., 1965, *Statistical Theories of Spectra Fluctuations* (Academic, New York).
Ratcliff, K. F., 1979, in *Multivariate Analysis V,* edited by P. R. Krishnaiah (North-Holland, Amsterdam).
Reif, F., 1957, Phys. Rev. **106**, 208.
Rhodes, H. E., P.-K. Wang, C. D. Makowka, S. L. Rudaz, H. T. Stokes, C. P. Slichter, and J. H. Sinfelt, 1982, Phys. Rev. B **26**, 3569.
Rhodes, H. E., P.-K. Wang, H. T. Stokes, C. P. Slichter, and J. H. Sinfelt, 1982, Phys. Rev. B **26**, 3559.
Rice, M. J., W. R. Schneider, and S. Strässler, 1973, Phys. Rev. B **8**, 474.
Rosenzweig, N., and C. E. Porter, 1960, Phys. Rev. **120**, 1698.
Ruppin, R., 1979, Phys. Rev. B **19**, 1318.
Saiki, K., T. Fujita, Y. Shimizu, S. Sakoh, and N. Wada, 1972, J. Phys. Soc. Jpn. **32**, 447.
Sako, S., and K. Kimura, 1984, J. Phys. Soc. Jpn. **53**, 1495.
Sako, S., and K. Kimura, 1985, Surf. Sci. **156**, 511.

Sashital, S. R., J. B. Cohen, R. L. Burell, Jr., and J. B. Butt, 1977, J. Catal. **50**, 479.
Sattler, K., J. Mühlbach, and E. Recknagel, 1980, Phys. Rev. Lett. **45**, 821.
Saunders, W. A., K. Clemenger, W. A. de Heer, and W. D. Knight, 1985, Phys. Rev. B **32**, 1366.
Schaber, H., and T. P. Martin, 1985, Surf. Sci. **156**, 64.
Schafer, C., 1921, Z. Phys. **7**, 287.
Schmeisser, H., 1974, Thin Solid Films **22**, 83.
Schmidt, V. V., 1966, Zh. Eksp. Teor. Fiz. **3**, 141 [Sov. Phys.—JETP **3**, 89 (1966)].
Schultz, S., G. Dunifer, and C. Latham, 1966, Phys. Lett. **23**, 192.
Schultz, S., M. R. Shanabarger, and P. M. Platzman, 1967, Phys. Rev. Lett. **19**, 749.
Sen, P. N., and D. B. Tanner, 1982, Phys. Rev. B **26**, 3582.
Shiba, H., 1976, J. Low Temp. Phys. **22**, 105.
Šimànek, E., 1977, Phys. Rev. Lett. **38**, 1161.
Šimànek, E., 1981, Solid State Commun. **37**, 97.
Šimànek, E., D. Imbro, and D. E. MacLaughlin, 1973, J. Low Temp. Phys. **11**, 787.
Slichter, C. P., 1978, *Principles of Magnetic Resonance,* 2nd ed. (Springer, Berlin).
Slichter, C. P., 1981a, Bull. Mag. Res. **2**, 73.
Slichter, C. P., 1981b, Surf. Sci. **106**, 382.
Smith, M. J. A., and D. J. E. Ingram, 1962, Proc. Phys. Soc. London **80**, 139.
Smithard, M. A., 1973, Solid State Commun. **13**, 153.
Smithard, M. A., 1974a, Solid State Commun. **14**, 407.
Smithard, M. A., 1974b, Solid State Commun. **14**, 411.
Sone, J., 1976, J. Low Temp. Phys. **23**, 699.
Sone, J., 1977, J. Phys. Soc. Jpn. **42**, 1457.
Sone, J., 1983, J. Low Temp. Phys. **50**, 559.
Stein, G. D., 1985, Surf. Sci. **156**, 44.
Stewart, G. R., 1977, Phys. Rev. B **15**, 1143.
Stokes, H. T., H. E. Rhodes, P.-K. Wang, C. P. Slichter, and J. H. Sinfelt, 1981, in *Nuclear and Electron Resonance Spectroscopies Applied to Materials Science,* edited by J. Kaufmann and G. K. Shenoy (Elsevier/North-Holland, Amsterdam), p. 253.
Stokes, H. T., H. E. Rhodes, P.-K. Wang, C. P. Slichter, and J. H. Sinfelt, 1982, Phys. Rev. B **26**, 3575.
Strässler, S., and M. J. Rice, 1972, Phys. Rev. B **6**, 2575.
Suzuki, T., and T. Tsuboi, 1977, J. Phys. Soc. Jpn. **43**, 444.
Takahashi, T., S. Kobayashi, and W. Sasaki, 1975, Solid State Commun. **17**, 681.
Tamura, A., K. Higeta, and T. Ichinokawa, 1982, J. Phys. C **15**, 4975.
Tanner, D. B., A. J. Sievers, and R. A. Buhrman, 1975, Phys. Rev. B **11**, 1330.
Tarczon, J. C., 1984, private communication.
Taupin, C., 1967, J. Phys. Chem. Solids **28**, 41.
Tavel, J. F., K. F. Ratcliff, and N. Rosenzweig, 1979, Phys. Lett. A **73**, 353.
Tran Thoai, D. B., and W. Ekardt, 1982, Solid State Commun. **41**, 687.
Turkevich, J., P. C. Stevenson, and J. Hillier, 1951, Discuss. Faraday Soc. **11**, 55.
Uchijima, T., J. M. Herrman, Y. Inoue, R. L. Burwell, Jr., J. B. Butt, and J. B. Cohen, 1977, J. Catal. **50**, 464.
Uyeda R., 1974, J. Cryst. Growth **24**, 69.
van der Klink, J. J., J. Buttet, and M. Graetzel, 1984, Phys. Rev. B **29**, 6352.
van Gelder, A. P., 1974, Phys. Rev. B **10**, 2144.
Vergara, O., D. Heitkamp, and H. V. Löhneysen, 1984, J. Phys. Chem. Solids **45**, 251.
Wada, N., 1967, J. Appl. Phys. **6**, 553.
Wada, N., 1968, J. Appl. Phys. **7**, 1287.
Walker, M. B., 1971, Phys. Rev. B **3**, 30.
Watson, J. H. P., 1966, Phys. Rev. **148**, 223.
Watson, J. H. P., 1970, Phys. Rev. B **2**, 1282.
Weinert, M., and A. J. Freeman, 1983, Phys. Rev. B **28**, 6262.
Wigner, E. P., 1951, Ann. Math. **53**, 36.
Wigner, E. P., 1955, Ann. Math. **62**, 548.
Wilenzick, R. M., D. C. Russell, R. H. Morriss, and S. W. Marshall, 1967, J. Chem. Phys. **47**, 533.
Wood, D. M., and N. W. Ashcroft, 1982, Phys. Rev. B **25**, 6255.
Wright, F., Jr., 1967, Phys. Rev. **163**, 420.
Yatsuya, S., S. Kasukabe, and R. Uyeda, 1973, Jpn. J. Appl. Phys. **12**, 1675.
Yatsuya, S., K. Mihama, and R. Uyeda, 1974, Jpn. J. Appl. Phys. **13**, 749.
Yatsuya, S., Y. Tsukasaki, K. Mihama, and R. Uyeda, 1978, J. Cryst. Growth **45**, 490.
Yatsuya, S., Y. Tsukasaki, K. Yamauchi, and K. Mihama, 1985, J. Cryst. Growth **70**, 533.
Yatsuya, S., R. Uyeda, and Y. Fukano, 1972, Jpn. J. Appl. Phys. **11**, 408.
Yatsuya, S., K. Yamauchi, T. Kamakura, A. Yanagida, H. Wakayama, and K. Mihama, 1985, Surf. Sci. **156**, 1011.
Yee, P., and W. D. Knight, 1975, Phys. Rev. B **11**, 3261.
Yu, I., 1980, "A Nuclear Magnetic Resonance Study of Small Platinum Particles," Ph.D. thesis (Northwestern University).
Yu, I., A. A. V. Gibson, E. R. Hunt, and W. P. Halperin, 1980, Phys. Rev. Lett. **44**, 348.
Yu, I., and W. P. Halperin, 1981a, J. Chim. Phys. **78**, 901.
Yu, I., and W. P. Halperin, 1981b, J. Low. Temp. Phys. **45**, 189.
Zeller, R. C., and R. O. Pohl, 1971, Phys. Rev. B **4**, 2029.
Zsigmondy, R., 1906, Z. Phys. Chem. (Leipzig), **56**, 65.

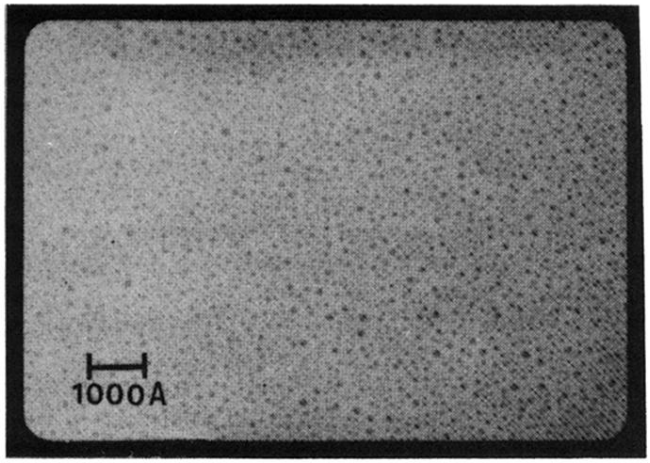

(a)

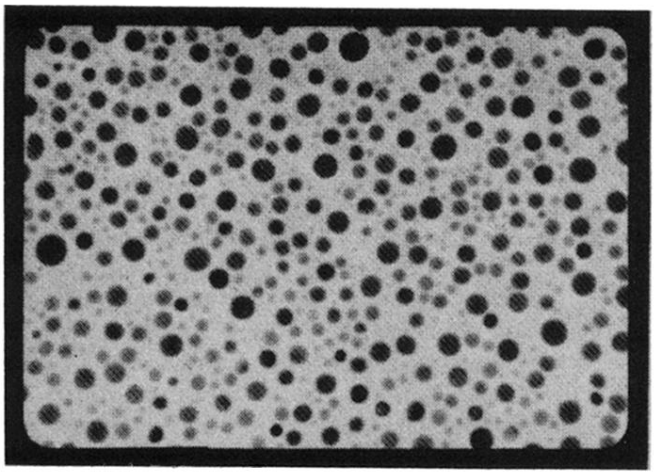

(b)

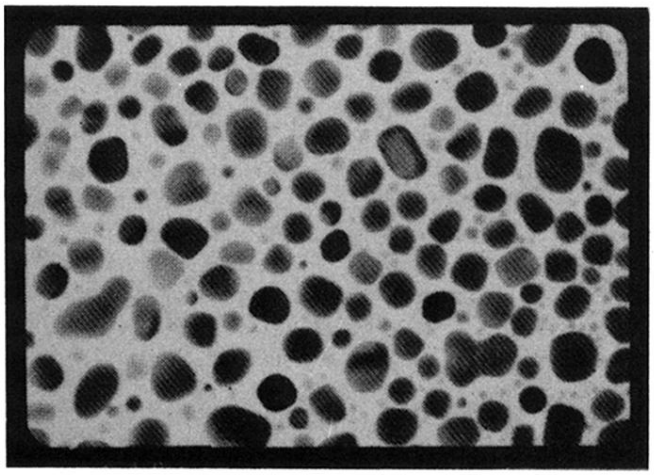

(c)

FIG. 32. Electron micrographs of three samples of Sn particles produced by the method of vacuum evaporation and subsequent island formation on Mylar substrates by Fukagawa, Kobayashi, and Sasaki (1982). The average diameters of these samples d' and the average cube root of the third moment of the size distributions $d=(6\overline{\Omega}/\pi)^{1/3}$, were found to be (a) $d'=75$ Å, $d=70$ Å; (b) $d'=330$ Å, $d=280$ Å; and (c) $d'=610$ Å, $d=450$ Å. In the above, $\overline{\Omega}$ is the average volume of a particle.